DESIGN OF SINGLE DEGREE-OF-FREEDOM PLANAR LINKAGES WITH ANTIPARALLELOGRAM LOOPS USING LOOP ASSEMBLY METHOD

**A Thesis Submitted to
the Graduate School of Engineering and Sciences of
İzmir Institute of Technology
in Partial Fulfillment of the Requirements for the Degree of**

MASTER OF SCIENCE

in Architecture

**by
Şebnem GÜR**

**July 2017
İZMİR**

We approve the thesis of **Şebnem GÜR**

Examining Committee Members:

_____
Assoc. Prof. Dr. Koray KORKMAZ
Department of Architecture, İzmir Institute of Technology

_____
Assoc. Prof. Dr. Gökhan KİPER
Department of Mechanical Engineering, İzmir Institute of Technology

_____
Assist. Prof. Dr. Özgür KİLİT
Department of Industrial Design, Yaşar University

21 July 2017

_____
Assoc. Prof. Dr. Koray KORKMAZ
Supervisor, Department of Architecture
İzmir Institute of Technology

_____
Assoc. Prof. Dr. Şeniz ÇIKIŞ
Head of the Department of Architecture

_____
Prof. Dr. Aysun SOFUOĞLU
Dean of the Graduate School of
Engineering and Sciences

ACKNOWLEDGEMENTS

ABSTRACT

DESIGN OF SINGLE DEGREE-OF-FREEDOM PLANAR
LINKAGES WITH ANTIPARALLELOGRAM LOOPS
USING LOOP ASSEMBLY METHOD

This research deals with the methodical derivation of single degree-of-freedom (dof) deployable and transformable linkages with antiparallelogram loops. The study starts with the review of literature on the mechanisms used in planar deployable structures, scissor mechanisms in particular. Scissor mechanisms have been subject of many research, including those that examine them in term of the loops formed. In this research, a summary of the loops observed in previous researches are mentioned. The simplest single-dof linkage is the four-bar linkage. Its loop geometry is quadrilateral. The loops defined formerly in the deployable structures literature are compared to the geometries classified under quadrilaterals and seen that use of antiparallelogram loops are yet to be discovered. While forming novel linkages with antiparallelogram loops, the loop assembly method that Hoberman utilized during his discovery of angulated scissor linkages is used. In order to lay out alternatives of loop arraying options, pattern generating methods are examined. Frieze group operations are found to be most suitable. Using those, loop assembly variations are formed. Later, links formed by these arrays are determined and linkages are formed, modelled and simulated using Solidworks®. Among many alternatives, five of them are chosen due to their novelties in specific aspects. In conclusion findings are compared to the previous research in the literature. Potentials of the novel linkages in terms of architecture are discussed and further research subjects are offered.

ÖZET

DEVRE BİRLEŞTİRME YÖNTEMİ KULLANILARAK TERS PARALELKENAR DEVRELER İLE TEK SERBESTLİK DERECELİ DÜZLEMSEL MEKANİZMALARIN TASARIMI

Bu araştırma ters paralelkenar devreli tek serbestlik dereceli katlanabilir/dönüştürülebilir yapıların metodik eldesi üzerinedir. Çalışma literatürdeki düzlemsel katlanabilir yapılarda kullanılan mekanizmaların ve özellikle de makas mekanizmaların bir incelemesi ile başlar. Makas mekanizmalar, oluşturdukları devre tipleri açısından da çalışılmış pek çok araştırmaya konu olmuştur. Bu araştırmada da önceki çalışmalarda incelenmiş devreler kısaca anlatılmıştır. Tek serbestlik dereceli bir dört-çubuk mekanizması devresinin geometrisi dörtgendir. Katlanabilir yapılar literatüründe daha önce belirlenmiş olan devreler dörtgen olarak tanımlanmış geometrik formlar ile kıyaslanmış ve ters paralelkenarların devre tipi olarak henüz keşfedilmediği görülmüştür. Ters paralelkenarlar kullanılarak yeni mekanizmalar oluşturulurken, Hoberman'ın açılı makas elemanları buluşu sırasında kullandığı devre birleştirme metodu kullanılmıştır. Tüm devre türetme tiplerinin bir dökümünü elde etmek için, patern oluşturma metotları incelenmiştir. Bunların arasında Frieze grubu işlemleri en uygun bulunmuştur. Bu işlemler kullanılarak devre türetme varyasyonları oluşturulmuştur. Daha sonra her türevin uzuvları çizilmiş ve mekanizmalar oluşturularak modellenmiş ve Solidworks® kullanılarak benzetimleri gerçekleştirilmiştir. Elde edilen pek çok alternatif mekanizma arasından belli yönlerden yenilikleri olan beş tanesi seçilerek detaylı olarak incelenmiştir. Sonuç bölümünde bulgular önceki çalışmalar ile karşılaştırılmıştır. Yeni mekanizmaların mimari alanındaki potansiyelleri tartışılmış ve ileride yapılabilecek araştırmalar için önerilerde bulunulmuştur.

TABLE OF CONTENTS

LIST OF FIGURES

CHAPTER 1

INTRODUCTION

1.1. Definition of the Study

Even though the first examples of deployable structures are quite ancient, as a research field at the intersection of architecture, mechanical engineering, civil engineering and mathematics, deployable structures are a recent subject. Their architectural applications offer novel solutions to the most significant problems of present times, such as the ever-changing needs of occupants, depletion of resources and environmental considerations. As an architect to be able to generate sustainable and responsive built environments, understanding and utilizing the potential of the motion of such structures is crucial.

Scissor mechanisms are primary choice to construct deployable structures. They attract a substantial attention, due to their capacity of motion, the simplicity of their elements and stowing efficiency. This entails many research to be conducted on the subject. Scissor mechanisms used in large-scale architectural designs were first introduced by Spanish architect Emilio Perez Piñero in the early 1960s and many researchers followed his lead from then on. Despite the subject has been extensively studies, it is still possible to find new approaches to the design.

Common approach of designing scissor linkages is focusing on the scissor elements and treating them as modules to create linkages, as Escrig (1985), Glassner (1996), Gantes et al. (1989) and You and Pellegrino (1997) did.

As an alternative, a loop formed by two adjacent scissor element pair can be considered as a module. Previous works on the translational and polar scissor units laid out parallelogram, rhombus, kite and dart loops. It was Chuck Hoberman, an artist and a mechanical engineer, who first utilized this approach. In his patented work on reversibly expandable doubly-curved truss structures Hoberman (1990), first rhombus loops were placed along an arbitrary polygon and then the edges of these loops are used to create the links. As a result of his work, Hoberman came up with angulated scissor unit, which was a great contribution to the field. Following Hoberman, Liao and Li (2005) and Kiper and

Söylemez (2010) used rhombus loops for their works on loop assembly method. In her work, Yar et al. (2017) analyzed scissor linkages and the loops forming between them. Using kite loops and a derivative of it, dart loops, she formed a single degree-of-freedom (DoF) linkage that can transform between concave and convex forms.

In this study first, a literature review on scissor structures is presented. It has been observed that according to the location of scissor hinge, there are three main groups of scissor units; translational, polar and angulated scissor units. Later, loop types of these scissor structures are examined. A loop is formed when two scissor units are connected at their end points. In a single-DoF four-bar linkage, the loop is a quadrilateral. Quadrilaterals are named according to their geometric constraints such as equal edges and parallelisms. After laying out quadrilateral types, loops formed between each type of scissor unit is examined. It is revealed that there are eight quadrilateral types defined in the literature; parallelogram, rhombus and kite loops with their special cases rectangle, square, dart loops and also convex and concave loops without any special geometric constraint. It has been seen that there were no loop definitions using complex quadrilaterals. A complex quadrilateral is composed of four edges, two of which are nonadjacent edges crossing each other. In this research, a more geometrically constraint complex quadrilateral, the antiparallelogram, is used to form planar linkages with single DoF.

An antiparallelogram loop has two equal nonadjacent short edges and two equal nonadjacent long edges which cross each other. At an arbitrary configuration it has a symmetry axis (and as a special case two orthogonal symmetry axes when short edges are parallel). In this research, loop assembly method is used to form linkages with antiparallelogram loops.

In the literature, a systematical method to formulate loop arrays was not observed. Therefore a mathematical approach called "Symmetry Operations" was analyzed to devise a method. Since this research is focusing only on planar loop chains, Frieze Groups were compatible with the work at hand. After introducing Frieze Group symmetry operations, arrays using antiparallelogram loops have been formed. Using each array, linkages were defined.

In order to achieve single degree-of-freedom linkages, two links from each adjacent loop should be combined to form two common links. It has been observed that there was most commonly more than one possible configuration of links for each array, concluding over a hundred alternatives outlined throughout the study. All defined

configurations were later modelled in Solidworks® to observe motion. Few of the alternatives laid interesting results due to their motion capacity. Those highlights wider examined and explained in proceeding chapters of the research.

1.2. Scope and Objectives of the Study

The aim of this thesis is to form single DoF linkages with antiparallelogram loops using the loop assembly method. In this process, primarily, a literature review on deployable scissor structures is conducted. The review is followed by a profound examination of the loops of the deployable structures.

Subsequently, the loop assembly method is explained. In order to produce assemblies with antiparallelogram loops, as a methodical way of loop multiplication, Frieze Group symmetry operations are proposed.

After explaining Frieze Group symmetry operations in detail, assembly variations using the method are laid out. Then, the links of the assemblies are defined to form alternative single degree-of-freedom mechanisms.

As the last step, novel mechanisms were chosen to be explained in detail.

1.3. Methodology

A literature review was the key to understand the basic geometry of scissor structures and loop formations. After the systematic derivation of loop arrays utilizing Frieze Groups of symmetry operations, two-dimensional drawing software packages are used to visualize the linkages and Solidworks® is used to simulate their motions. Microsoft Excel is used to create parametric calculations and two dimensional graphics that visualize the position of the joints throughout the motion.

1.4. Significance of the Study and Contributions

This study presents a novel methodology to form antiparallelogram loop arrays in order to form single degree-of-freedom linkages using the loop assembly method. As the outcome of the method, there are five novel linkages, four of which are able to transform and one able to deploy in a ring formation.

1.5. Organization of Thesis

This thesis is composed of six chapters:

In Chapter 1, definition of the study, scope and objectives, methodology, significance of the study and contributions and outline of the thesis are mentioned.

In Chapter 2, an introduction to the deployable scissor mechanisms and relevant studies in the literature is made.

Chapter 3 explains the planar scissor linkages, kinematic properties of their units in detail. The quadrilateral geometry is introduced and the loop types formed in these linkages are examined in correspondence with quadrilaterals yielding the lack of antiparallelograms loops in linkages used in modular deployable structures. Later the loop assembly method and properties of antiparallelogram as a loop are explained.

In Chapter 4 symmetry operations are explored. Frieze Group symmetries are examined. Then their applications with antiparallelogram loops are produced. After that, while producing linkages from loop arrays, the link formations are explained.

Chapter 5 consists of detailed explanations of five novel linkages among the results.

In Chapter 6 all the findings from previous chapters are summarized and contribution of the research is expressed.

CHAPTER 2

REVIEW OF LITERATURE

2.1. Deployable Pantograph Structures

"Deployable Structure" refers to mechanisms that can transform between a compact stowed and a deployed functional configuration (Merchan and Henrique, 1987). They are also known as erectable, expandable, extendible, developable or unfurlable structures (Jensen, 2004). As a field of research, deployable structures are recognized as a subject around 1960's, however, the concept of transformable objects and spaces is as old as civilization itself. It is possible to find various applications: Hunter chairs and umbrellas in Egyptian civilization, Mongolian yurts, velum of Roman Coliseum and folding chairs… etc. In modern age, applications of deployable structures can be seen in many fields such as aerospace industry as space antennas and masts (Wang et al., 2015; Zheng and Chen, 2015; Qi et al., 2016), in architecture as retractable roofs (Mao and Luo, 2008; Jiang and Wang, 2010; Cai et al., 2016) and kinetic building skins (Pesenti et al., 2015), and in engineering as bridges (Ario et al., 2013; Lederman et al., 2014; Bouleau and Guscetti, 2016) and lifts.

Hanaor and Levy (2001) categorized deployable structures according to their structural-morphological properties (Figure 2.1.1). Focus of the review of literature in this thesis report is on the pantographic structures with rigid links and without cables as indicated with red frame in Figure 2.1.1. Pantographic elements, also called scissor-like elements (SLEs) are made up of two straight bars connected with an intermediate hinge, which is a revolute joint that allows the bars to pivot about an axis perpendicular to the common plane of the bars. If these units are connected at their end nodes, a two-dimensional deployable linkage is achieved. The position of the intermediate hinge together with the shape of the bars lead to three different scissor units: *translational*, *polar* and *angulated units*.
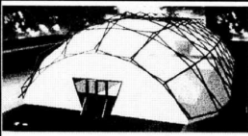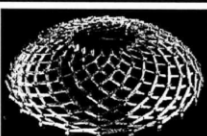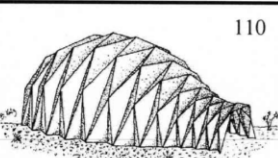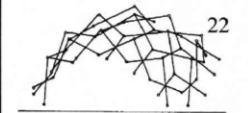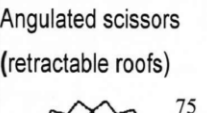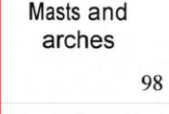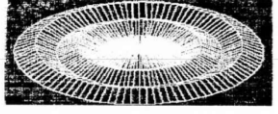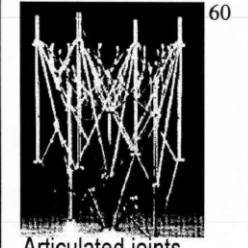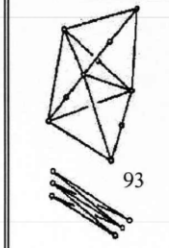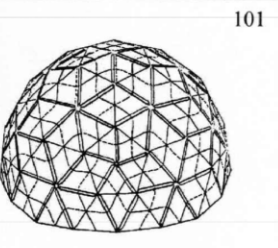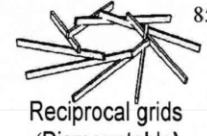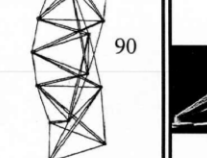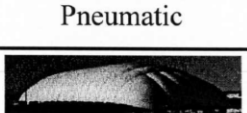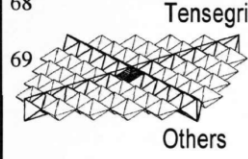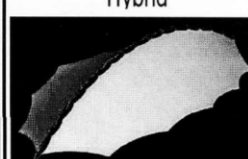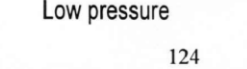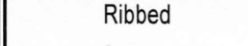
Figure 2.1.1. Deployable structures classification chart; numerals indicate references given in the paper (Source: Hanaor and Levy, 2001)

It was Emilio Pérez Piñero who first published about the use of deployable structures in architecture. His movable theater (Figure 2.1.2) was composed of scissor-like elements (SLEs) and was made up of rigid bars and cables. His application was not

stable after deployment and additional cables for stabilization were needed. Later on he developed his designs with deployable bar structures (Pinero, 1961; Pinero, 1961).
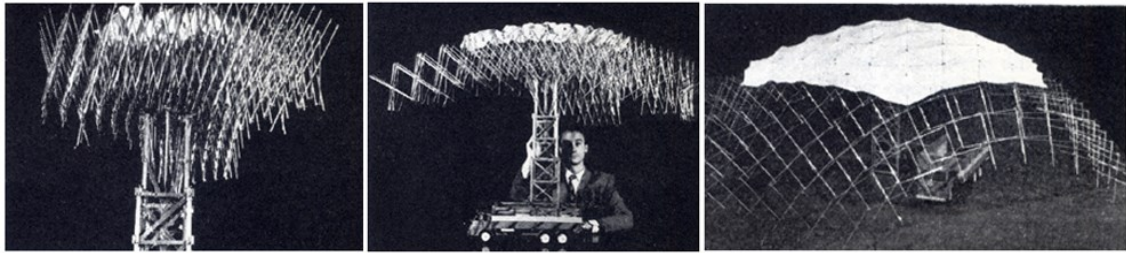
Figure 2.1.2 Movable theatre by Piñero
(Source: Cook, 1967)

Piñero's latter works such as pavilions, retractable domes and temporary enclosure were developed using SLEs as well (Pinero, 1962; Perez, 1965). The foldable reticular dome he designed was made up of seven modules expanding from compact bundles (Figure 2.1.3). During the erection process, modules were expanded and stiffened on the ground later to be lifted up and locked together (Belda, 2013). However, the system was no longer deployable after the process.
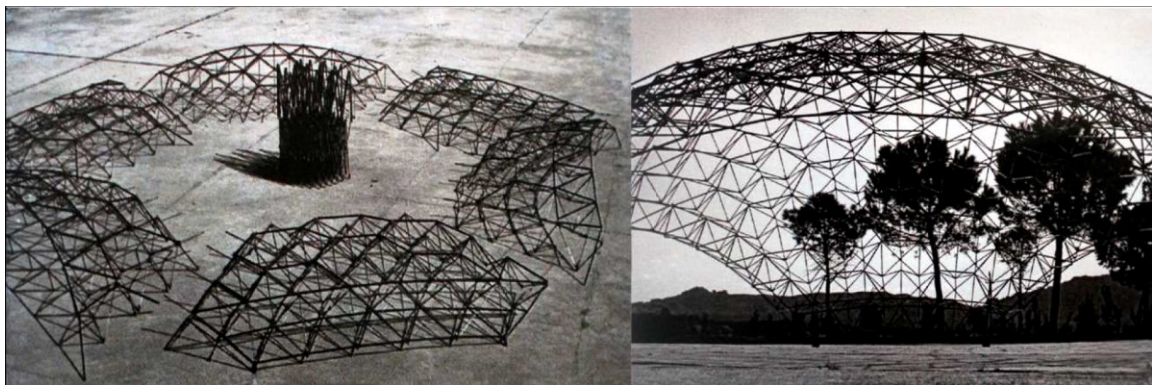
Figure 2.1.3. Foldable reticular dome
(Source: © Fundación Emilio Pérez Piñero, 2017)

Another pioneer in the field, Félix Escrig, worked extensively on deployable bar structures and laid out the geometric and deployability conditions of SLEs. He also studied the relation between the elements and the span of the structure (Escrig, 1984; Escrig, 1985). His works include generating three-dimensional structures using planar translational SLEs (Figure 2.1.4) in various directions to form grids (Figure 2.1.5).
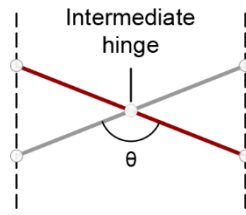
Figure 2.1.4. Translational scissor unit
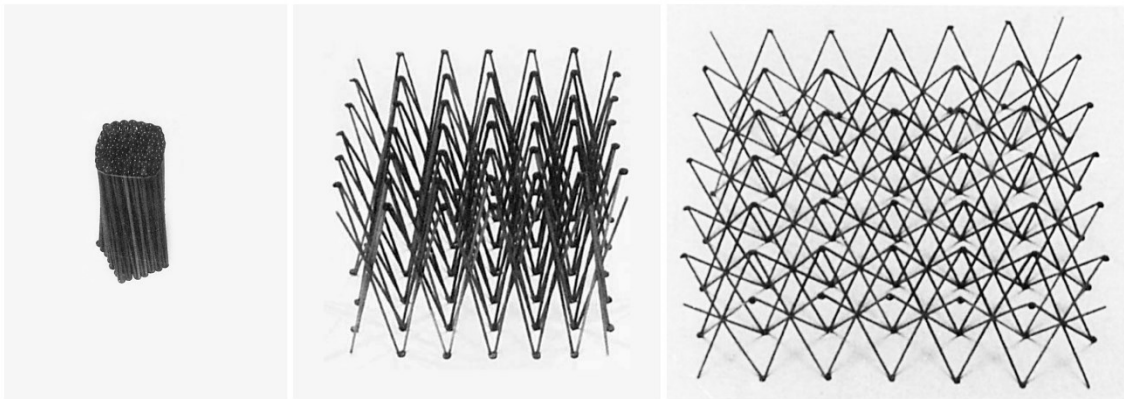
Figure 2.1.5. Two-way grid composed of translational scissor units
(Source: Escrig, 1985)

With the unit formed by changing the location of the intermediate hinge of SLEs, which is called the *polar unit* (Figure 2.1.6) Escrig obtained curved grids (Figure 2.1.7). Polar units deploy along an arc, giving the opportunity to form curved surfaces that can be stowed in a compact form.
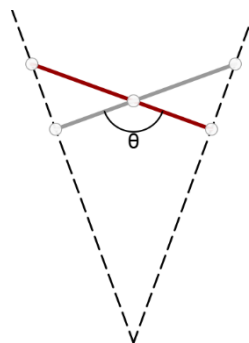
Figure 2.1.6. Polar Scissor Unit
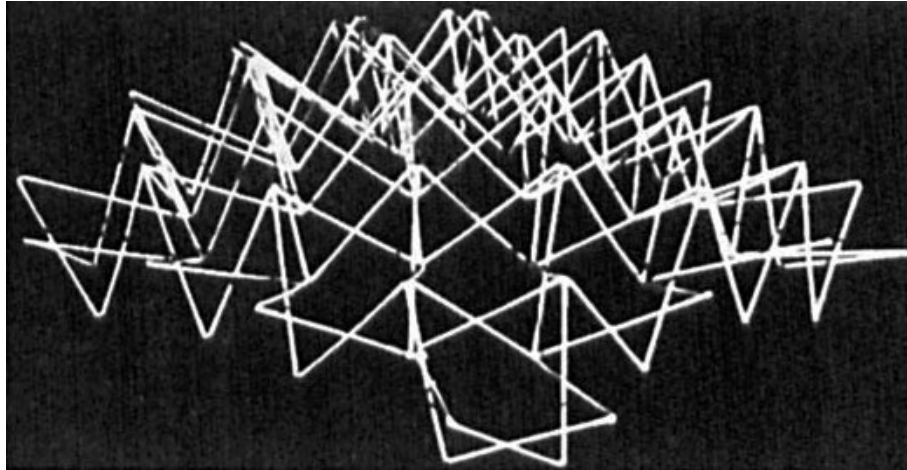
Figure 2.1.7. Expandable space-frame structure
(Source: Escrig, 1985)

Escrig also developed spherical grid structures using two-way and three-way scissors (Escrig and Valcarcel, 1986; Escrig and Valcarcel, 1987). Some other works by him and together with Valcárcel are spherical and geodesic structures, an expandable umbrella, and deployable polyhedra and compactly folded cylinder (Escrig and Valcarcel, 1986; Escrig and Valcarcel, 1993; Escrig, 1996).

One well-known real-life application by Escrig (1996) is the roof structure of the swimming pool of San Pablo Sports Centre in Seville (Figure 2.1.8). The 30m by 60m roof structure consists of two identical rhomboid spherical scissor grids covered with fabric. Grids are made up of equal quadrilateral SLEs.
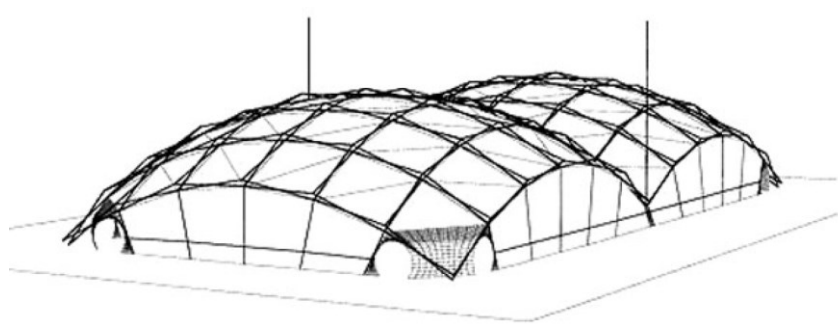
Figure 2.1.8. Swimming pool in Seville
(Source: Kassabian et al., 1999)

Langbecker (1999) developed the foldability conditions of SLEs. He worked on the deployability and kinematics of translational, polar and angulated units. Using *curved translational scissor units* (De Temmerman, 2007) (Figure 2.1.9) he formed barrel vaults

(Langbecker and Albermani, 2001) and doubly-curved synclastic and anticlastic structures (Langbecker and Albermani, 2000) (Figure 2.1.10).
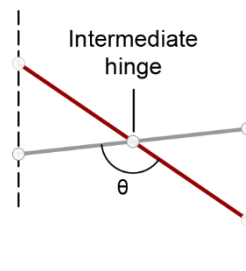
Figure 2.1.9. Curved translational scissor unit
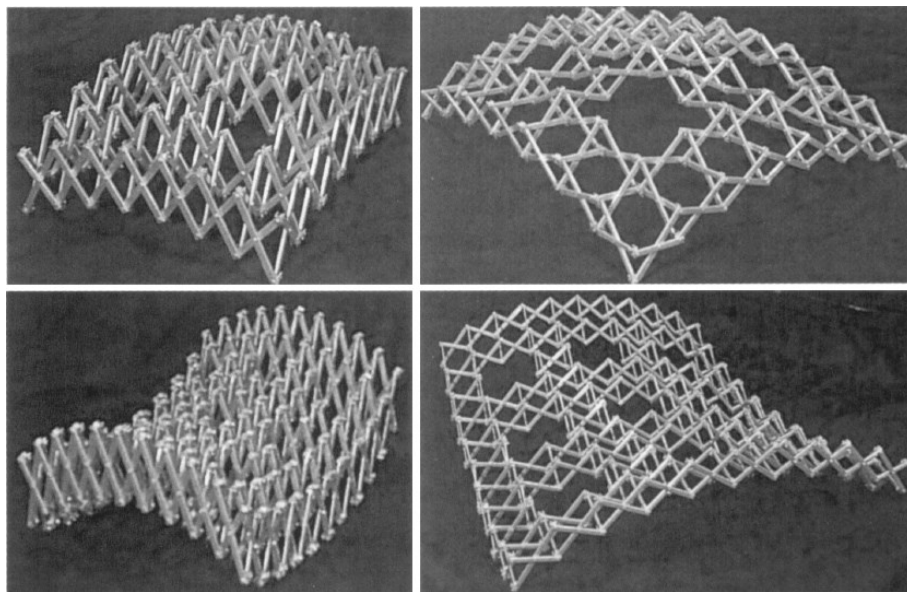
Figure 2.1.10. Synclastic and anti-clastic structures
(Source: Langbecker & Albermani, 2000)

Although many researchers kept working on translational and polar scissors with straight bar links, in 1990 Chuck Hoberman discovered a third type of scissor link, the angulated link. The scissor pair he created was made up of two identical mirror symmetric angulated bars connected with a revolute joint at the kink point and the linkage he constructed expanded radially keeping a fixed center point (Figure 2.1.11).
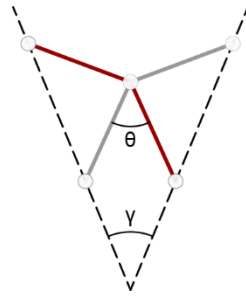
Figure 2.1.11. Angulated scissor pair with identical links

Using the angulated scissors he developed many structures such as arches, domes and spheres; also some well-known structures such as his trademark toy sphere (Hoberman, 1990), Iris Dome at EXPO 2000 (Hoberman, 1991) and Hoberman Arch which was presented at 2002 Winter Olympics at Salt Lake City (Figure 2.1.12).

Figure 2.1.12. Hoberman Sphere (up left), Expanding Geodesic Dome (up right),
Hoberman Arch (down left), open and closed Iris Dome (down right)
(Source: Hoberman Assc. and Salt Lake Tribune webpages, 2017)

Hoberman's angulated scissor unit was further examined in detail by You and Pellegrino (1997). They laid out the necessary geometric conditions of angulated scissors for radial deployment. They did not only worked on pairs of identical links but also different link pairs. They named the links they defined as *generalized angulated elements* (GAEs) (Figure 2.1.13).
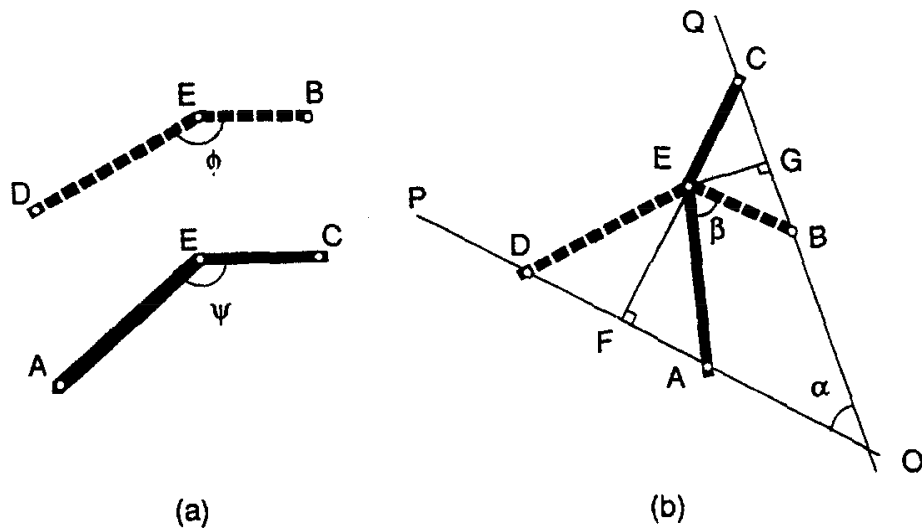
Simplest Type I GAE, formed by angulated rods with equal semi-length but different kink angles $\overline{AE} = \overline{DE}$, $\overline{BE} = \overline{CE}$, $\psi \neq \varphi$. ADE and BCE are isosceles triangles.
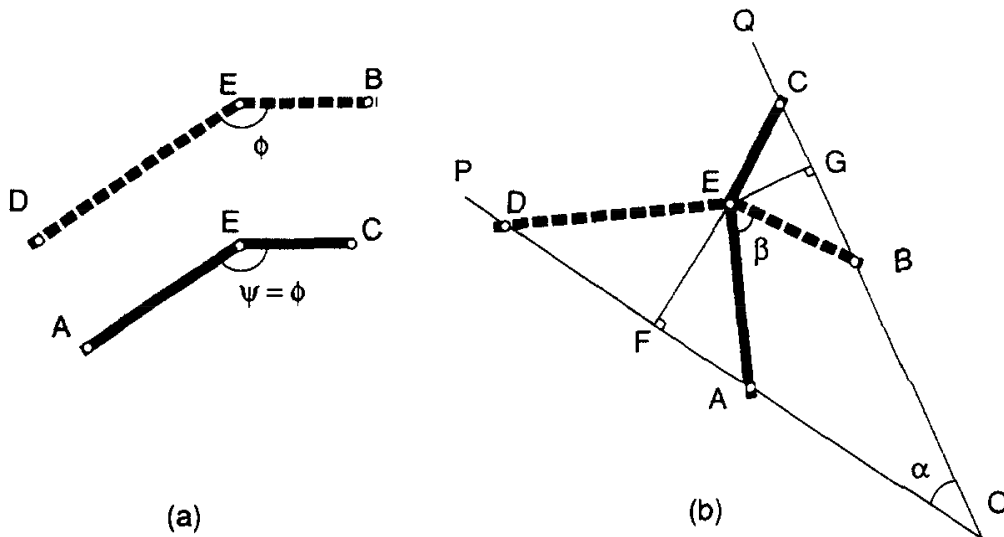
Simplest Type II GAE, formed by angulated rods with proportional semi-lengths and equal kink angles $\overline{AE}/\overline{DE} = \overline{CE}/\overline{BE}$, $\psi = \varphi$. ADE and BCE are similar triangles.

Figure 2.1.13. Generalized angulated elements
(Source: You and Pellegrino, 1997)

You and Pellegrino expanded their research forming rings of scissors and adding inner rings to achieve a structure that can radially close and retract like an iris. Their observations led them to form multi-angulated links which avoided complex joints and an excessive number of links (Figure 2.1.14).
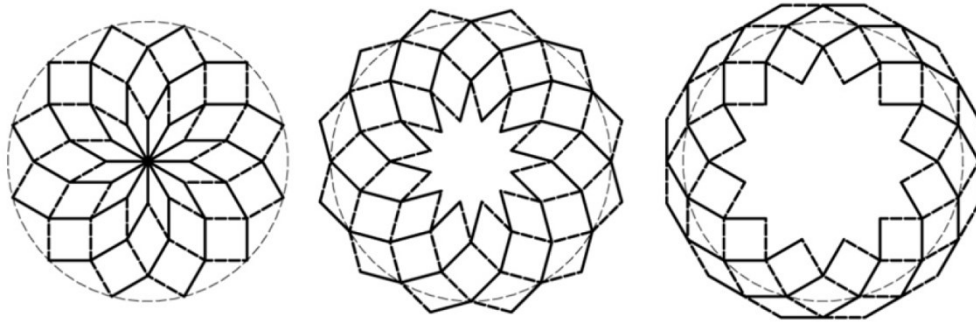
Figure 2.1.14. Multi-angled ring structure developed by You and Pellegrino
(Source: Friedman, 2011)

Kassabian, You and Pellegrino (1999) developed a structure that rests on columns with pin joints (Figure 2.1.15). They generated the dome form by projecting the hinges vertically on a sphrical surface. Although it had less complex joints, the structure was susceptible to wind effects due to its form in open configuration (Kovács and Tarnai, 2004). Kokawa took You and Pellegrino's work one step further with his retractable dome structure by using non-parallel joint axes to form a deployable dome (Kokawa, 2000).
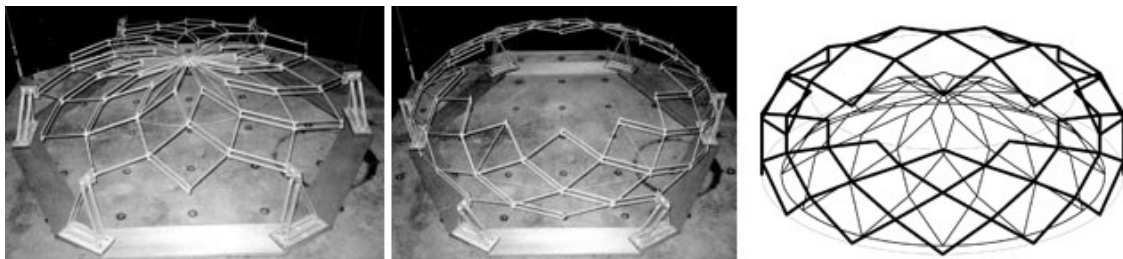
Figure 2.1.15. Retractable dome structure developed by You and Pellegrino
(Source: Deployable Structures Laboratory, 2017; Kovács & Tarnai, 2004)

Van Mele is another researcher who worked with angulated scissors. In his design to cover a tennis arena (Van Mele, 2008), he proposes a barrel vault made up of two angulated scissor arches carried by pin connected arches (Figure 2.1.16). The scissor arches are covered with a membrane and they are pinned to the spectator area at one end to form two halves of a barrel vault.
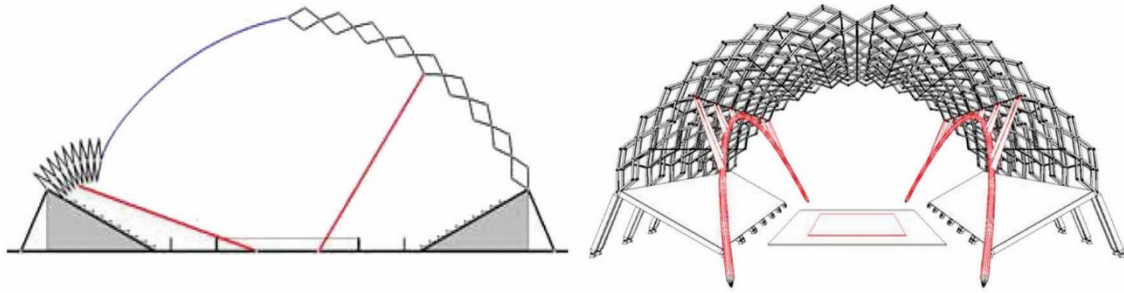
Figure 2.1.16 Deployable roof of a tennis hall by T. Van Mele
(Source: Van Mele, 2008)

Rippmann and Sobek constructed curved structures using the scissor module with various intermediate hinge points they developed (Rippmann, 2007). By connecting the units at different intermediate hinge positions, they formed curved shapes as they desired. When a different shape was needed, the units simply dismantled and assembled according to the new form once more.
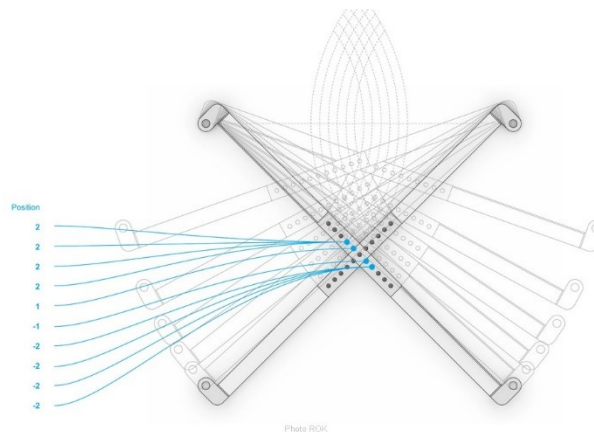
Figure 2.1.17 Scissor unit with various intermediate hinge points
(Source: Rippmann, 2007)

CHAPTER 3

SCISSOR LINKAGES

3.1. Planar Scissor Mechanisms

As the most basic scissor unit, translational units, are made up of two straight bars connected by an intermediate hinge located at the midpoint of the bars. There are two types of translational scissor units. *Plane translational units* (De Temmerman, 2007) are made up of two identical bars connected whereas the second type, the curved unit, is made up of different length bars, both connected at midpoint. The imaginary line connecting the ends of the bars are called *unit lines* (De Temmerman, 2007). Unit lines of a translational scissor unit are parallel and stay as such during deployment. In order to deploy a scissor mechanism the angle between the bars called the *deployment angle*, shown as θ in Figure 3.1.1, is changed. When two translational units are connected at their end nodes the resulting linkage has single DoF. The simplest translational unit with equal length bars is called a plane unit (Figure 3.1.1). Well-known lazy-thong mechanism is made up of such units.
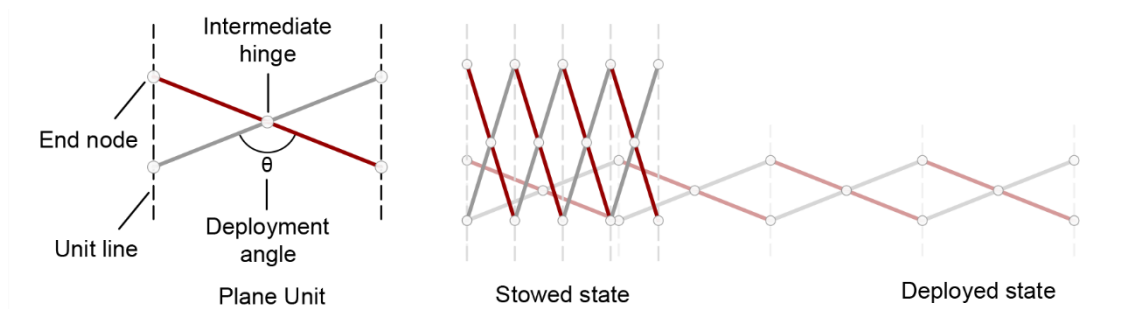
Figure 3.1.1. Deployment of translational scissor linkage composed of plane unit
(Source: Redrawn from De Temmerman, 2007)

Another type is the curved translational unit, which has different length links that are also connected from their midpoints. Depending on the array of units, whether they are repeated (Figure 3.1.2a) or mirrored (Figure 3.1.2b) along a line, the deployment direction changes. If more than one type curved unit is used, it is possible to form deployable curved linkages (Figure 3.1.2c).
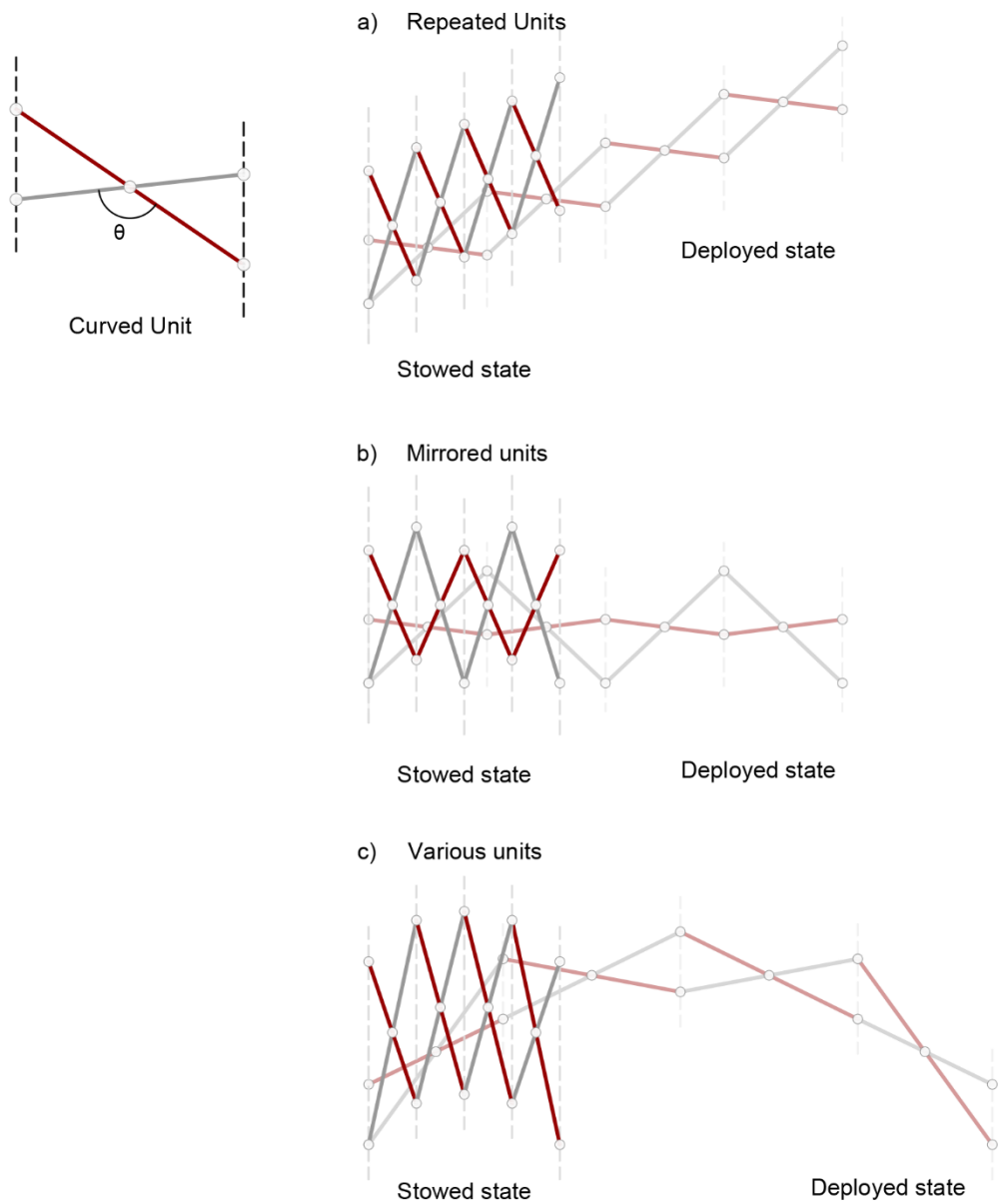
Figure 3.1.2. Deployment of translational scissor linkages composed of curved units
(Source: Redrawn from De Temmerman, 2007)

In a polar unit, the unit lines passing through the end points intersect (Figure 3.1.3). The unit deploys along an arc without a fixed center point and radius. As the linkage deploys, the angle between the unit lines increase and the intersection of the unit lines move closer to the unit. The radius of the arc defined by the linkage gets smaller as well.
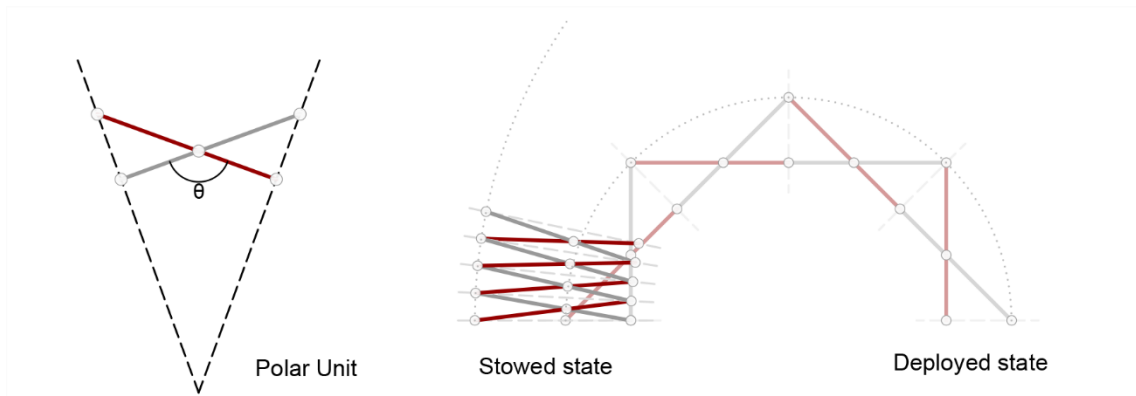
Figure 3.1.3. Deployment of polar scissor linkage
(Source: Redrawn from De Temmerman, 2007)

In 1990 Hoberman introduced the first angulated scissor elements. Unlike straight bars of translational and polar units, angulated elements have a kink and they are attached with an intermediate hinge at this point (Figure 3.1.4). The simplest angulated element is made up of two identical kinked bars with equal arm lengths. Unit lines of an angulated element intersect at a point which is also the center of the arc defined by the linkage. The linkage deploys radially and the angle between the unit lines keeps unchanged during the deployment. This is called the subtended angle, shown as γ in Figure 3.1.4.
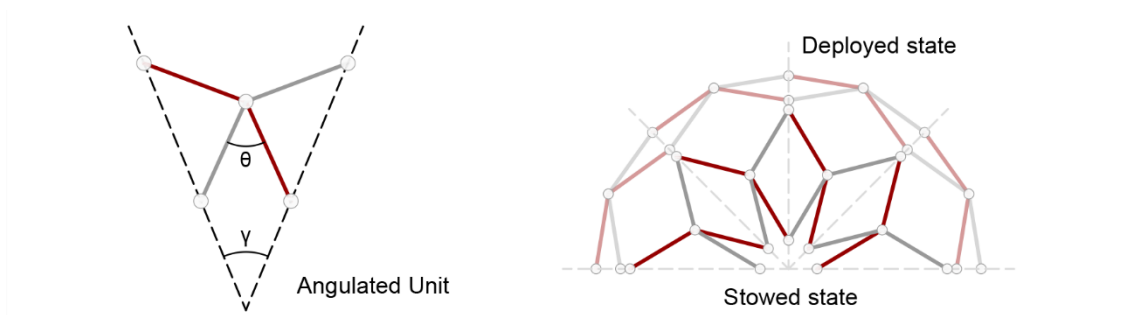
Figure 3.1.4. Deployment of angulated scissor linkage
(Source: Redrawn from De Temmerman, 2007)

Although scissor mechanisms are commonly preferred to form deployable mechanisms, they can also form transformable mechanisms. In Yar et al. (2017) angulated elements are used to generate transformable mechanisms that can take concave or convex forms (Figure 3.1.5). A detailed research on the geometric principles and design methods of scissor structures was conducted by Maden et al. (2011).
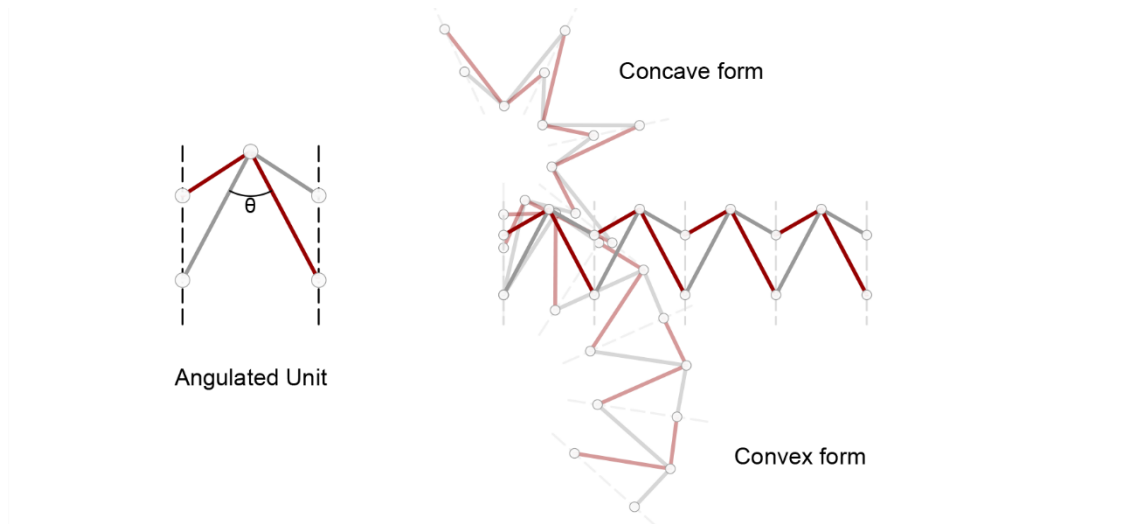
Figure 3.1.5. Transformable angulated scissor linkage

3.2. Loop Types of Planar Scissor Linkages

The simplest planar single DoF linkage consists of four bars on the same plane connected to each other at their end nodes with revolute joints forming a quadrilateral loop, also named as quadrangle or tetragon (Coxeter, 1969; Leonard et al., 2014). In Euclidian geometry the name of a quadrilateral depends on its geometric conditions such as edge lengths, inner angles and parallelism. In Figure 3.2.1 parallel edges are marked with black arrows while equal length edges are drawn with same colors and grey dashed lines refer to mirror axes. The quadrilateral names in Figure 3.2.1 are well established in the literature (for ex. see Usiskin et al., 2008).
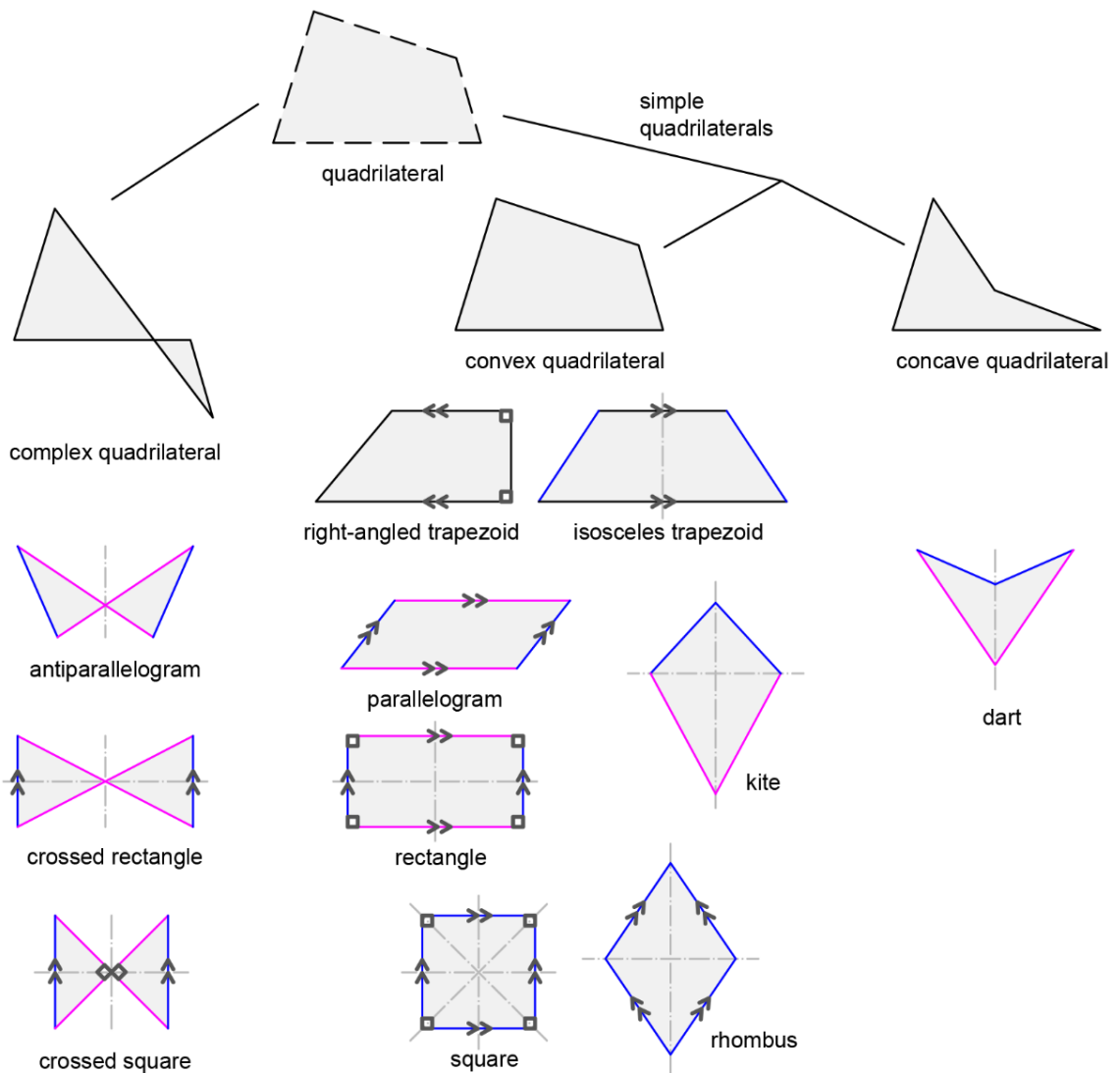
Figure 3.2.1. Quadrilateral specifications

In a linkage of plane translational units, since the bars are identical, the loop formed in between units have four equal length edges and defined as a rhombus loop. Square is a special case of a rhombus where the inner angles are all right-angles. During deployment, the inner angles change and at some point, a square loop is also formed (Figure 3.2.2).
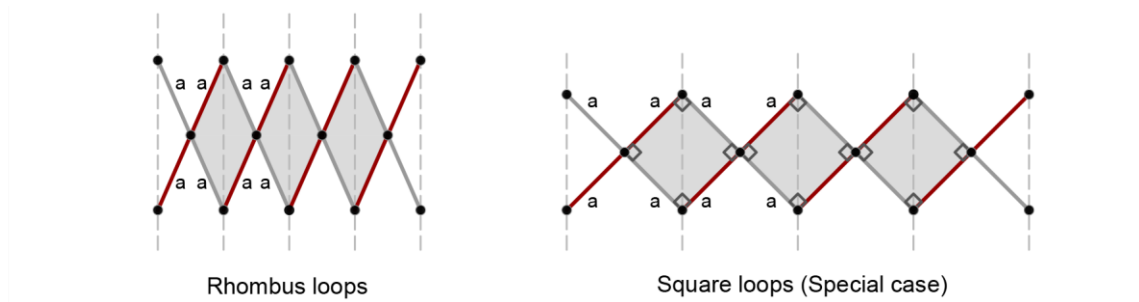
Figure 3.2.2. Loops of translational linkage composed of plane units

Using curved translational units, there are two possible deployment forms. First one is a rectilinear deployment. In this configuration same pairs of scissors are repeated to form the linkage, which has two different length bars connected at their midpoints. The loop formed has two of the short and two of the long edges. Since unit lines always stay parallel in translational scissor linkage, the parallel relation of the edges is never broken. With two pairs of parallel edges, the loop is a parallelogram or a rectangle at one point, as a special case of parallelogram (Figure 3.2.3).
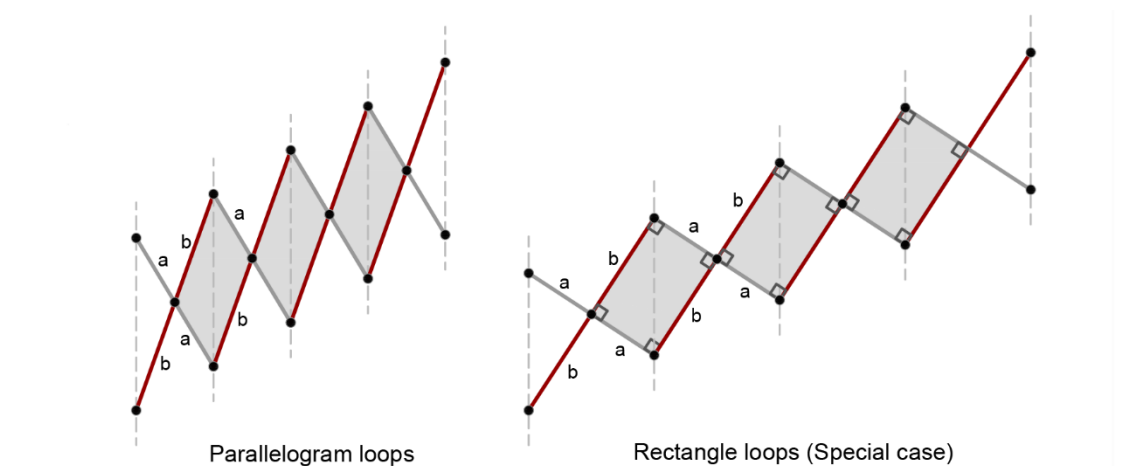
Figure 3.2.3 Curved translational linkages with parallelogram and rectangle loops

If the linkage is formed with a mirror symmetric repetition of the unit, then a loop with adjacent equal edge pairs is obtained. In this case, the loop is either a kite loop or a dart loop as a special case (Figure 3.2.4).
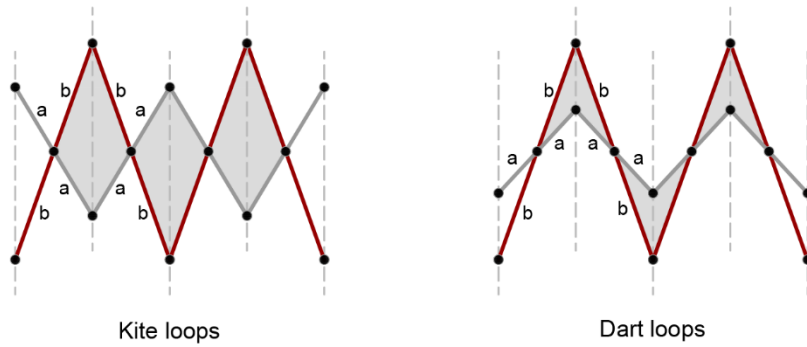
Figure 3.2.4 Curved translational linkages with kite and dart loops

When more than one variation of curved scissor units is used, the edge lengths of the loop are all different, resulting in a concave or convex quadrilateral without any special geometric conditions (Figure 3.2.5).
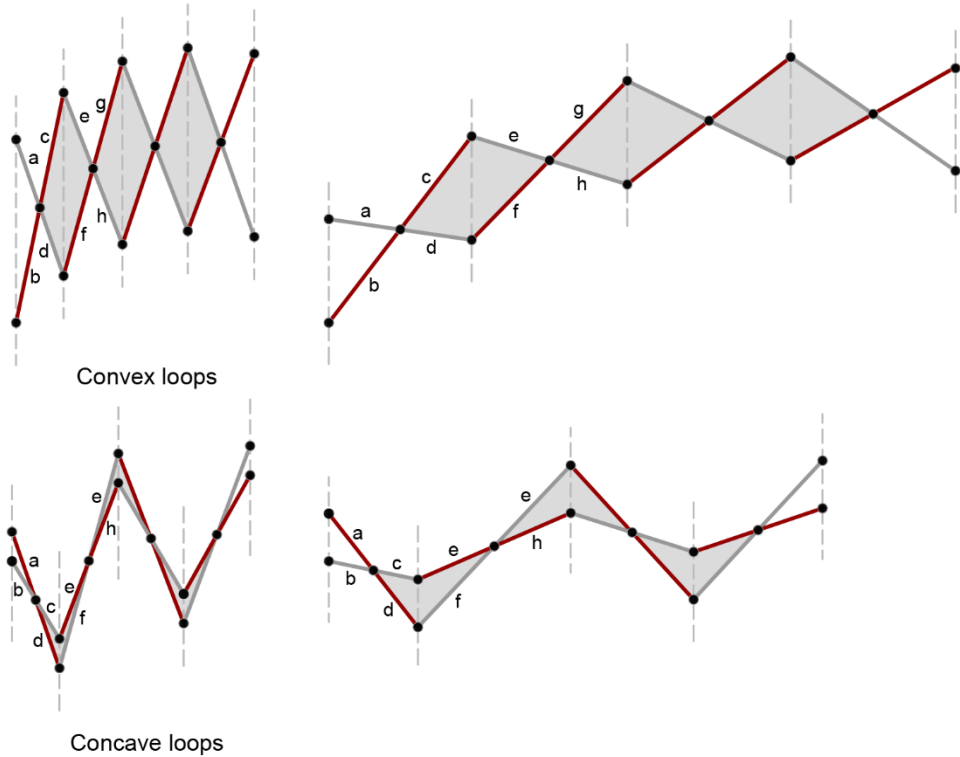
Figure 3.2.5. Curved translational linkage composed of convex and concave loops

In a polar unit since intermediate hinge is not located in the middle, two sides of a bar of a polar unit has different lengths. In one possible assembly, the loops formed in between polar units have two adjacent short and two adjacent long edges without any parallelism. The geometry of the loop is a kite (Figure 3.2.6).
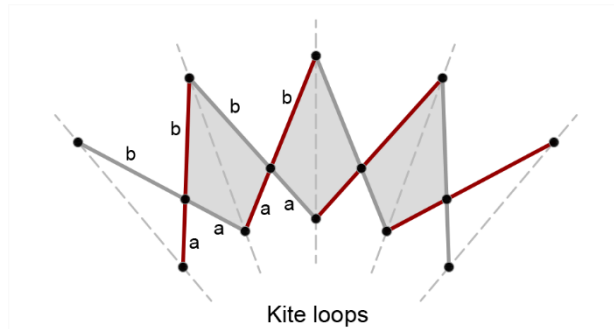
Figure 3.2.6. Polar scissor linkage with kite loops

Another possible assembly of polar scissor units is to multiply the unit with glide symmetry. This time, short side of one link connects to the long side of the next link. The loop is composed of non-adjacent short and long edges, forming a parallelogram (Figure 3.2.7).
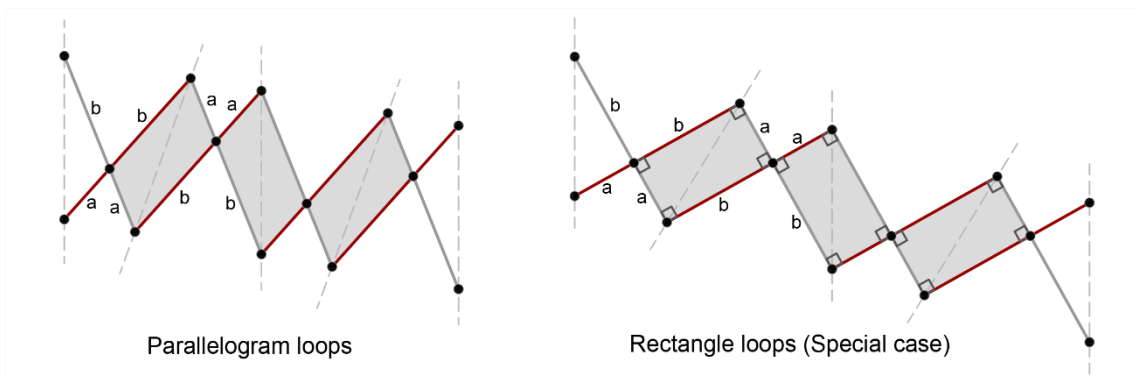
Figure 3.2.7 Polar scissor linkage with parallelogram and rectangle loops

In 1990 Hoberman introduced the angulated scissor units that are composed of angulated bars connected at their kink point. Angulated units yield a variety of loops with various arm lengths and kink angles. The general unit Hoberman identified had two identical bars. Use of such units forms rhombus loops which also take a square form momentarily during deployment (Figure 3.2.8).
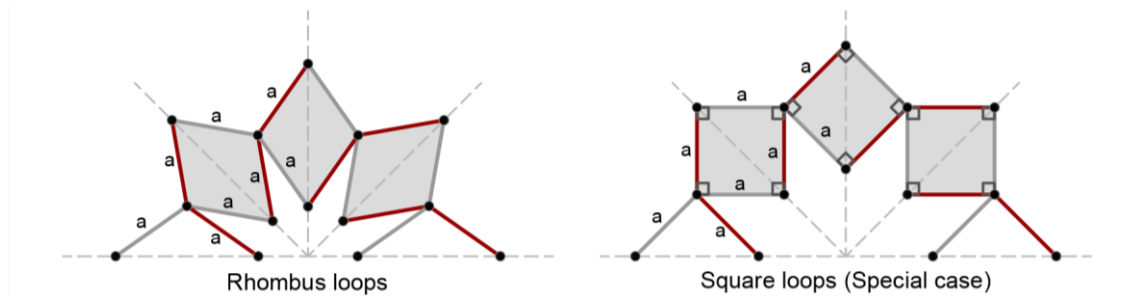
Figure 3.2.8. Angulated linkage with rhombus loops made up of Hoberman's units

You and Pellegrino's further research yielded generalized angulated elements (GAE's). The types of GAE's defined by them had different arm lengths and kink angles. Using their units, it is possible to form parallelogram and rectangle loops within a linkage (Figure 3.2.9).
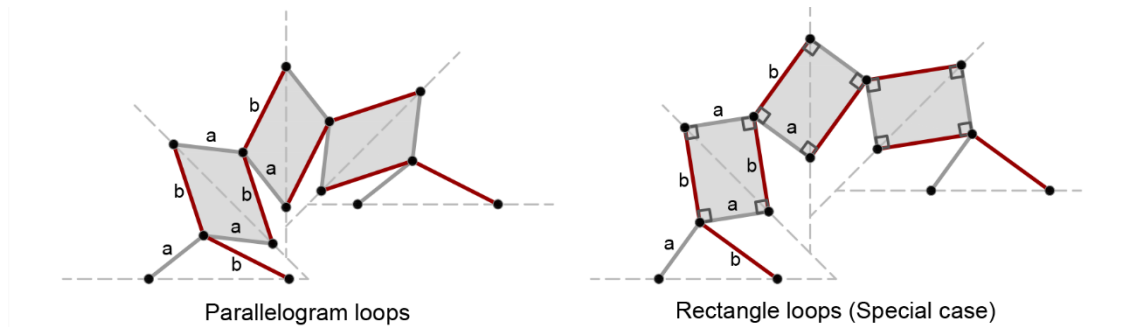
Figure 3.2.9. Angulated linkage with parallelogram loops made up of GAE's

Using GAE's it is also possible to create transformable linkages. Such a linkage is presented by Yar et al. (2017) where kite and dart loops are formed within the linkage (Figure 3.2.10).
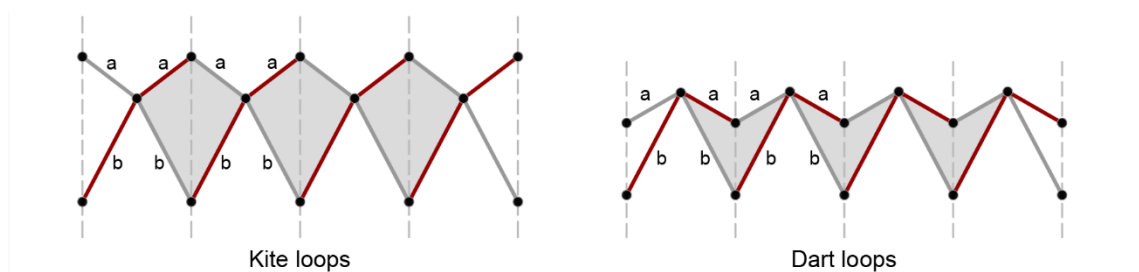
Figure 3.2.10. Angulated linkage with kite and dart loops made up of GAE's

Although many forms of concave and convex quadrilateral loops can be observed within scissor linkages, complex quadrilaterals are not specified as a loop type. In this

study, the potential of an antiparallelogram loop in the construction of single DoF deployable linkages will be explored.

3.3. Loop Assembly Method

It was Hoberman who devised a method to form the links using loops. While designing the linkage, he aligns identical rhombus loops on a curve such as a circle to derive the links (Figure 3.3.1). This way, he is able to form units with identical suspended angles. The unit lines of units intersect at the center of the circle.
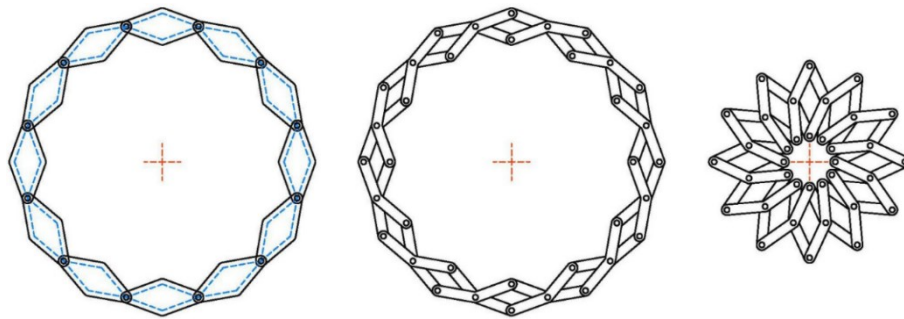
Figure 3.3.1. Assembly of rhombi loops on a circle
(Source: Hoberman et al., 2013)

The same method is also proved to be effective when used on curves with non-constant curvature such as an ellipse (Figure 3.3.2). However, in this form, adjacent unit lines intersect at various points.
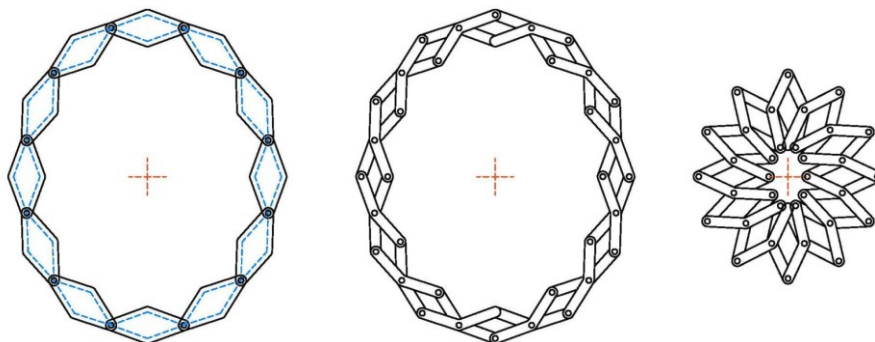
Figure 3.3.2. Assembly of rhombi loops on an ellipse
(Source: Hoberman et al., 2013)

Expanding his research, Hoberman experimented with different scales of the same rhombus loop aligned on a polygon (Figure 3.3.3) which also yielded deployable

mechanisms. In this design, every edge of the polygon is made up of one rhombus loop scaled to fit. Since each rhombus is a different size, they are not stowed equally hence the linkage cannot be stowed efficiently.
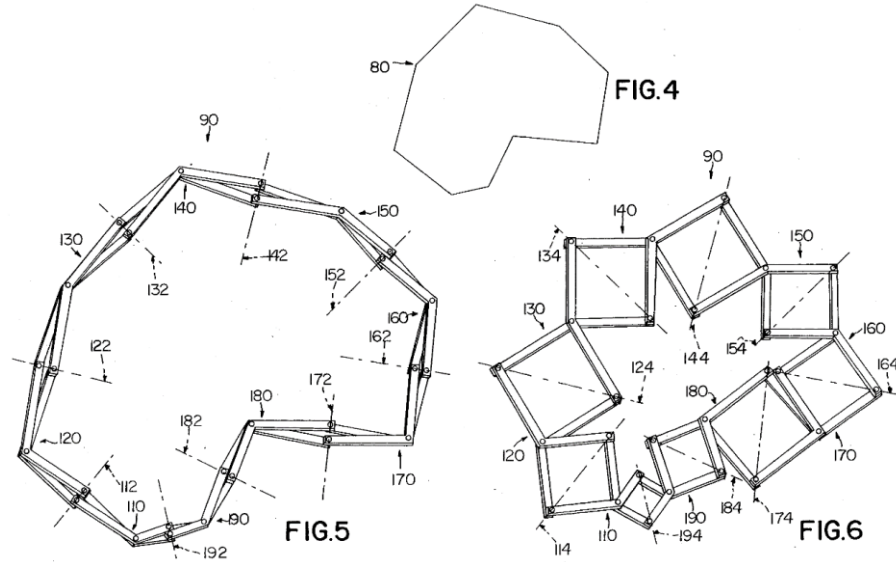
Figure 3.3.3. Drawing from Hoberman's patent
(Source: Hoberman, 1990)

Also the research conducted by Liao and Li (2005) and Kiper and Söylemez (2010) yielded similar results. Most recent research using this method is conducted by Yar et al. (2017) who used kite and dart loops to form transformable single DoF planar linkages (Figure 3.3.4). The linkages designed are able to transform from a linear form to concave and convex curves (Figure 3.1.54).
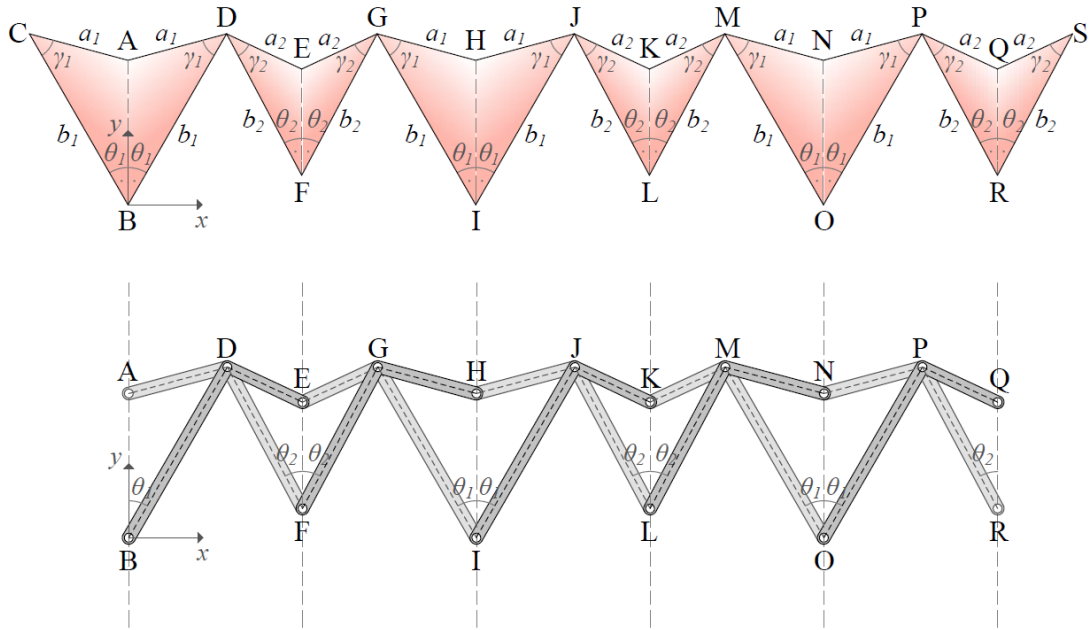
Figure 3.3.4. Dart loop assembly along a line and the resulting linkage
(Source: Yar, 2016)

3.4. Antiparallelogram Loop

In this thesis report, antiparallel loops will be used to form single DoF planar linkages.

Using the same links and connections, there can be more than one configuration to form a linkage. These are called assembly modes. A planar linkage may pass from one assembly mode to another during the motion by passing through the so-called dead-center position at which some links are aligned. In a parallelogram mechanism, there are four bars that don't cross. The linkage can be folded into a line and if the motion is continued, the opposite long bars would cross, yielding an antiparallelogram loop. An antiparallelogram, therefore, is also referred as a crossed-parallelogram or a contra-parallelogram.

The antiparallelogram has two equal nonadjacent short edges and two equal crossing long edges. A linkage forming an antiparallelogram loop has four hinges at the end points of the links but it has no hinge at the crossing point. It has single mirror-symmetry about a line passing through the cross point (Figure 3.4.1).
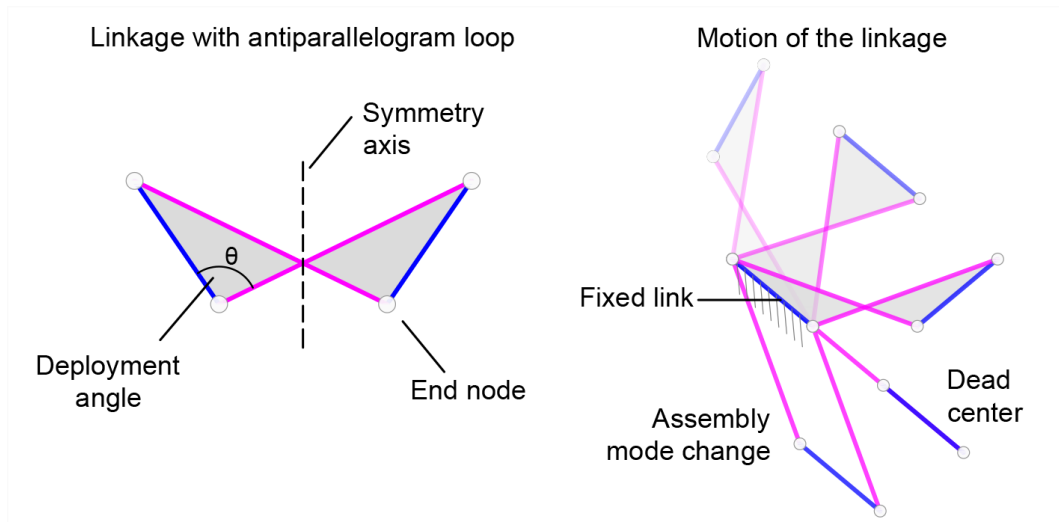
Figure 3.4.1. A linkage with an antiparallelogram loop and its motion

While examining the geometry of an antiparallelogram, drawing guide lines, s1 and s2 (Figure 3.4.2), connecting the upper and lower two corners would contribute understanding the geometry. The symmetry axis of the form passes through the midpoints of s1 to s2 (P and R respectively), passing through the crossing point (Q). This axis is also perpendicular to s1 and s2 lines. Then four sets of equal edges are obtained, which are $\overline{AB} = \overline{CD}$, $\overline{AD} = \overline{BC}$ as conditions to form an antiparallelogram and $\overline{BQ} = \overline{CQ}$, $\overline{AQ} = \overline{DQ}$ as the result of symmetry on both sides of the cross point. Since ABQ and CDQ are identical triangles their inner angles are also same.

Figure 3.4.2. Geometrical analysis of an antiparallelogram

$\overline{AB}$ edge is chosen as fixed link and $\widehat{DAB}$ is the deployment angle named as θ. Let $\widehat{CAD}$ angle be α. Since AQC is an isosceles triangle, $\widehat{AQB}$ is 2α. Within AQC triangle, inner angles of A and Q are θ and 2α, respectively, leaving the $\widehat{ABQ}$ angle $\pi - 2\alpha - \theta$. Since s1 and s2 lines are parallel, $\widehat{ABQ} = \widehat{QBD} = \alpha$. Z is the point where the extensions of AB and CD edges intersect with the symmetry axis. At point B, following counterclockwise, two angles are defined as $\pi - 2\alpha - \theta$ and α, that results as $\widehat{PBZ} = \theta + \alpha$. Within BPZ triangle, two angles are known, B and P angles: $\theta + \alpha$ and $\pi/2$ respectively. Therefore it is known that $\widehat{BZP} = \pi/2 - \theta - \alpha$. If edge $\overline{AB}$ is chosen to be perpendicular to the horizontal axis, then it can be seen that the angle between the horizontal axis and s2 is also $\pi/2 - \theta - \alpha$. During the motion, at one point, $\overline{AB}$ and $\overline{CD}$ edges become perpendicular and there is no intersection point Z available at that time. Depending on the value of θ the intersection point can be achieved on the other side of the mechanism.

CHAPTER 4

SYMMETRY OPERATIONS

4.1. Frieze Groups

In a scissor linkage, loops or units are multiplied to form a chain. The most basic way of doing that is to repeat the unit/loop many times one after another by translating it. In geometry, there are defined methods of multiplying a form, commonly named as symmetry operations and the resulting array of forms is a pattern. Although symmetries in a 2D plane may consist of multiplications on more than one direction, such as wallpaper groups, the aim of forming a curve-like linkage restricts the options with those that are multiplied in one direction only. This restriction led the research to Frieze groups (Pólya, 1924). In architecture 'frieze' means "The part of an entablature between the architrave and the cornice" (Dictionary, 2007). In mathematics, a pattern that repeats regularly in one direction on 2D plane, hence has a translational symmetry, is called a *Frieze pattern* (Guy and Woodrow, 1994). A frieze pattern may have more than just translational symmetry. There are four main symmetry operations that can be conducted on a 2D plane. These are translation, rotation and reflection and glide-reflection (Figure 4.1.1).
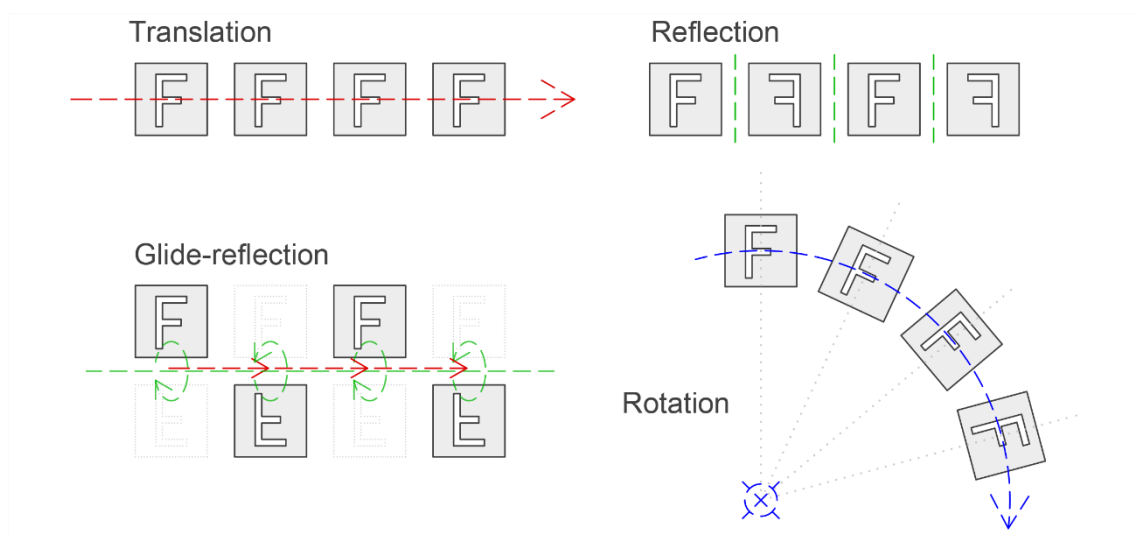
Figure 4.1.1. Basic array operations

All other operations are generated combining these four, even multiple times over (Singh, 2015). There are 7 array types defined under Frieze symmetry groups (Figure 4.1.12).
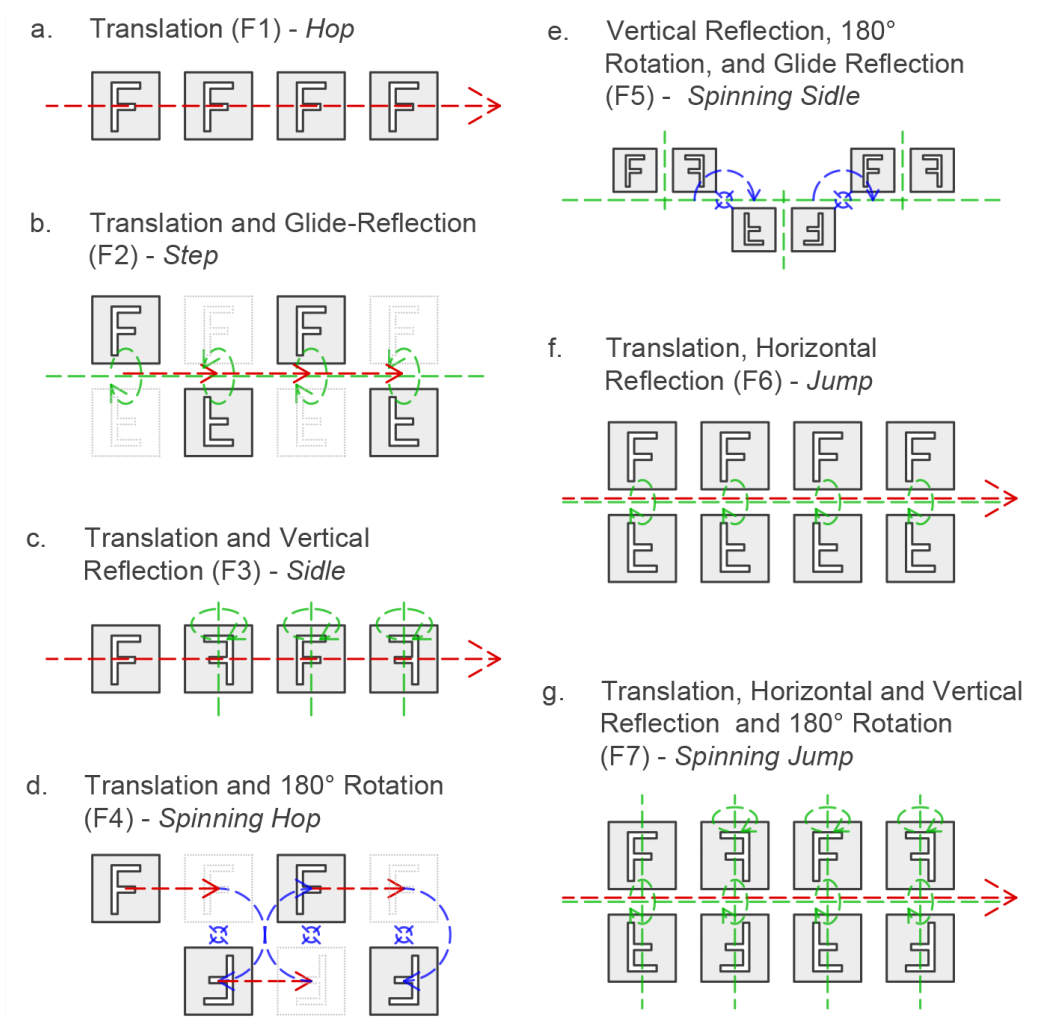
Figure 4.1.2. Frieze symmetry groups
(Source: Redrawn from Glassner, 1996)

In the previous loop assembly studies, researchers have offered ways of multiplying the loops and examined the potentials of the resulting linkage. However, rhombus, square and rectangle loops with doubly-symmetrical forms do not yield much variety. If a rhombus loop is multiplied along one of the diagonals using Frieze groups, all end up being the same pattern. Also the kite and parallelogram loops possess more symmetries compared to antiparallelogram loops. This being so, a methodology to multiply the loops was not offered in previous studies. An antiparallelogram has a single symmetry axis and due to its rather complex form, the array operations yield various connections, therefore a method was needed to classify them.

When designing polar linkages, loops or units are polar arrayed (Figure 3.2.6.) They are repeated while rotating around a point, which means they are aligned on a circular arc. Also rhombuses are multiplied in a rotational array around a point in Figure 3.3.1. When the loops are aligned on a non-constant curvature curve, such as an ellipse (Figure 3.3.2), it is also a rotational array since each loop can be achieved by rotating the previous one at one point on a plane but not necessarily using a common point for all the loops. These array patterns along a curve can again be obtained by using Frieze groups (Figure 4.1.3).

a. Rotation (F1) - *Hop*

b. Rotation and Glide-Reflection (F2) - *Step*

c. Rotation and Vertical Reflection (F3) - *Sidle*

d. Rotation and 180° Rotation (F4) - *Spinning Hop*

e. Rotation, Vertical Reflection, 180° Rotation and Glide Reflection (F5) - *Spinning Sidle*

f. Rotation and Horizontal Reflection (F6) - *Jump*

g. Translation, Horizontal and Vertical Reflection and 180° Rotation (F7) - *Spinning Jump*
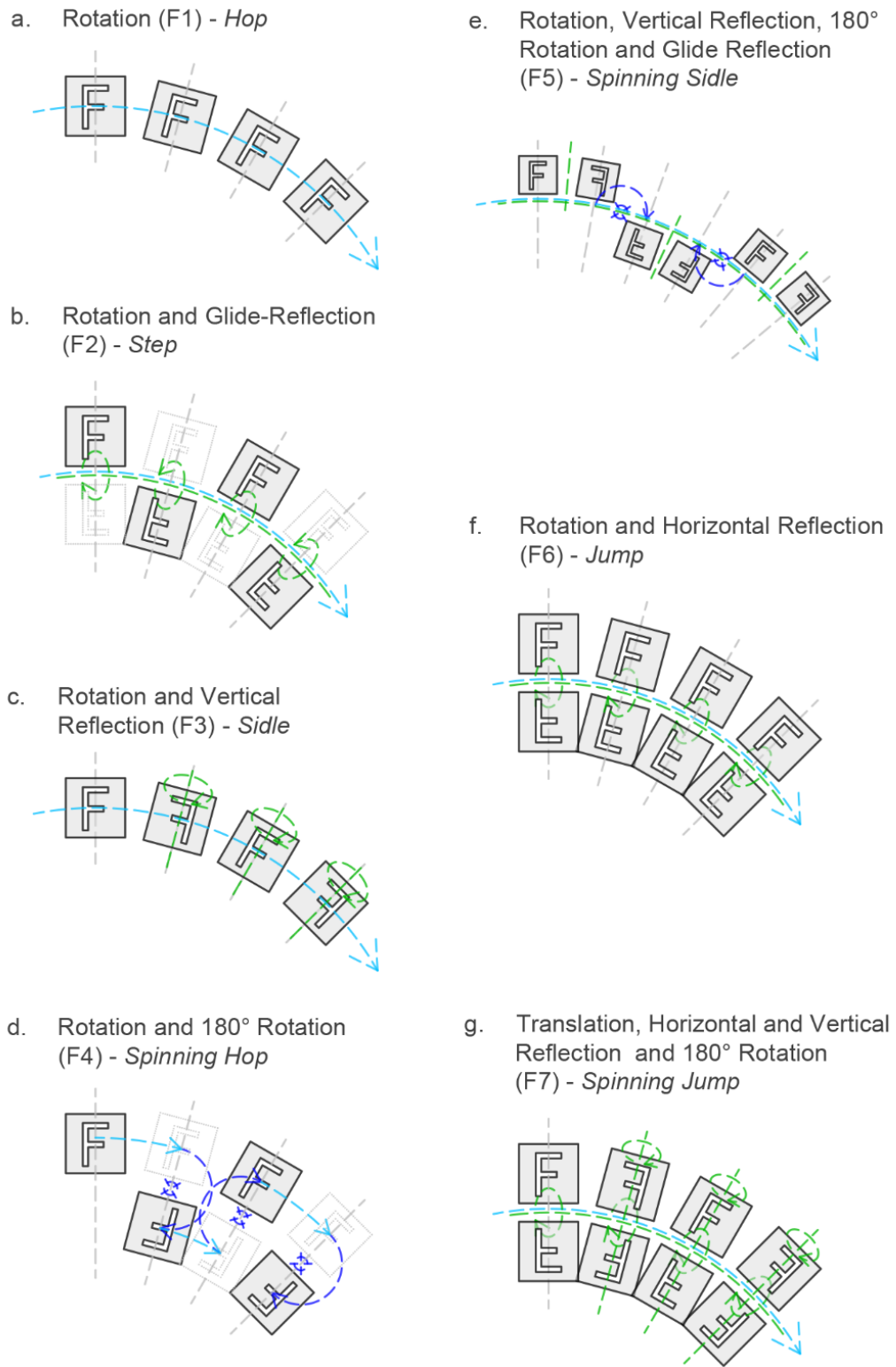
Figure 4.1.3. Frieze groups on a curve

4.2. Symmetry Operations of Antiparallelogram Loop

The antiparallelogram is a shape with a single mirror symmetry axis, therefore reflection of it about an axis parallel to the symmetry axis is the same. The crossed-rectangle is a special case of antiparallelogram with two symmetry axes, which makes reflections about vertical or horizontal axes result in the same shape as itself (Figure 4.2.1).
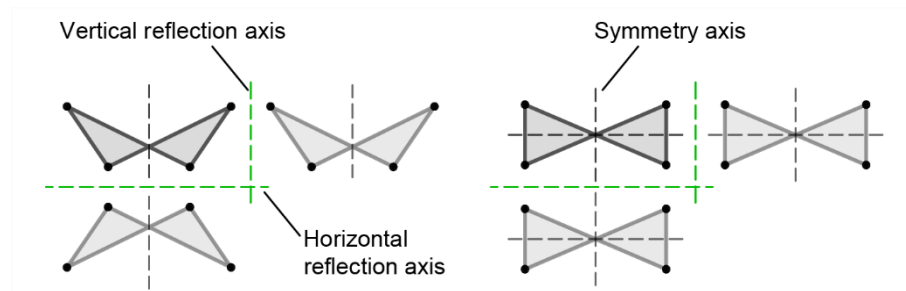
Figure 4.2.1. Reflections of antiparallelogram and cross-rectangle

An antiparallelogram has four corners which also represents joints of a linkage with such a loop. When the loop is multiplied, they are attached at these points. Depending on the direction of translation it is possible to formulate alternative arrays for each Frieze group operation. In the figure below, there are three alternatives for the *Hop* group; using horizontal, vertical and diagonal translations (Figure 4.2.2). However, a vertical array is not applicable since the loops cannot be connected at their corners.
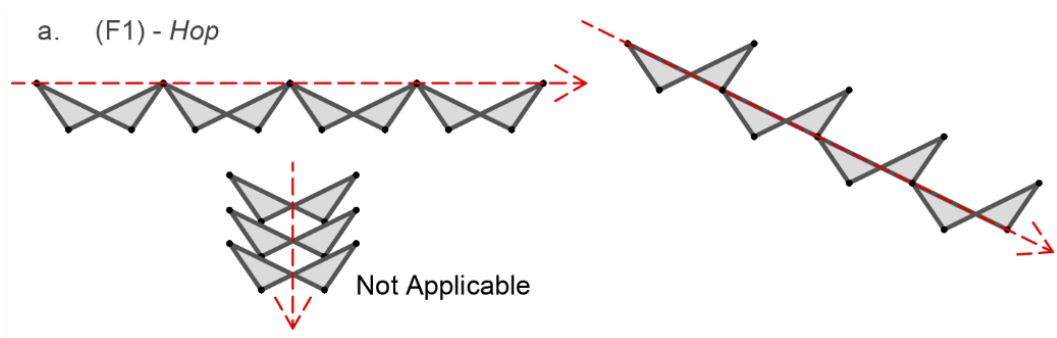
Figure 4.2.2. Hop group arrays of antiparallelogram

When a cross-rectangle, a special case of antiparallelogram, is used for array operations, Hop operation yields different possibilities (Figure 4.2.3). Its perpendicular edges make it possible to connect two corners at the same time, meaning they can share

and edge. In addition, a vertical multiplication becomes possible. Due to the double-symmetry mentioned above, it also happens that *Hop* and *Sidle* group operations yield same results.
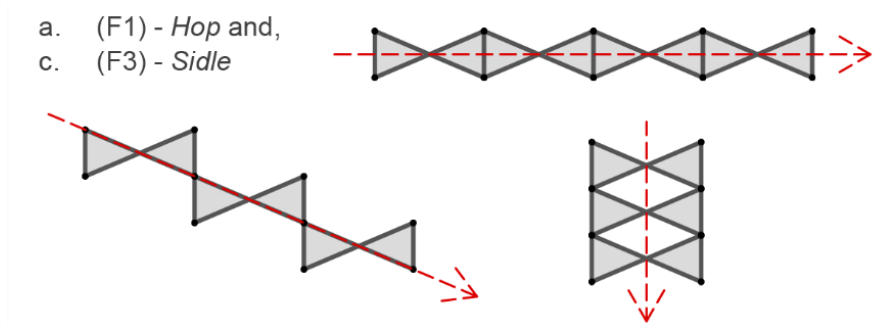
Figure 4.2.3. Hop and Sidle group arrays of cross-rectangle

On the other hand, arrays produced with *Sidle* group operations are not the same with *Hop* group for the general antiparallelogram, except for the one marked with dotted lines (Figure 4.2.4). The one with dotted lines has a reflection axis parallel to the symmetry axis of the shape, making it same as the corresponding *Hop* array.
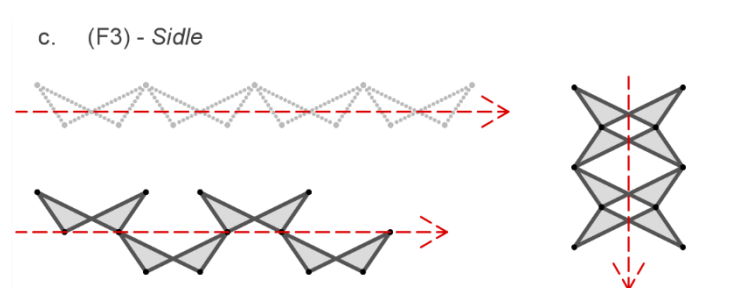
Figure 4.2.4. Sidle group arrays of antiparallelogram

Two other Frieze groups are *Step* and *Spinning Hop* groups. These two arrays when constructed with cross-rectangle loops, they end up being the same (Figure 4.2.5). There are two alternatives; horizontal or vertical directions.

b.   (F2) - *Step* and,
d.   (F4) - *Spinning Hop*
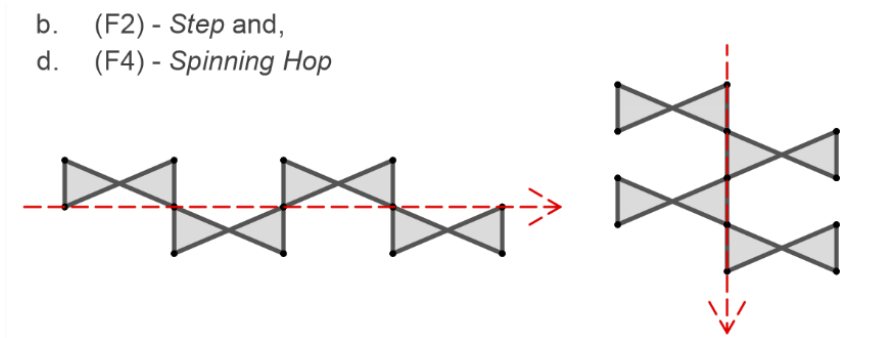
Figure 4.2.5. Step and Spinning Hop group arrays of cross-rectangle

Once again, the results of these groups are not the same for antiparallelogram loops, except for two (Figure 4.2.6).

b.   (F2) - *Step*
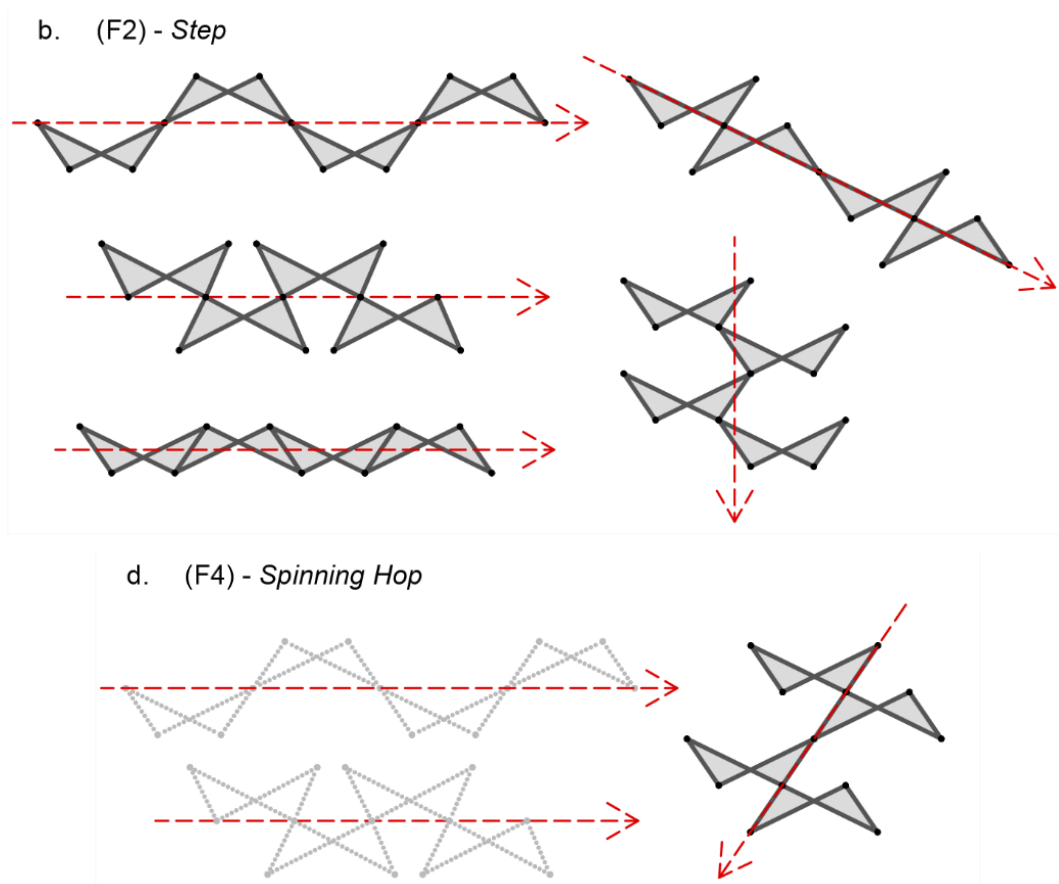
d.   (F4) - *Spinning Hop*

Figure 4.2.6. Step and Spinning Hop group arrays of antiparallelogram

When cross-rectangle loops are multiplied using *Spinning Sidle* group (Figure 4.2.7), the result does not reflect the mirror and rotation operations of the group. Due to the double symmetry of the loop, the resulting array is rather perceived as a double repetition of the loop in an over and under fashion. Whereas, when antiparallelograms are

used, one less symmetry of the form lets the mirror operation to be perceived (Figure 4.2.8).
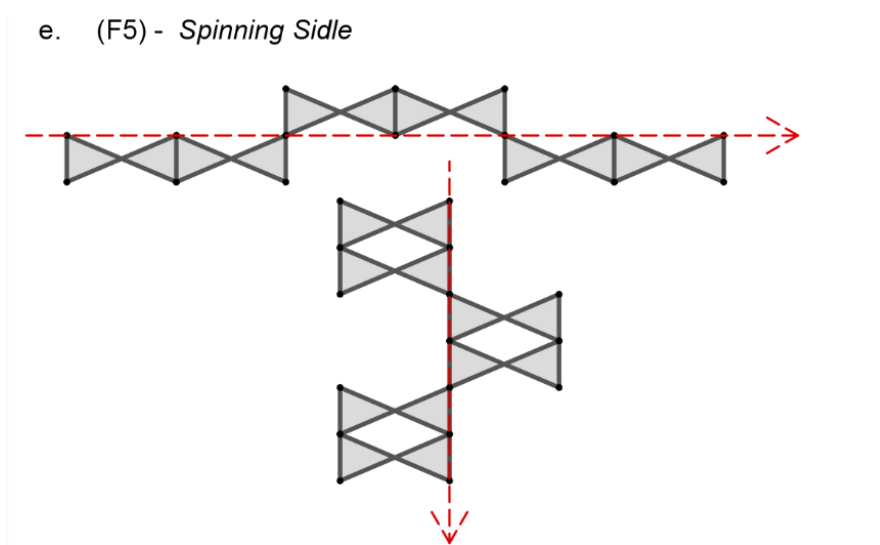
e. (F5) - *Spinning Sidle*

Figure 4.2.7 Spinning Sidle group array of cross-rectangle
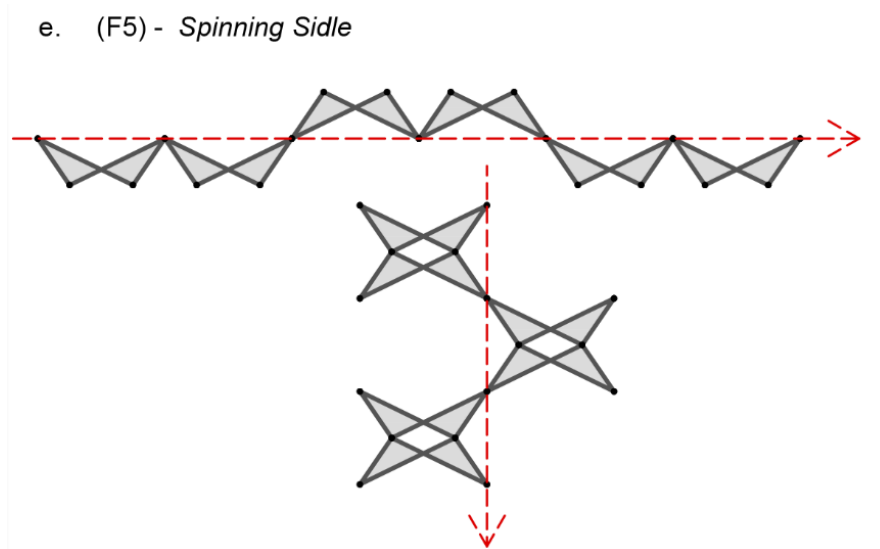
e. (F5) - *Spinning Sidle*

Figure 4.2.8 Spinning Sidle group array of antiparallelogram

Although Frieze groups consist of seven types, in this study five of the variations are examined and two are eliminated. The reason is, in Figure 4.1.2 f and g groups are made of two rows of items, which in this case would translate as two connected parallel linkages. Such a formation is not aimed in this study.

As mentioned before there are also rotational arrays already used in the literature, Hoberman's rhombus assembly on a circle being one of them. Using the Frieze groups along a curve gave rise to new array options. Translation operations within each Frieze

operation is switched with a rotation, which is the center of a curve the loops array along. Using only this rotation, we get *Hop* group along a curve. Once again, while the results of Hop and Sidle groups are the same for cross-rectangle loops (Figure 4.2.9), they differ for antiparallelogram ones except for one that is shown with dotted lines (Figure 4.2.10, Figure 4.2.11).
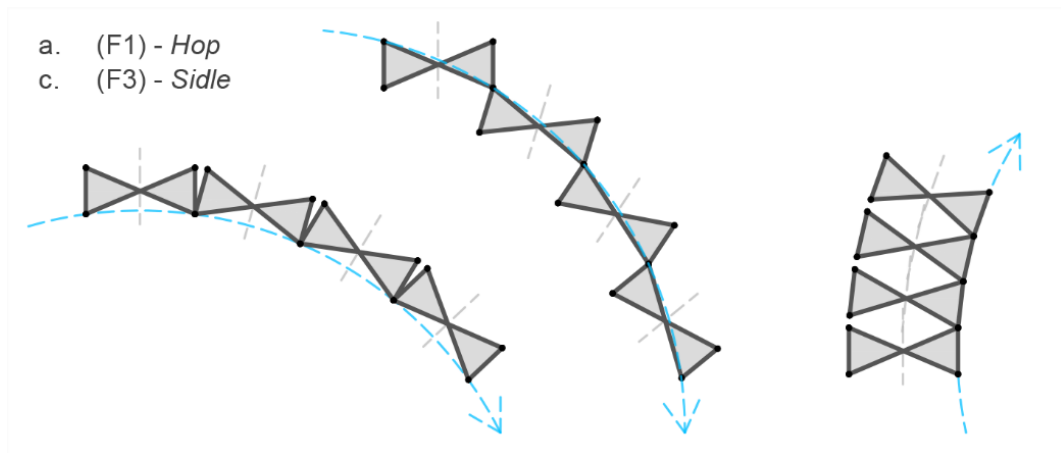
Figure 4.2.9. Curved Hop and Sidle group arrays of cross-rectangle
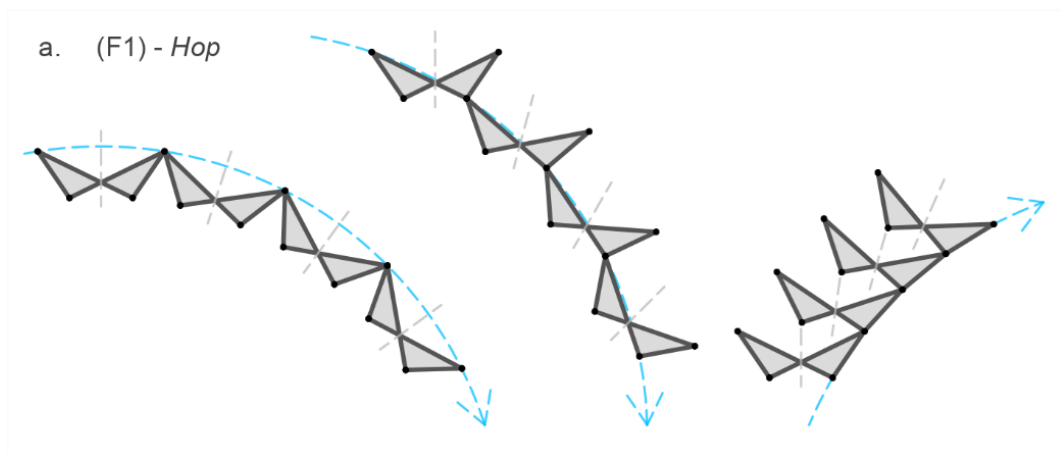
Figure 4.2.10. Curved Hop group arrays of antiparallelogram
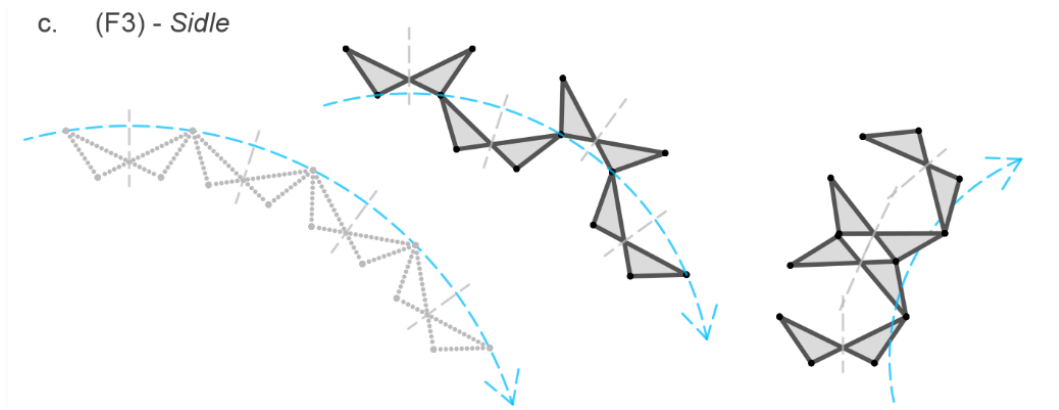
Figure 4.2.11. Curved Sidle group arrays of antiparallelogram

When *Step* and *Spinning Hop* groups applied along a curve, it is seen that a cross-rectangle yield only two options, same for both (Figure 4.2.12). However, an antiparallelogram loop can be arrayed in four ways to form *Step* group (Figure 4.2.13) and one more for *Spinning Hop* group together with the common one shown with dotted lines (Figure 4.2.14).
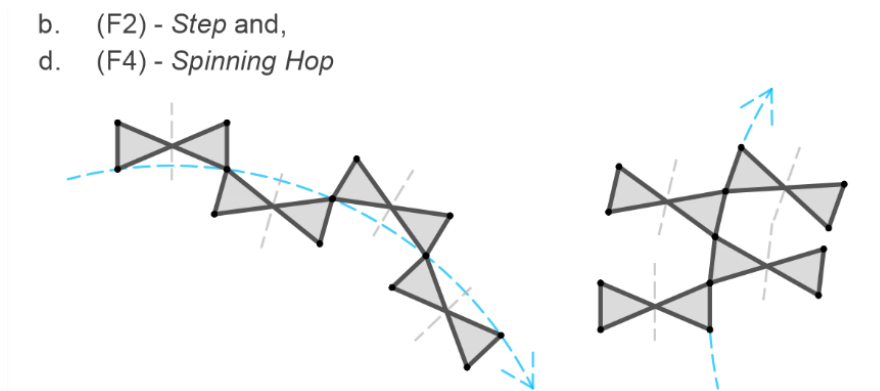
Figure 4.2.12. Curved Step and Spinning Hop group arrays of cross-rectangle

b.   (F2) - *Step*
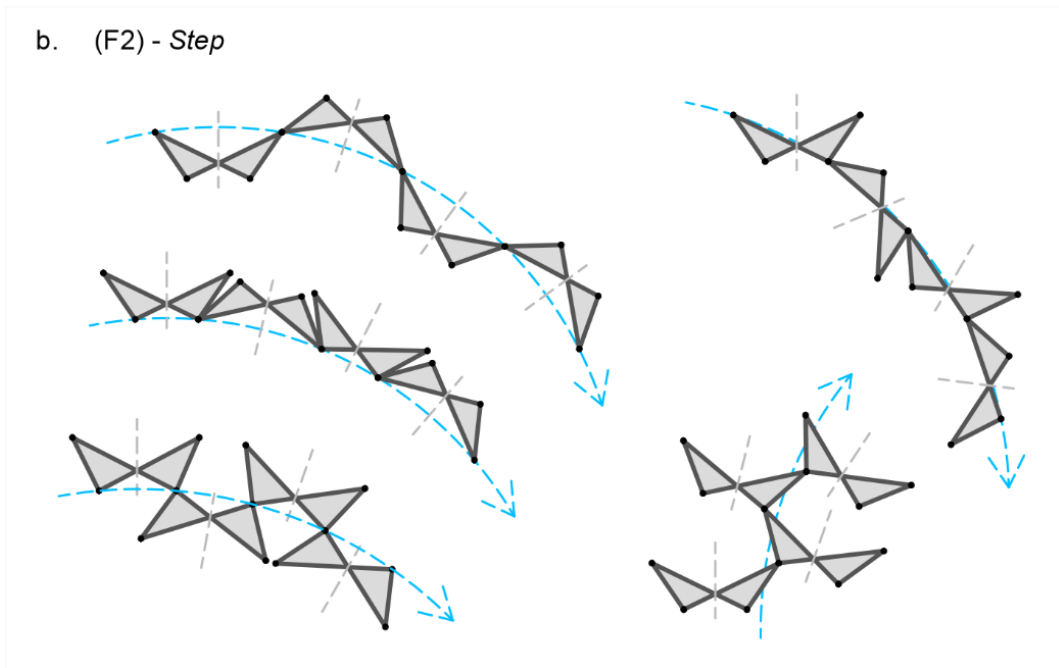
Figure 4.2.13. Curved Step group arrays of antiparallelogram
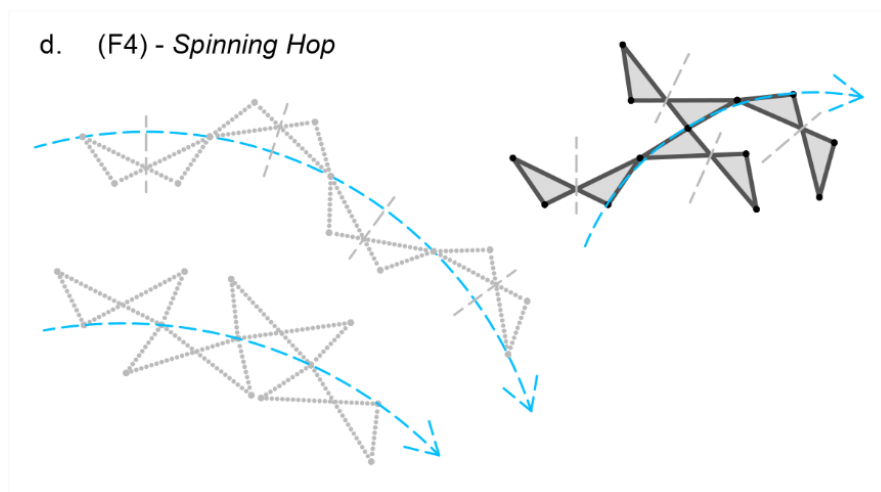
d.   (F4) - *Spinning Hop*

Figure 4.2.14. Curved Spinning Hop group arrays of antiparallelogram

When *Spinning Sidle* group is applied, for both cross-rectangle (Figure 4.2.15) and antiparallelogram (Figure 4.2.16) two options can be formed. In order to see all variations as a whole, an outline is given in Figure 4.2.17 and Figure 4.2.18.
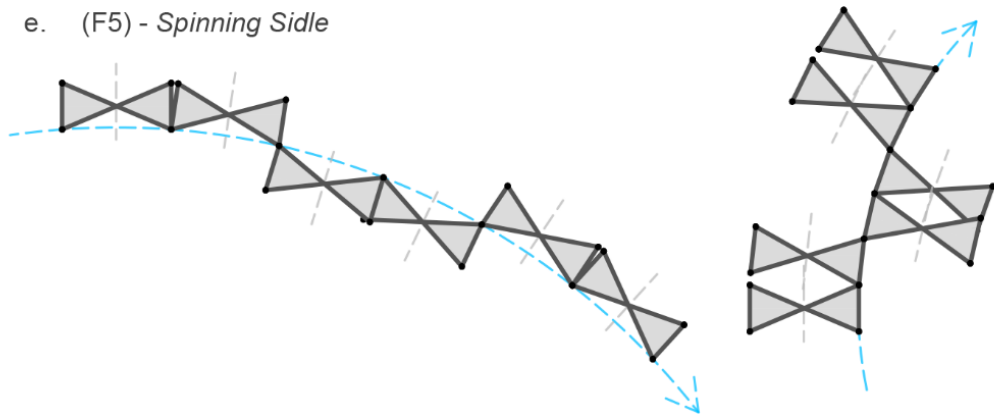
Figure 4.2.15 Curved Spinning Sidle group array of cross-rectangle
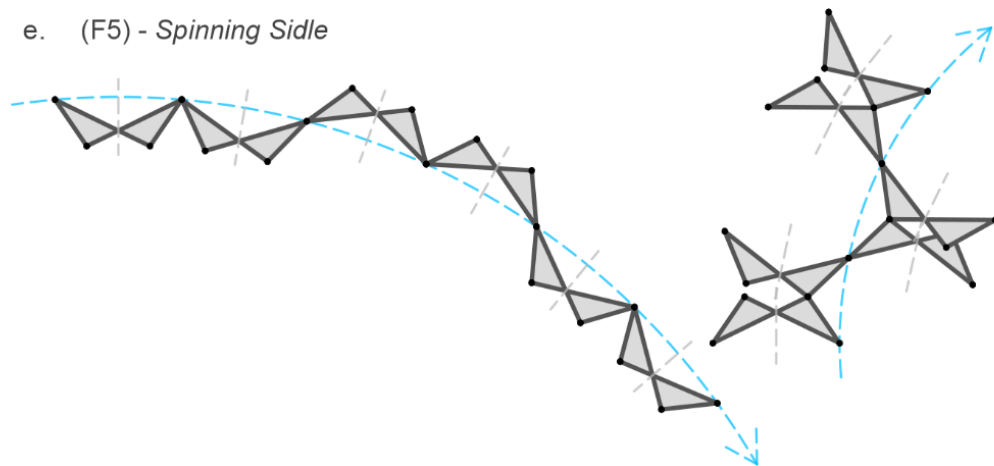
Figure 4.2.16 Curved Spinning Sidle group array of antiparallelogram

Figure 4.2.17 Outline of array alternatives according to Frieze groups

Figure 4.2.18 Outline of array alternatives with rotations

4.3. Linkage Formation from Loop Arrays

Once the arrays are formed, the next step to form the linkages is to draw the links following the edges of the loops. In order to form single degree-of-freedom linkages, there should be at least two common links between the loops. Therefore, at each connection, two edges from each loop should be considered as a single link common to both as shown in Figure 4.3.1.
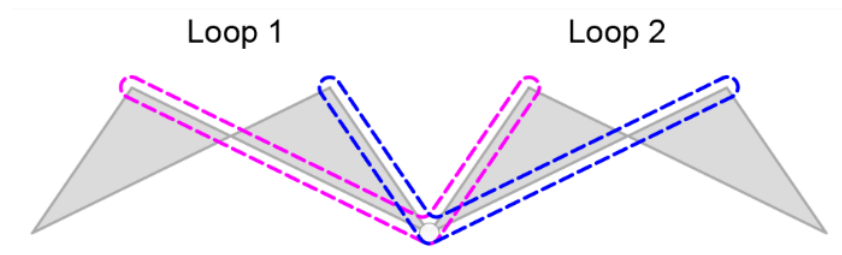
Figure 4.3.1 Common link formation

Since there are only two edges meeting at each corner, it is possible to conclude that, there are only two ways of forming the links. A rotational array example is given in Figure 4.3.2 and the possible links that can be formed for this array are shown in Figure 4.3.3.
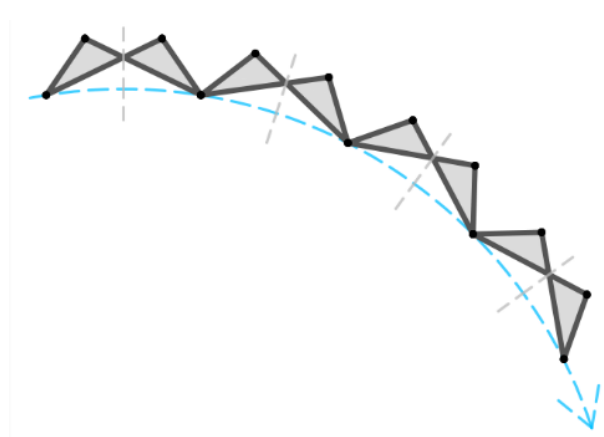
Figure 4.3.2. A rotational array

Even though the common links seem to be the only source of alternative link forms, they are not. One other factor adding to variation is the rotation angle of the loops in the array. In Figure 4.3.2 none of the loop edges are collinear, but it is possible to array the so that some edges become collinear.
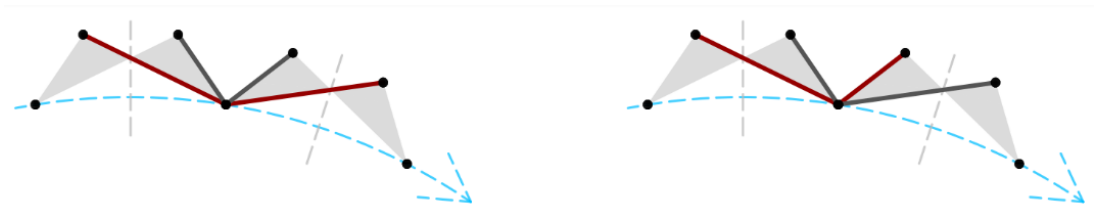
Figure 4.3.3. Link form alternatives for given array

In Figure 4.3.4 there are three more alternatives of the same array. The only difference is the curvature of the curve. These arrays make it possible to form linear links, therefore, yield linkages with different motion capabilities. A point to mention is that even these still have secondary options due to the choice of common links as mentioned at the beginning. There were over a hundred linkages that could be determined in total. All of them were drawn in Solidworks®, simulated and their motions were observed.
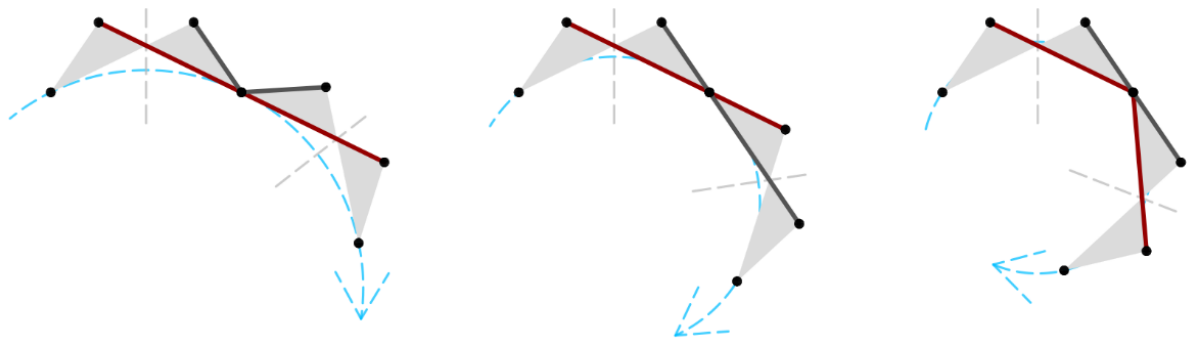
Figure 4.3.4 Link form alternatives due to array angle

CHAPTER 5

ANALYSIS OF SELECTED LINKAGES

When all array types and possible linkages formed with them are examined, five linkages stood out due to their motion and link types. In this chapter, the five novel linkages are examined in detail.

5.1. Linkage 1

The array in Figure 5.1.1 is formed using the *Step* Frieze group. It consists of cross-rectangles which are repeated along a line in one-over, one-under formation. The loops are connected along their long side. Since there are no rotations, the only factor to form link variations is the choice of the common ones.
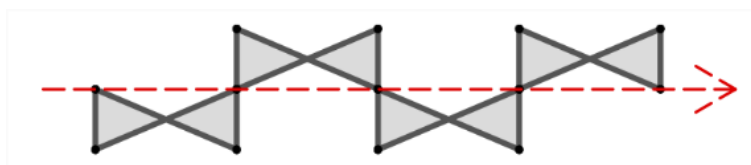
Figure 5.1.1. Array type of the linkage-1

In Figure 5.1.2a one long edge is connected to one short edge of the adjacent loop, the links formed are identical angulated ternary links. On the other hand, in Figure 5.1.2b short edges are connected to short, and long edges are connected to long ones. In this alternative, since edges are collinear, the links formed are straight bars. When their motions are observed, it is seen that linkage with angulated links was able to transform from straight to concave and convex forms, while the one with straight bars was able only to lengthen and shorten in a linear form during rotation. To understand the motion of the linkage with angulated links a geometrical analysis is done.
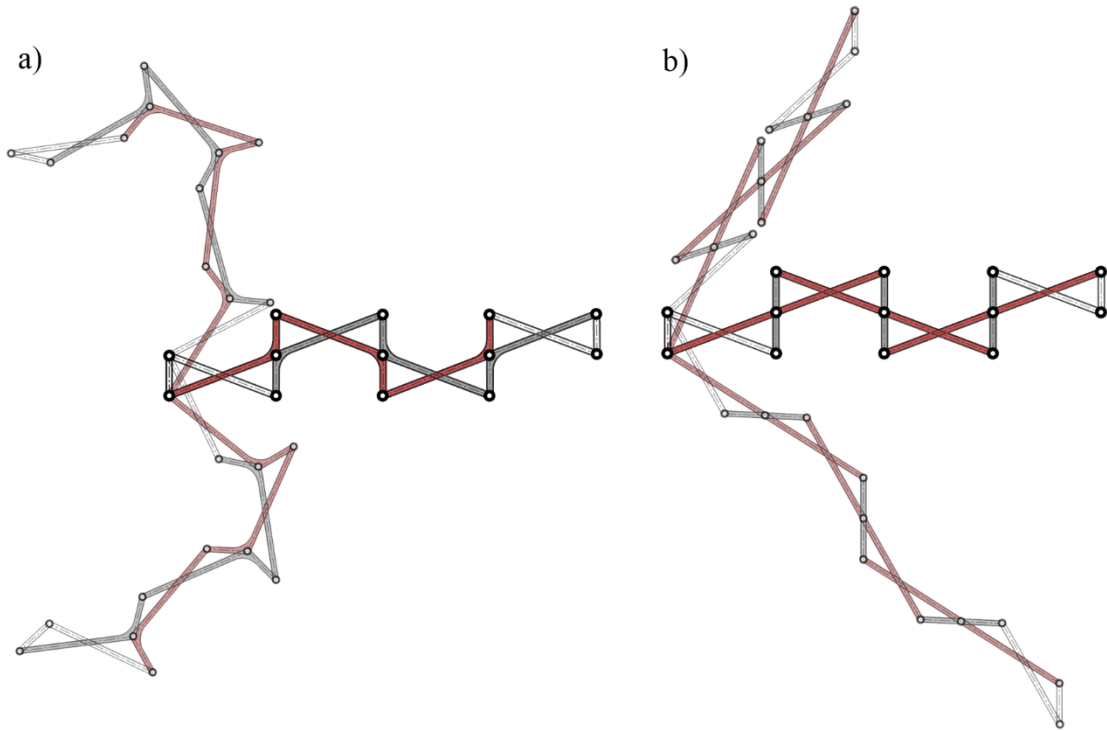
Figure 5.1.2. Linkage alternatives of the array and their motion

Since the relation of the two adjacent loops come from the array typology, it is essential to see the relations at the start position (Figure 5.1.3). ABCD and DEFG are cross-rectangles; Short edges are $\overline{AB} = \overline{CD} = \overline{DE} = \overline{FG} =$ a, they are all perpendicular to horizontal axis and parallel to each other. Long edges are $\overline{BC} = \overline{AD} = \overline{DF} = \overline{EG} =$ b. Since a cross-rectangle is a doubly symmetric form all the inner angles at the corners are the same, α. In addition, the inner angles at crossing point are also equal, $\pi - 2\alpha$. The links are formed by connecting a long edge and a short edge from each loop. Therefore, the kink angle of the links is, $\widehat{ADE} = \widehat{CDF} = \pi - \alpha$. When the link AB is chosen as the fixed link, ADE link is rotated to reconfigure the linkage. The amount the ADE link is rotated is noted as the rotation angle and named as θ.
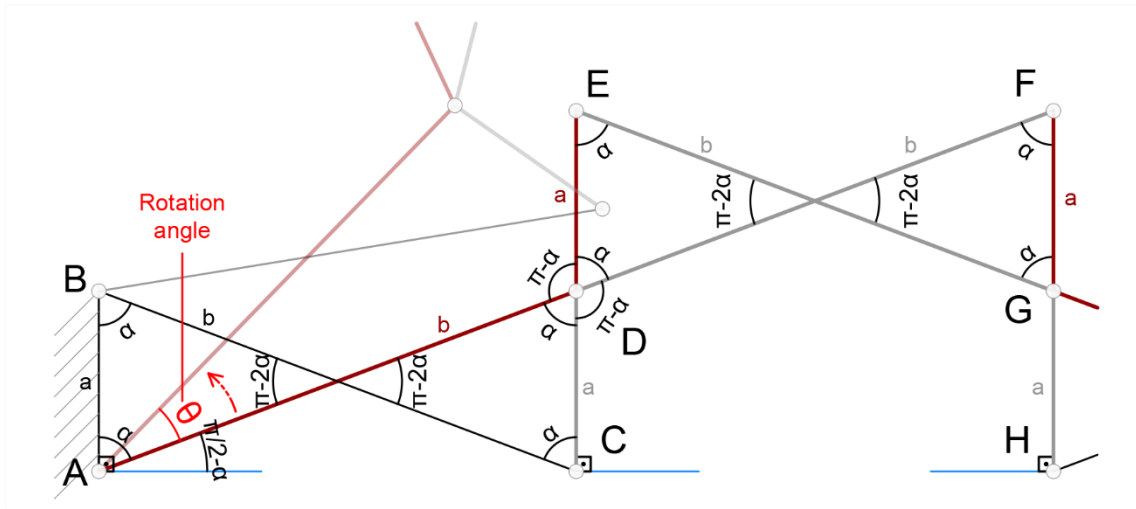
Figure 5.1.3. Geometry analysis at start position of the linkage-1

When the linkage is deployed by rotating ADE link counterclockwise by θ, the whole linkage is also curved counterclockwise. In the new configuration, the loops are now regular antiparallelograms. When an antiparallelogram's upper and lower corners are connected (as shown with blue dashed lines in Figure 5.1.4) they are parallel to each other. The line passing through the midpoint of these dashed lines is the symmetry axis which is perpendicular to them. Also when the short edges are extended to intersect, this intersection point is (W, X, Y points in Figure 5.1.4) on the symmetry axis.

The curve defined by the linkage is a circle which B, D, G and J points are located on. To prove that, method of finding the center of a circle should be considered. To locate the center of a given circle, two chords and their perpendiculars passing from the midpoint of the chord is drawn. The point where perpendiculars of the chords intersect gives the center of the circle. In order to prove that the points B, D, G and J are on a circle, one must trace back the steps of finding the center of a circle. There are two imaginary lines $\overline{BD}$ and $\overline{DG}$ which have perpendicular symmetry axis passing from their midpoints. Therefore the intersection point of these axes is the center point of the circle (point Z). Since D is a common point, they are unavoidably on the same circle. If we consider $\overline{DG}$ and $\overline{GJ}$ lines, same reasoning apply to them, too. Hence B, D, G, J and so on are on the same circle. The length of the all line segments drawn to these points from the center is the radius. Since each antiparallelogram is symmetrical, the angles on either side of the symmetry axis are equal.
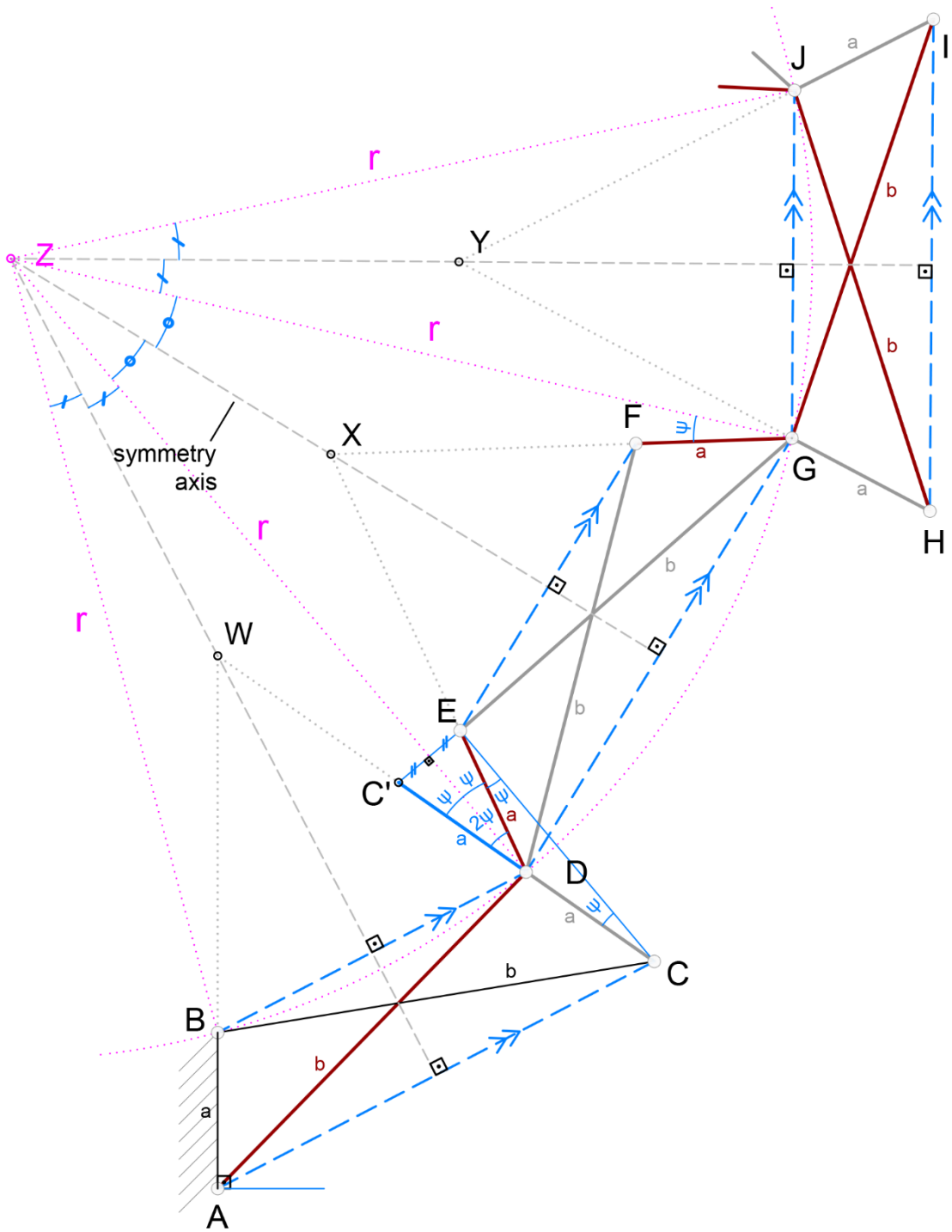
Figure 5.1.4. Geometric specifications of the linkage-1

One other point about the linkage is that $\widehat{WDZ} = \widehat{EDZ}$. To observe this relation, first imaginary line $\overline{CE}$ should be drawn. Since $\overline{DC} = \overline{DE} = $ a, then $\widehat{DCE} = \widehat{DEC} = \psi$. If an edge of length a was drawn on $\overline{WD}$ (the extension of $\overline{CD}$), then it would make an isosceles triangle with $\widehat{C'DE} = 2\psi$. If the bisector of the $\widehat{C'DE}$ is drawn it is perpendicular to $\overline{C'E}$. Following the same logic of finding the center of the circle, C', E and F are proven

to be on a circle aith center at Z. Since $\widehat{EDZ}$ is symmetric to $\widehat{FGZ}$, the bisector of $\widehat{C'DE}$ passes through the point Z, the center of the linkage.

When the linkage is deployed by rotating ADE link by θ degrees, in the new configuration as seen in Figure 5.1.5, $\widehat{BAD} = \alpha - \theta$. Using the edges $\overline{AB} =$ a and $\overline{AD} =$ b together with $\widehat{BAD} = \alpha - \theta$, it is possible to determine the edge length of s1. Again with cosine theorem using s1 length, $\overline{AB}$ and $\overline{AD}$, $\widehat{BDA}$ angle can be found. Let $\widehat{BDA} = \widehat{DBC} = \beta$. Then the inner angle at cross point is 2β and $\widehat{ABC} = \pi + \theta - \alpha - 2\beta$. From here on, it is possible to calculate $\widehat{BDW}$ angle which is equal to $\widehat{DBW} = \alpha - \theta + \beta$. As we know the angle $\widehat{BDW}$, angle between the symmetry axis and $\overline{WD}$ can be calculated as $\pi/2 + \theta - \alpha - \beta$. Up to this point all the angles of the first loop are defined.

When the angles around point D is examined, the kink angles of ADE and CDE links are the key to solving the angles of the second loop. Those are known due to their positions at the start configuration, $\pi - \alpha$ for both. From here on, to calculate $\widehat{WDE} = \pi + \theta - 2\alpha - 2\beta$, $\widehat{BDA}$ and $\widehat{BDW}$ angles are subtracted from the kink angle of ADE. Now, the only angle left around point D which is $\widehat{EDF}$ can be calculated as $3\alpha + 2\beta - \pi - \theta$. This is the only angle known in the second loop up to now.

As done in the first loop, with the cosine theorem using edges $\overline{ED}$ and $\overline{DF}$ together with $\widehat{EDF}$ angle, s2 edge length can be determined. Once more using the cosine theorem using edges s2, $\overline{ED}$ and $\overline{DF}$, we may find $\widehat{EFD}$ to be let's say φ. Then the inner angle at the cross point of the second loop is 2φ and $\widehat{DEG} = 2\pi + \theta - 3\alpha - 2\beta - 2\varphi$. Following the same calculations as done in first loop, $\widehat{FEX} = 3\alpha + 2\beta + \varphi - \pi - \theta$ and the angle between the symmetry axis of the second loop and $\overline{XF}$ is $3\pi/2 + \theta - 3\alpha - 2\beta - \varphi$.

As mentioned before, when a bisector is drawn dividing $\widehat{WDE}$, the bisector passes through the center point of the circle defined by the linkage. So as half of $\widehat{WDE}$, the angle $\widehat{WDZ} = \pi/2 + \theta/2 - \alpha - \beta$. It can also be calculated as $\widehat{DWZ} = \alpha + \beta - \pi/2 - \theta$ since it is a complementary of a known angle. When the triangle WDZ is examined, the only angle left is $\widehat{WZD}$, which comes up as $\theta/2$, half of the rotation angle.

Due to the symmetric placement of the loops within the array, when further calculated it is seen that the first and third loops are composed of same angles and s1 and s3 lengths are equal. Consequently, it can be seen that every other loop are similar.
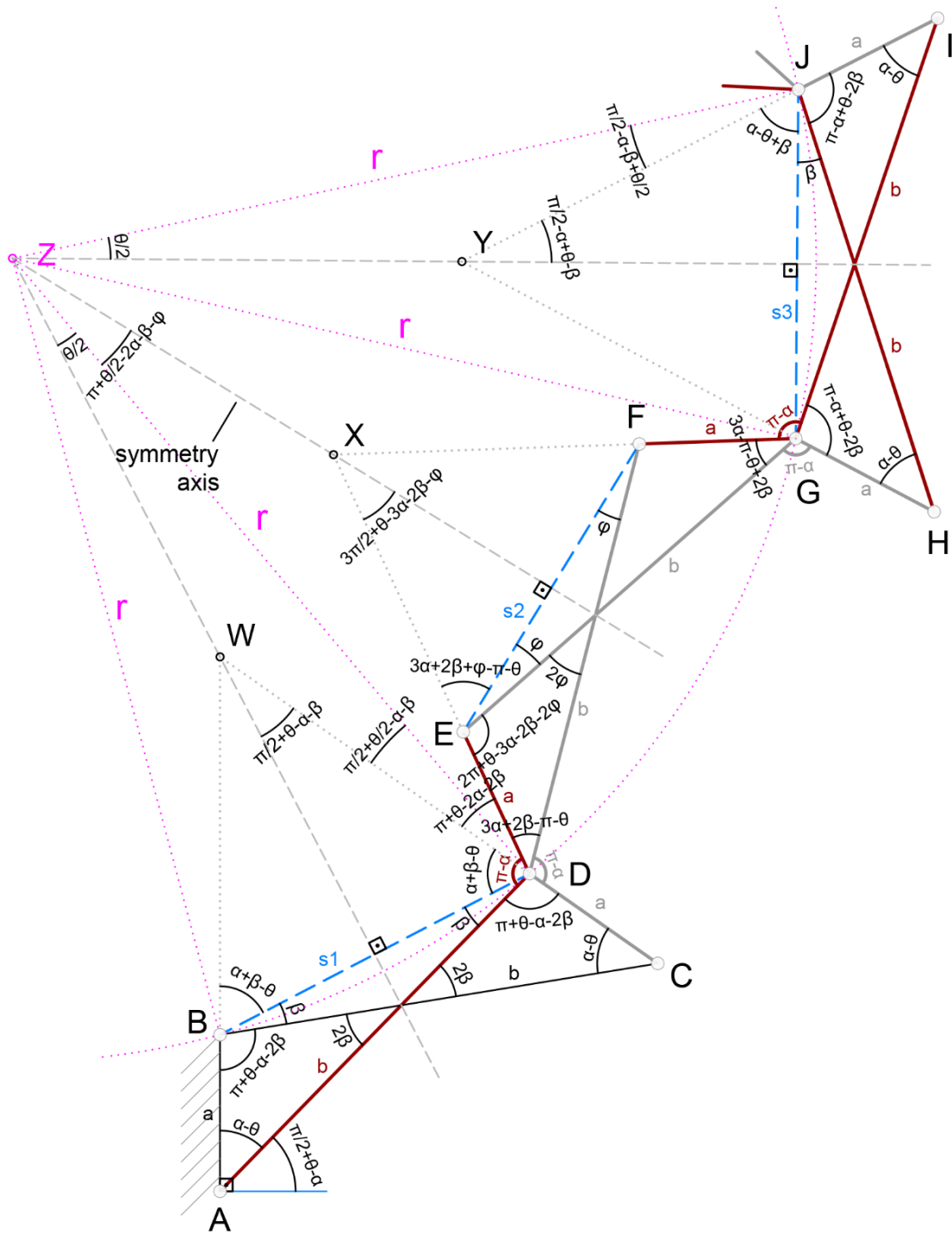
Figure 5.1.5. Analysis of relations and angles of the linkage-1

The linkage can be transformed from convex to concave form. During deployment the curvature of the linkage changes and only at the start position the curvature is zero. This is a novel mechanism since such motion was observed only with angulated scissor units before.

A parametric model of the linkage, is implemented in a Microsoft Excel® sheet as seen in Figure 5.1.6. The method of calculating the positions of the joints of a mechanism

uses triangulation (Söylemez, 2010). In the method, edge lengths and kink angles are given as inputs (shown with blue cells). Cells without a color means they are derived from the input, and orange cells are the result of the analysis.

One of the links in the linkage is selected as fixed link. In the analysis below, $\overline{AB}$ link is chosen to be fixed and ADE link is chosen to be rotated in order to transform the mechanism. Therefore, the angle $\widehat{BAD}$, denoted as $\theta 1$ in the analysis, is changed using the buttons with arrows to move the linkage.

For each joint position, necessary angles named as θ and β are calculated using trigonometric functions in correlation to the input parameters. Once an input parameter changes, so does the angle calculations. In the end, position of every joint as x and y value is gathered in a two-dimensional space.

In order to triangulate the geometry, imaginary lines are needed between some points. These are the edges named as s1, s2, s3… etc. and they are shown with blue dashed lines in the kinematic scheme within the analysis. These are the distances between joints and they change during the motion. They are calculated using the cosine theorem again in correlation with the input data.
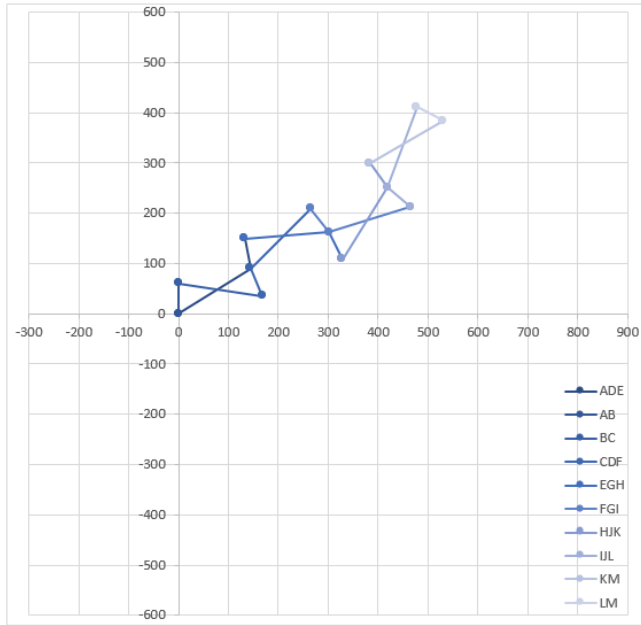
Angle	Degrees	Radians
θ1	32,00	0,559

Kink	Degrees	Radians
α1	111,00	1,937
α2	111,00	1,937
α3	111,00	1,937
α4	111,00	1,937
α5	111,00	1,937
α6	111,00	1,937

Coor.	x	y
A	0,00	0
B	0,00	60
C	168,17	35,09
D	144,17	90,09
E	132,72	148,98
F	265,26	209,40
G	302,21	162,13
H	327,98	107,94
I	464,77	211,86
J	419,49	251,21
K	383,85	299,48
L	477,60	410,97
M	531,27	384,14

Edge	Length (cm)		Edge	Length (cm)
AB	60		GH	60
BC	170		GI	170
CD	60		HJ	170
AD	170		IJ	60
DE	60		JK	60
DF	170		JL	170
EG	170		KM	170
FG	60		LM	60

θ2	351,58	6,136
θ3	101,00	1,763
θ4	44,58	0,778
θ5	364,43	6,361
θ6	115,43	2,015
θ7	126,43	2,207
θ8	29,87	0,521

S1	147,27
S2	171,79
S3	145,66
S4	173,69
S5	171,79
s6	145,66

Angle	Degrees	Radians
β1	58,00	1,012
β2	58,00	1,012
β3	11,79	0,206
β4	20,21	0,353
β5	81,58	1,424
β6	56,42	0,985
β7	56,42	0,985
β8	24,50	0,428
β9	20,07	0,350
β10	24,50	0,428

Angle	Degrees	Radians
β11	20,07	0,350
β12	17,01	0,297
β13	81,58	1,424
β14	37,22	0,650
β15	20,21	0,353
β16	81,58	1,424
β17	56,42	0,985
β18	70,01	1,222
β19	20,07	0,350
β20	49,94	0,872
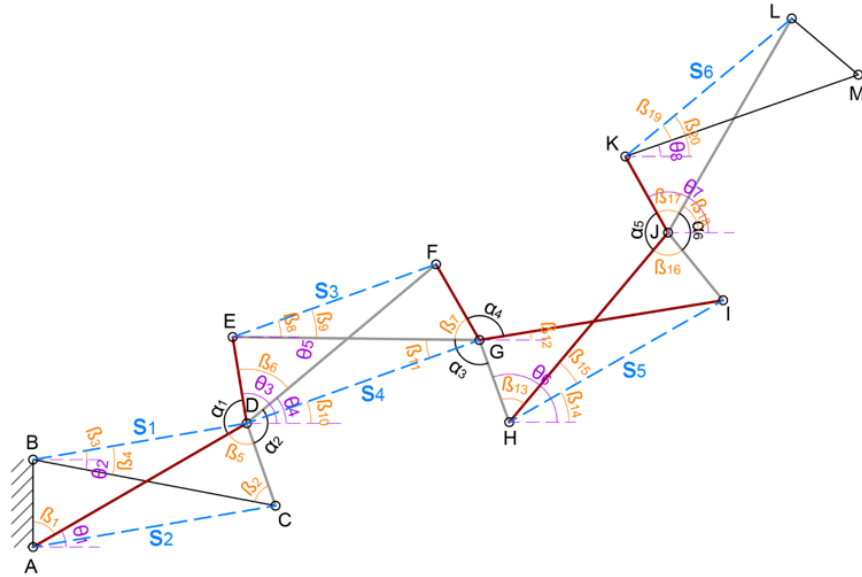
Figure 5.1.6 Position Analysis of Linkage 1

5.2. Linkage 2

The array in Figure 5.2.1 is formed using the *Hop* Frieze group. It consists of cross-rectangles which are repeated along a line in a diagonal formation.
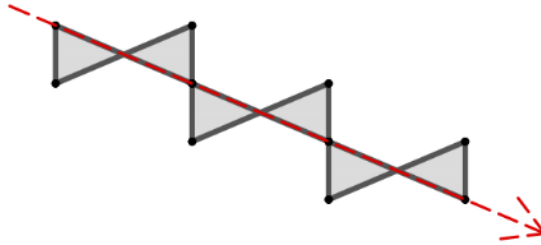
Figure 5.2.1. Array type of the linkage-2

In Figure 5.2.2a one long edge is connected to one short edge of the adjacent loop, the links formed are angulated. However in the diagonal configuration, one link of a loop is common to that of one before and one after it, turning it into a quaternary link. On the other hand, in Figure 5.2.2b short edges are connected to short, and long edges are connected to long ones. In this alternative, since edges are collinear, the links formed are straight bars. Being common with the loop before and after, the long bar becomes a single link continuing through the entire linkage, common to all loops, with many kinematic elements on it. When their motions are observed, it is seen that linkage with angulated links was able to transform from straight to concave and convex forms, while the one with straight bars was able only to flatten. To understand the motion of the linkage with angulated quaternary links a geometrical analysis is done.
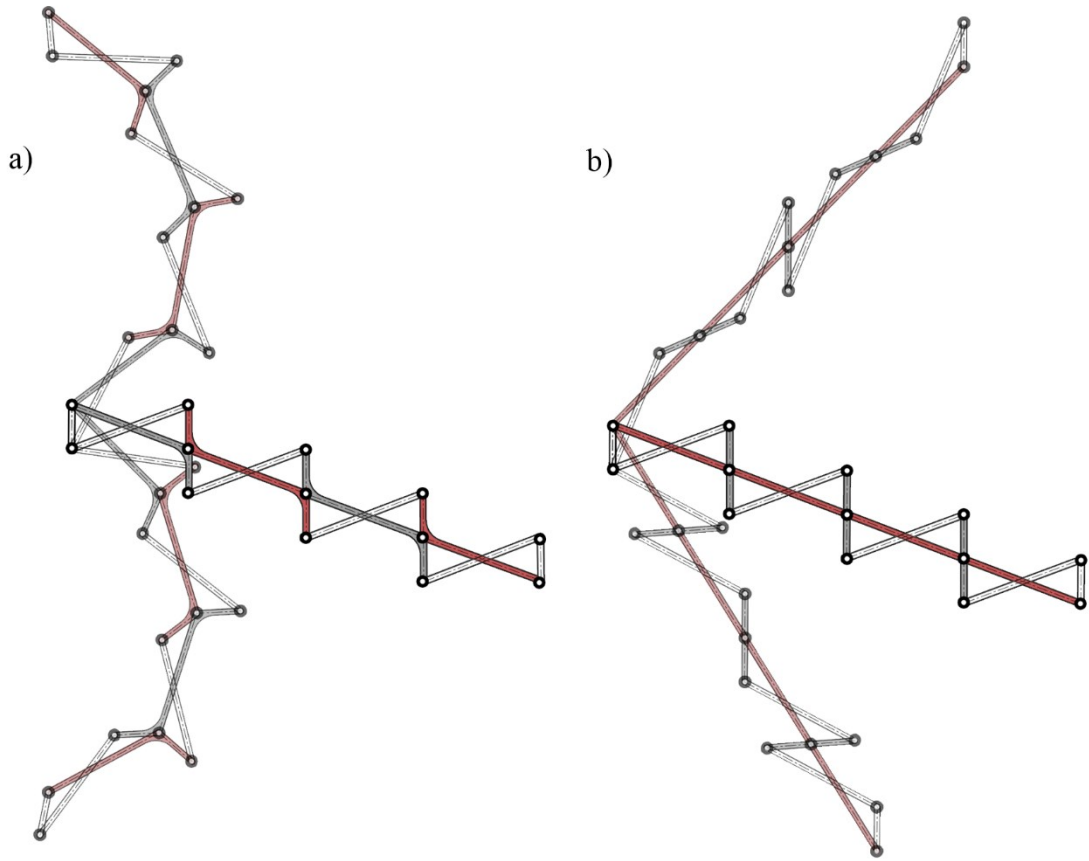
Figure 5.2.2. Linkage alternatives of the array and their motion

Since the relation of the two adjacent loops come from the array typology, it is essential to see the relations at the start position (Figure 5.2.3). ABCD and DEFG are cross-rectangles; Short edges are $\overline{AB} = \overline{CD} = \overline{DE} = \overline{FG}$ = a, they are all perpendicular to horizontal axis and parallel to each other. Long edges are $\overline{BC} = \overline{AD} = \overline{DF} = \overline{EG}$ = b. Since cross-rectangle is a doubly symmetric form all the inner angles at the corners are the same, α. In addition, the inner angles at crossing point are also equal, $\pi - 2\alpha$. The links are formed by connecting a long edge and a short edge from each loop. Therefore, the kink angle of the links is, $\widehat{ADE} = \widehat{CDF} = \widehat{DGH} = \pi - \alpha$. The quaternary links formed have two kink angles that are equal. When the link AB is chosen as the fixed link, AC link is rotated to move the linkage. The amount the AC link is rotated is denoted as θ.
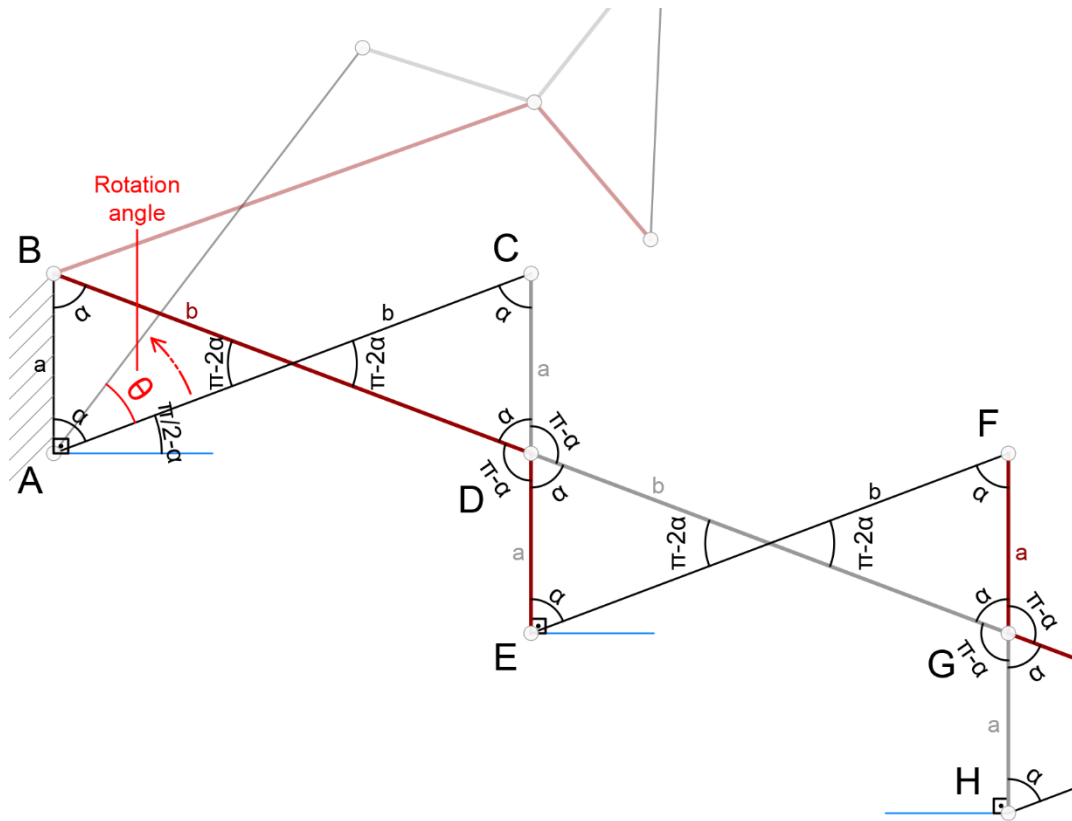
Figure 5.2.3. Geometry analysis at start position of the linkage-2

When the linkage is deployed by rotating AC link counterclockwise by θ, the linkage is also curved counterclockwise (Figure 5.2.4). In the new configuration, the loops are now antiparallelograms. When an antiparallelogram's upper and lower corners are connected, as shown with blue dashed lines in Figure 5.2.4, they are parallel to each other. Since antiparallelogram is a symmetrical form, the line passing through the midpoint of these dashed lines is the symmetry axis which is perpendicular to them. Also when the short edges are extended to intersect, this intersection point is (W, X, Y points in Figure 5.2.4) on the symmetry axis. The intersection point of the symmetry axis is denoted by point Z.
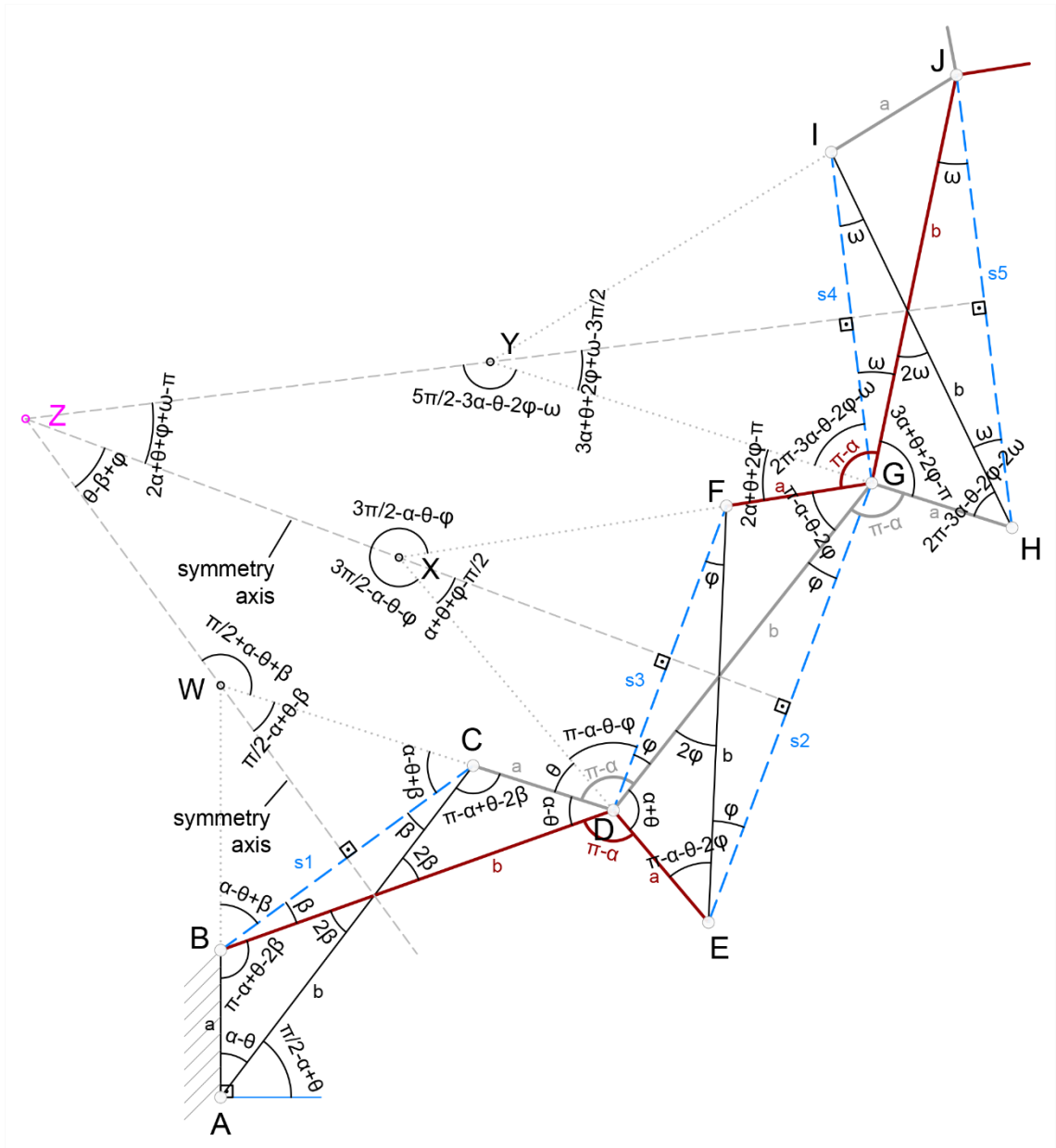
Figure 5.2.4. Analysis of relations and angles of the linkage-2

When the linkage is deployed by rotating AC link by θ degrees, in the new configuration as seen in Figure 5.2.4, $\widehat{BAC} = \alpha - \theta$. Using the edges $\overline{AB} =$ a and $\overline{AC} =$ b together with $\widehat{BAC} = \alpha - \theta$, it is possible to determine the edge length of s1. Again with cosine theorem using s1 length, $\overline{AB}$ and $\overline{AC}$, $\widehat{BCA}$ angle can be found. Let $\widehat{BCA} = \widehat{CBD} = \beta$, then the inner angle at cross point is 2β and $\widehat{ABD} = \pi - \alpha + \theta - 2\beta$. From here on, it is possible to calculate $\widehat{BCW}$ angle which is equal to $\widehat{CBW} = \alpha - \theta + \beta$. As we know the angles $\widehat{BCA}$ and $\widehat{BCW}$, angle between the symmetry axis and $\overline{WC}$ can be calculated as $\pi/2 - \alpha + \theta - \beta$. Up to this point all the angles of the first loop are defined.

56

When the angles around point D is examined, the kink angles of BDE and CDF links are the key to solving the angles of the second loop. Those are known due to their positions at the start configuration, $\pi - \alpha$ for both. $\overline{DX}$ is the extension of $\overline{ED}$ edge. Since $\widehat{BDE}$ and $\widehat{CDG}$ angles are known, it is possible to calculate $\widehat{CDX} = \theta$, which is the rotation angle. From here on, we may find the $\widehat{EDG}$ angle by subtracting $\widehat{CDB}$ and two kink angles from 2π, resulting as $\alpha + \theta$. This gives the first angle of the second loop.

Similar to the first loop, using cosine theorem, $\widehat{DGE}$ angle can be calculated with the help of imaginary s2 line. $\widehat{DGE}$ angle is equal to $\widehat{FEG}, \widehat{DFE}, \widehat{FDG}$ angles, let's say φ. Then $\widehat{FDX}$ angle being complementary angle of FDE triangle, can be solved to be $\pi - \alpha - \theta - \varphi$. From here on angle between the symmetry axis of the second loop and $\overline{XD}$ can also be calculated as $\alpha + \theta + \varphi - \pi/2$. With the methods used for second loop, third loop angles can be identified.

The intersection point of the symmetry axis of loops is point Z. This point is also the center of the spiral defined by the linkage when deployed (Figure 5.2.5). This point goes to infinite when the linkage is as the start configuration and the loops are parallel. This mechanism is novel because such motion was observed only with angulated scissor units with ternary links before.
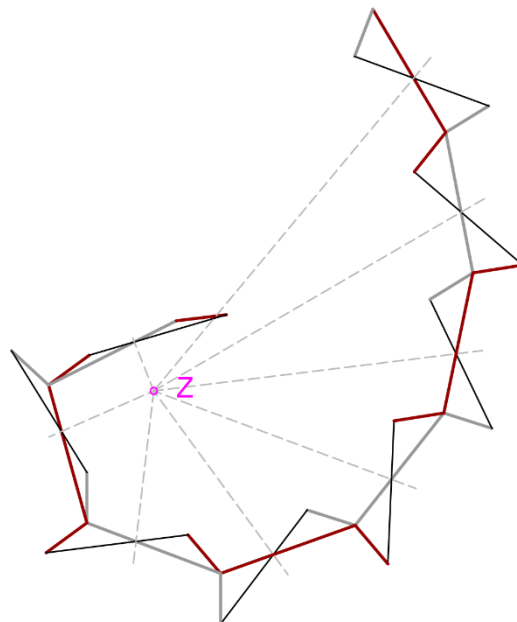
Figure 5.2.5 Spiral form of Linkage 2

5.3. Linkage 3

The array in Figure 5.3.1 is formed using the *Hop* Frieze group with rotation. It consists of antiparallelograms which are repeated along a circular arc.
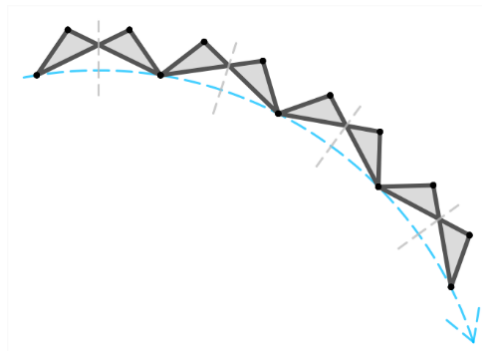
Figure 5.3.1. Array type of the linkage-3

Using this array type there are many linkage alternatives to be formed. The rotation angle of the loops in the array leads to straight bars at specific points, such as in c, d, e and f in Figure 5.3.2. As the forms of the links differ, so does the motion capabilities of the linkages.
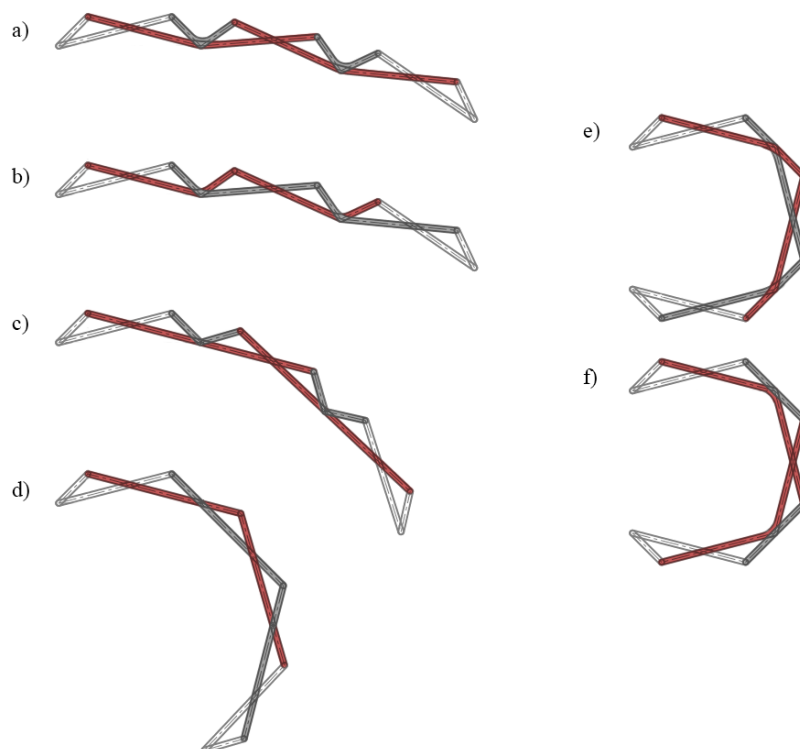
Figure 5.3.2. Linkage alternatives of the array

Within the alternatives of the array, one stands out due to its motion and link type. In Figure 5.3.2d the linkage is made up of identical straight bars. They are connected with

an eccentrically placed intermediate hinge, just like the polar unit (Figure 5.3.3). However unlike a polar scissor chain (Figure 5.3.3a), when two units come together in this novel linkage, the short side is attached to the long side of the next unit (Figure 5.3.3b).
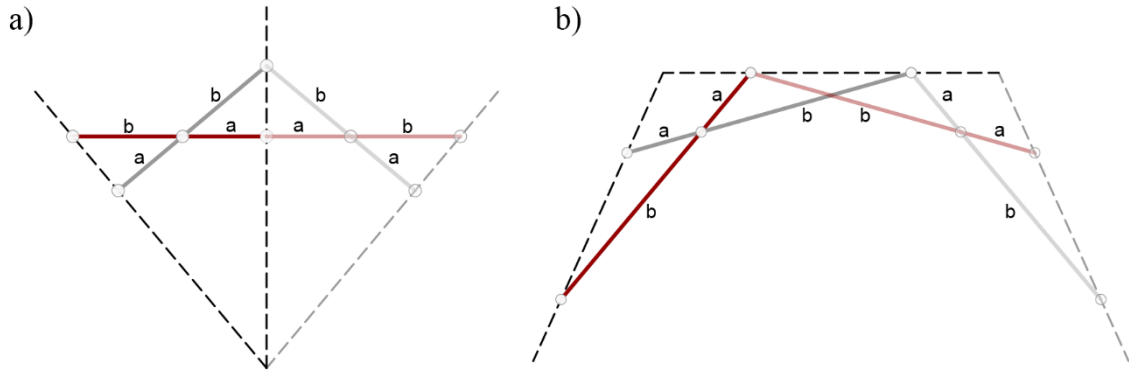
Figure 5.3.3 Polar unit vs Linkage 3 unit

When the linkage is deployed, it is seen that it can transform from convex to the concave configuration as in Figure 5.3.4. This kind of movement hasn't been observed in linkages with straight bars before.
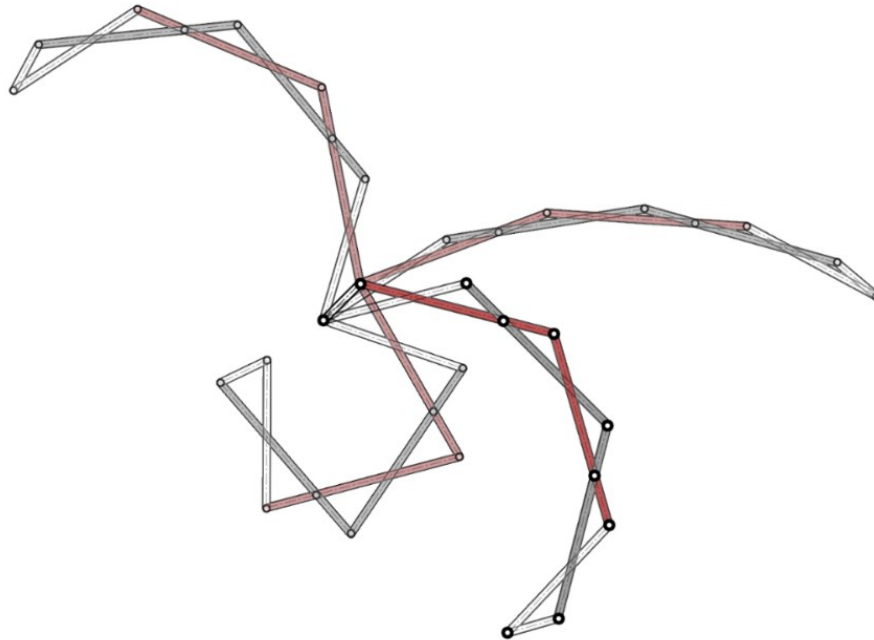
Figure 5.3.4. Motion of the linkage-3

At the start position, the loops are aligned such that short edge of the second loop is collinear with the long edge of the first loop. This way, one long edge connect with one short edge and form straight links.

At the start position, the loops are aligned along a curve whose radius is known. Since the loops are equal, the curve is divided equally, making the loops symmetric on the radius passing through the joints connecting them, as seen with pink dotted lines in Figure 5.3.5.
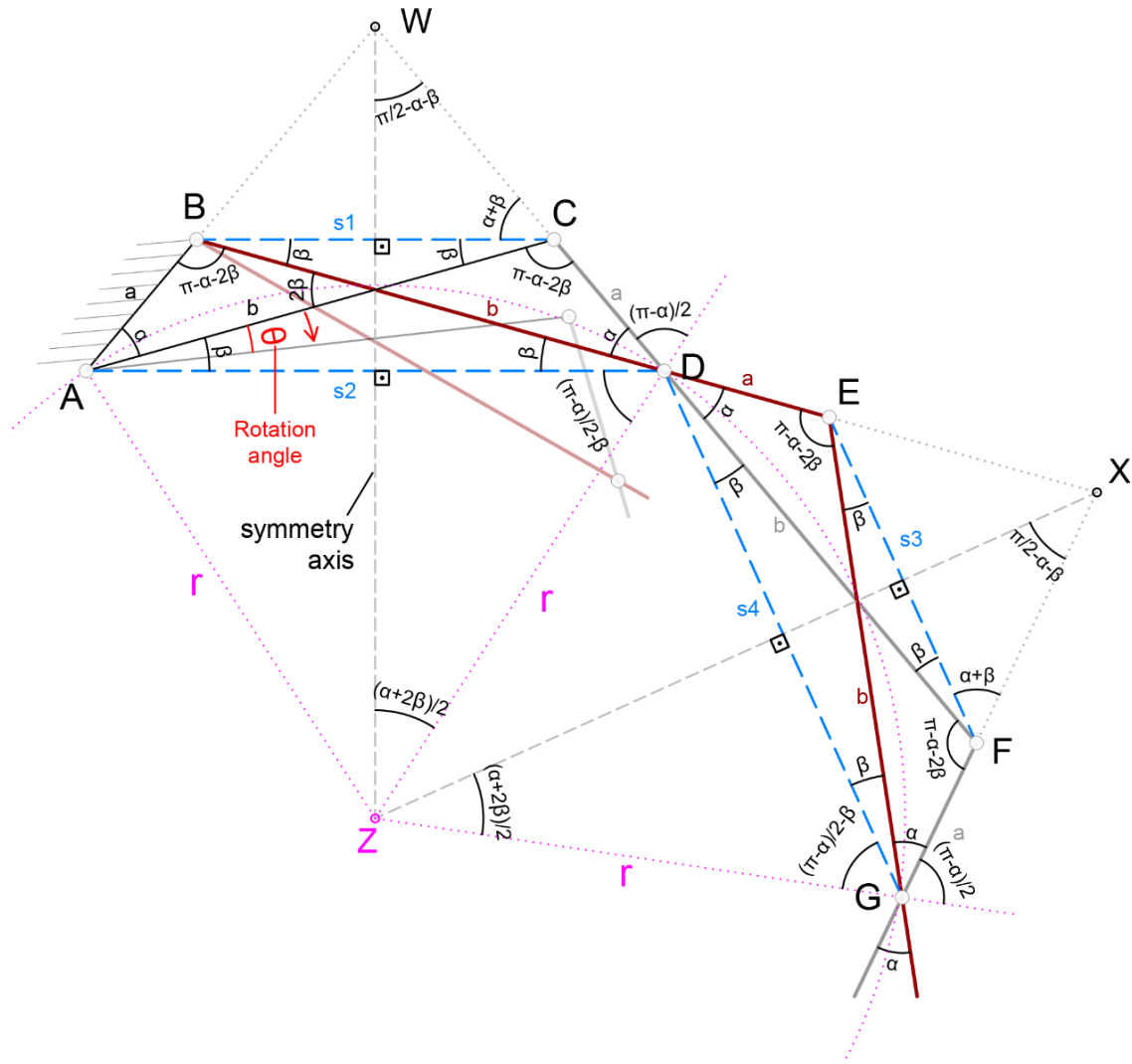
Figure 5.3.5. Geometry analysis at start position of the linkage-3

In the first loop, the angles $\widehat{BAC} = \widehat{CDB} = \alpha, \widehat{BCA} = \widehat{CBD} = \widehat{CAD} = \widehat{BDA} = \beta$ as found in Linkage 1&2 and $\widehat{ABD} = \widehat{ACD} = \pi - \alpha - 2\beta$. Because of the symmetrical array, it is known that $\widehat{ADZ} = \widehat{ZDG}$. Since $\overline{BD}$ and $\overline{DE}$ are collinear and $\widehat{BDA}, \widehat{GDF}, \widehat{FDE}$ are known, then $\widehat{ADZ} = \widehat{ZDG} = (\pi - \alpha)/2 - \beta$. Using this angle $\widehat{DZW}$ can be calculated as $(\alpha + 2\beta)/2$. Being complementary to BCD triangle $\widehat{BCW}$ angle is $\alpha + \beta$ and $\widehat{CWZ} = \pi/2 - \alpha - \beta$.

When AC link is rotated clockwise by θ, then $\widehat{BAC} = \widehat{CDB} = \alpha + \theta$ in the new configuration shown in Figure 5.3.6. The new length of s1 is calculated with cosine theorem again, and $\widehat{BCA} = \widehat{CBD} = \widehat{CAD} = \widehat{BDA}$ are notated as φ. Following the same steps as start position calculations, all other angles can be found for the first loop. Since the system is symmetric, the angles of the first loop are the same for all the other loops.

During the motion, while transforming from concave to convex form, at one point all the links become collinear, which might result in assembly mode change. Although same motion is observed in other linkages examined in this research, only this linkage faces this situation. The cause for this is the form of the loops at the point between concave and convex, at the linear position. In other linkages, their loops are not compacted so that the joints are not at the dead center. However in this linkage, at the linear position, all links are aligned so that it is at the same time the dead center.
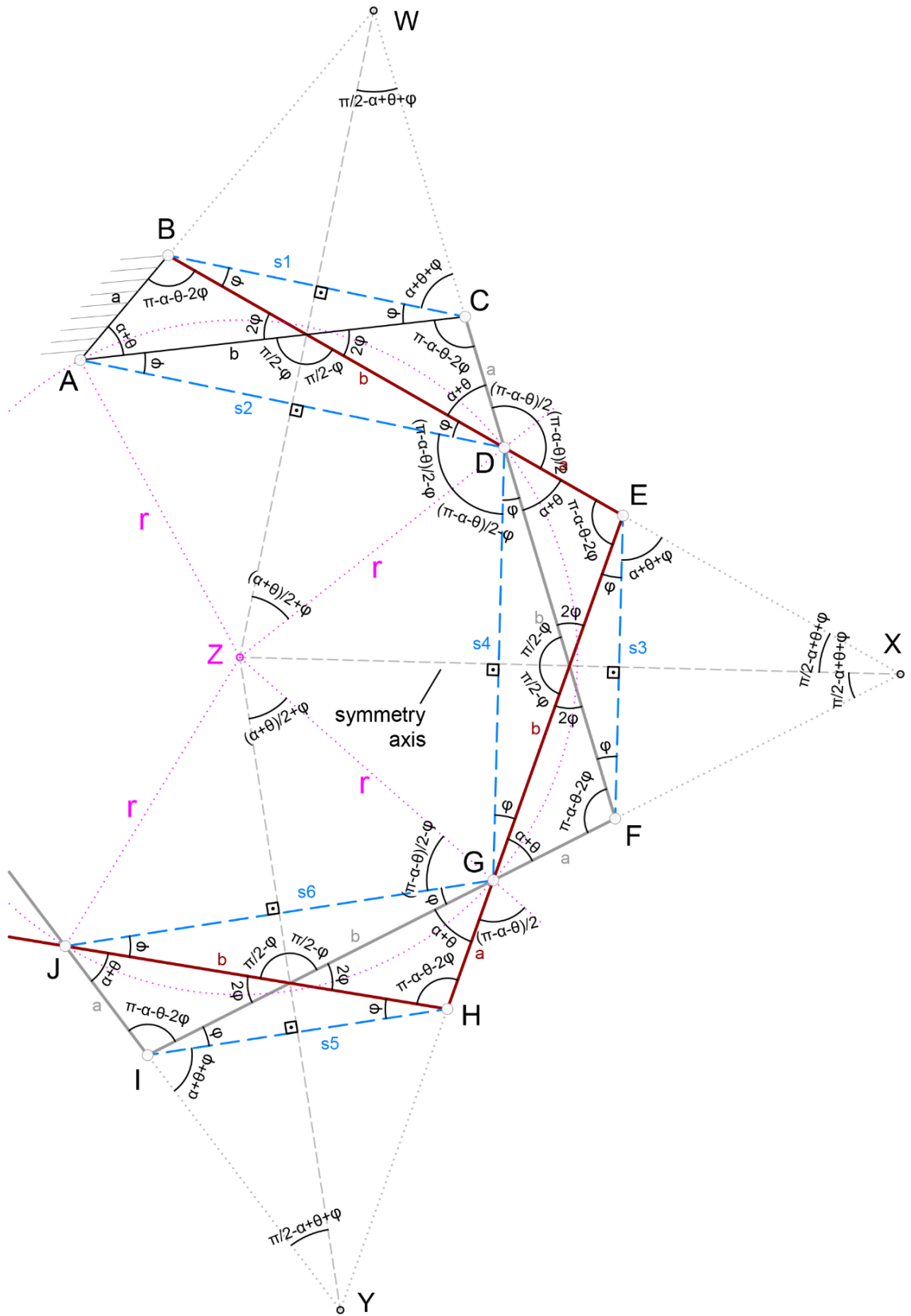
Figure 5.3.6. Analysis of relations and angles of the linkage-3

5.4. Linkage 4

The array in Figure 5.4.1 is formed using the *Step* Frieze group with rotation. It consists of cross-rectangles which are repeated along a circular arc in one-over, one-under formation.
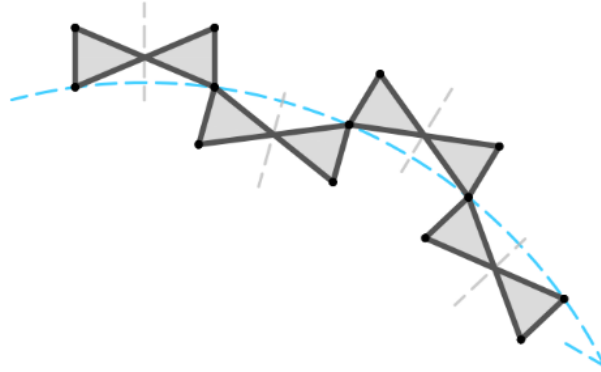
Figure 5.4.1. Array type of the linkage-4

In Figure 5.4.2a one long edge is connected to one short edge of the adjacent loop, the links formed are angulated. When the linkage is deployed it is able to transform from straight to concave and convex forms just like Linkage 1, with ternary links. Differing from Linkage 1 is that, the links are not identical. They both have the same arm lengths but different kink angles.

On the other hand in Figure 5.4.2b short edges are connected to short, and long edges are connected to long ones. Both links are angulated ternary links with equal arms but the lengths are different for each link. The novel aspect of this linkage is in its motion. It can form a ring that can be expanded and stowed.

At the start position, the rotation angle of the loops along the curve, which is β in the Figure 5.4.3, is a given. Also at the start, the cross-rectangles are perpendicular and short edges are parallel to each other. Therefore, if $\widehat{BAC} = \alpha$ then $\widehat{ABD}, \widehat{ACD}, \widehat{BDC}, \widehat{EDF}$, $\widehat{DEG}, \widehat{EGF}$ and $\widehat{DFG}$ are all equal to α. Also $\widehat{DAC}, \widehat{ADB}, \widehat{CBD}, \widehat{BCA}, \widehat{GDF}, \widehat{DGE}, \widehat{EFD}$ and $\widehat{FEG}$ are all equal to $\pi/2 - \alpha$ because of the perpendicularity.
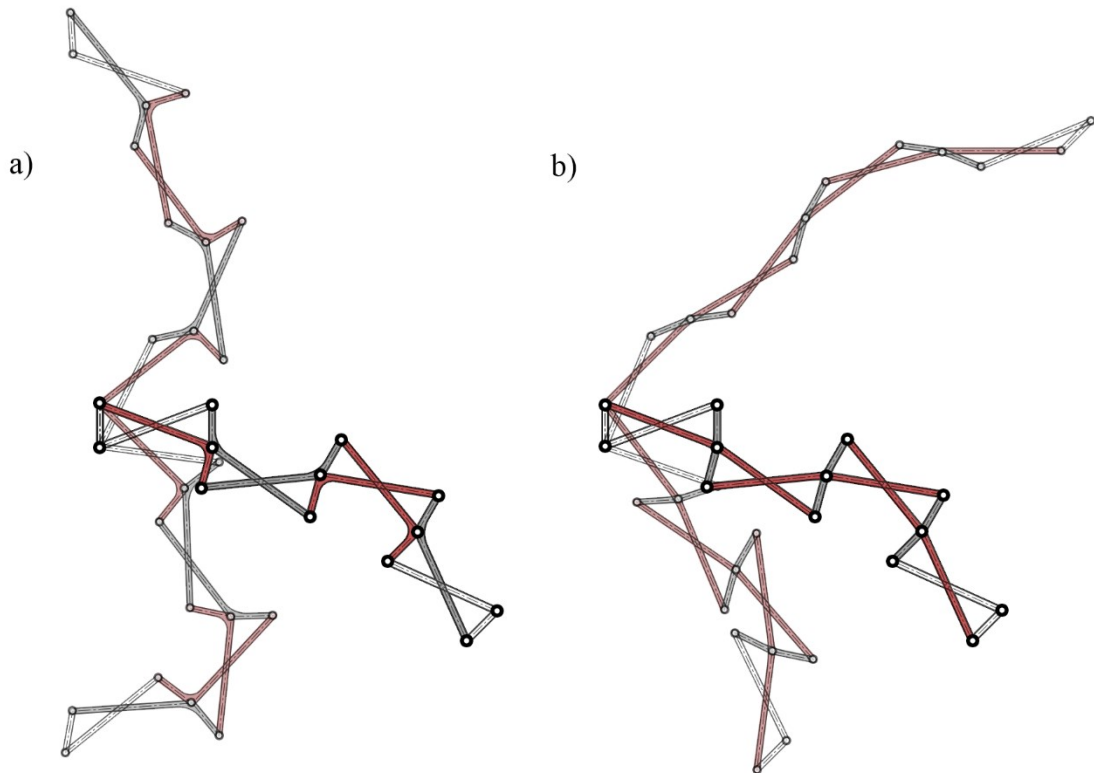
Figure 5.4.2 Linkage alternatives of the array and their motion

Edges $\overline{AD}$ and $\overline{DG}$, drawn with blue dashed lines, are equal in length and perpendicular lines drawn from their midpoint intersect at point Z, which is the center of the curve. ZD line is the radius of the curve. The symmetry axis of the first loop and $\overline{CD}$ edge are parallel. Therefore, when ZD line is traced, the angle between it and the symmetry axis is equal to the angle between it and $\overline{CD}$ edge, which is $\beta/2$.

Second loop is rotated by β in the array at around the point D. The imaginary line s3 is equal to s1 and s2 at the start position. To help understanding the kink angles, an imaginary second loop is drawn above the original, defined with D, E', F' and G. In this geometry, the angle between the symmetry axis and ZD line is equal to $\beta/2$ and since $\overline{DE'}$ is collinear with $\overline{ED}$, $\widehat{EDZ}$ is also equal to $\beta/2$. After this it is possible to calculate the angle $\widehat{ADE} = \pi/2 - \beta$. Now all the angles to calculate the kink angles of BDF and CDE links exist. When the calculation is done, it is seen that both kink angles are equal, $\pi - \beta$.
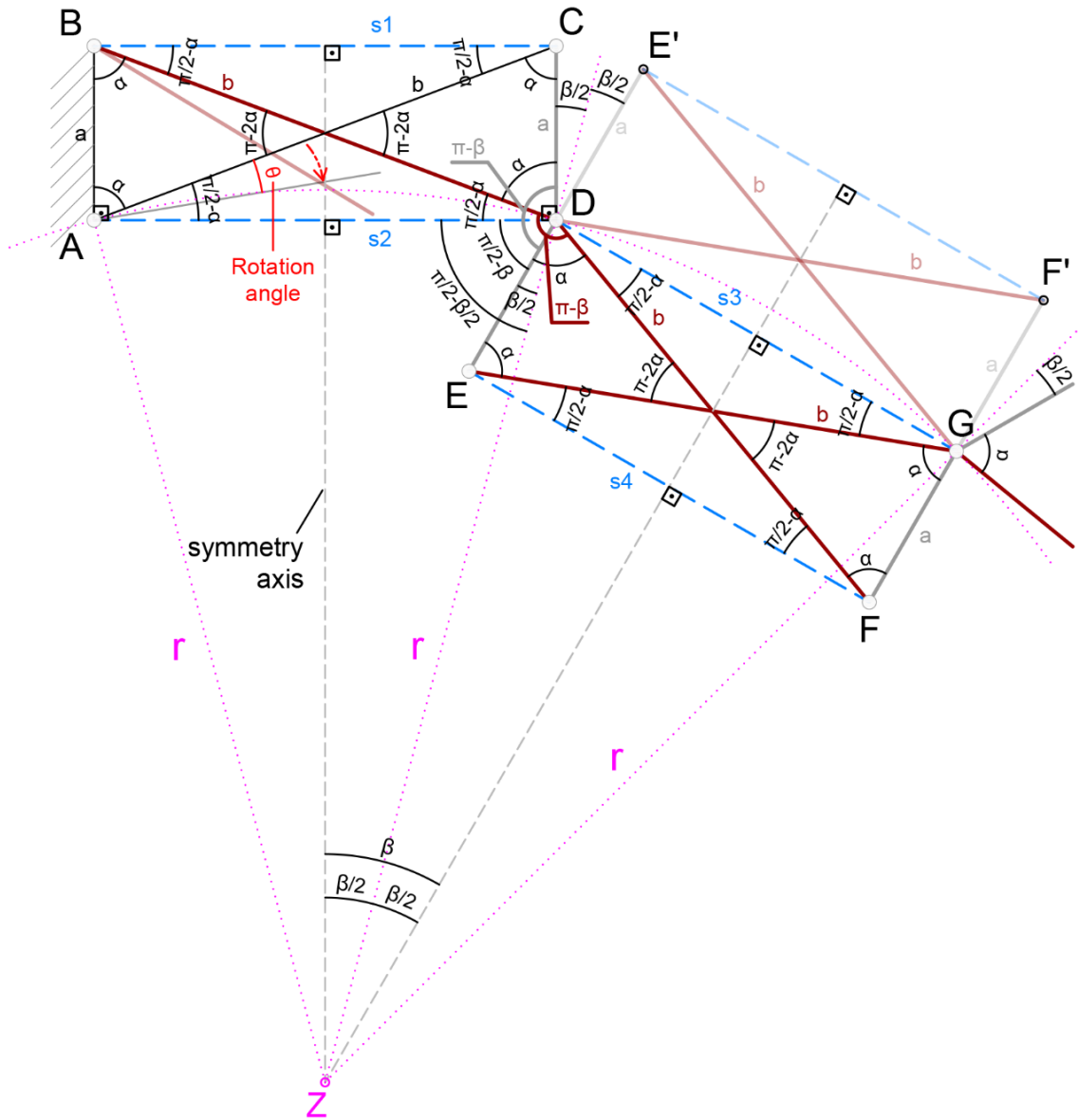
Figure 5.4.3. Geometry analysis at start position of the linkage-4

When AC link is rotated clockwise by θ, linkage also rotates clockwise (Figure 5.4.4). Now $\widehat{BAC} = \widehat{BDC} = \alpha + \theta$. Using the cosine theorem, as in the linkages before, s1 length and $\widehat{BCA} = \widehat{CBD} = \widehat{CAD} = \widehat{BDA} = \varphi$ is found.

In order to continue to second loop, kink angles are used. On CDE link, kink angle is known to be $\pi - \beta$. When angles $\widehat{CDB}$ and $\widehat{BDA}$ are subtracted, $\widehat{ADE} = \pi - \beta - \alpha - \theta - \varphi$ is found. Now if BDF link is observed, $\widehat{BDA}$ and $\widehat{ADE}$ angles are known, so that $\widehat{EDF} = \widehat{EGF}$ can be calculated as $\alpha + \theta$. Using the cosine theorem, since edges are same length as the first loop, it can be proven that s4 is equal to s1, s3 is equal to s2 and $\widehat{GDF} = \widehat{DGE} = \widehat{GEF} = \widehat{EFD} = \varphi$.
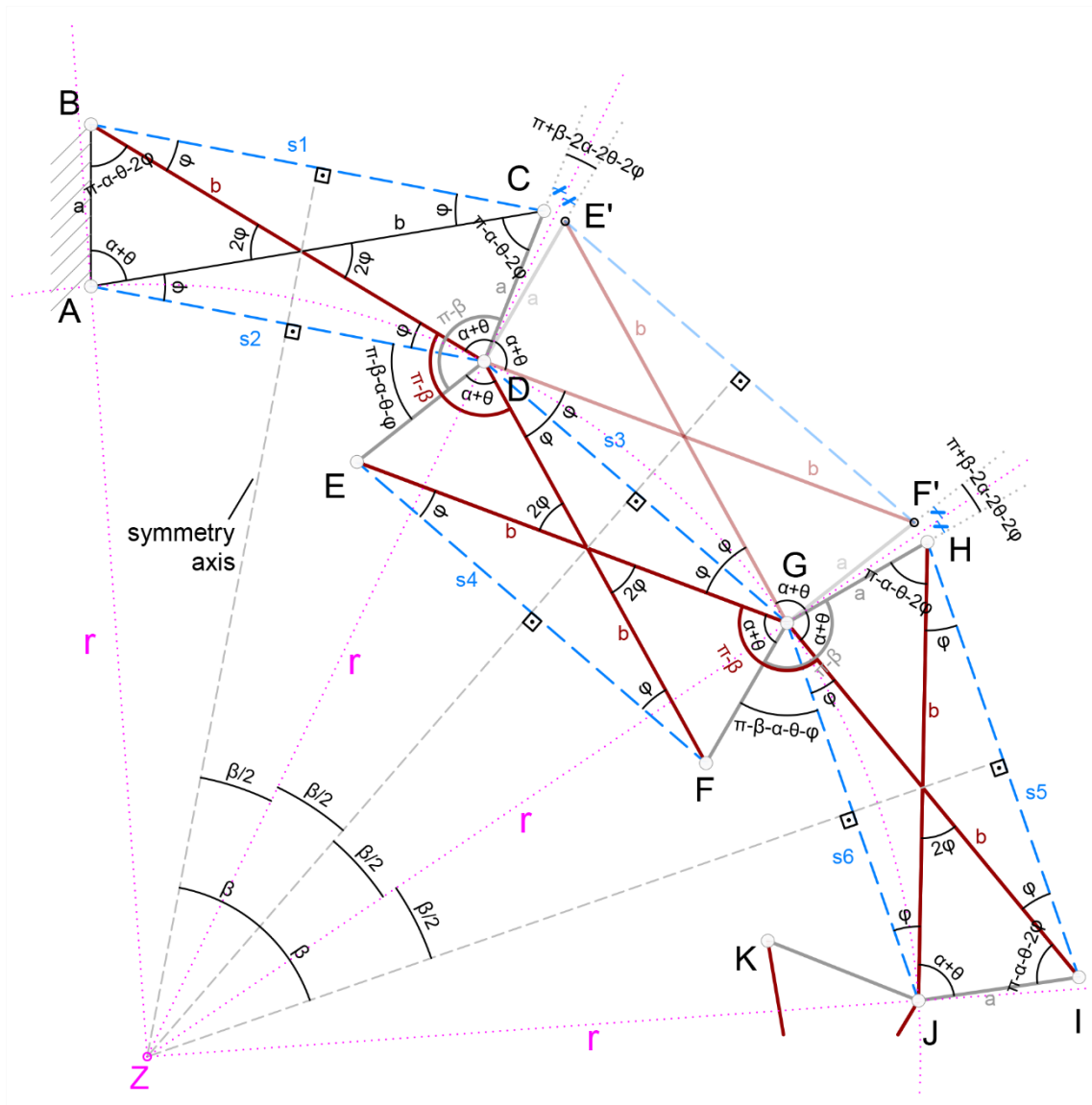
Figure 5.4.4. Analysis of relations and angles of the linkage-4

When the quadrilateral formed between the symmetry axis and D point, it is seen that the form is a kite with two equal short and two equal long edges. $\widehat{ADG} = \pi - \beta$ which is same as the kink angle, therefore the angle between the symmetry axis is β, which is the array rotation angle. This proves that during motion, the symmetry axes preserve their relative positions and the joints remain on the axis making an angle of $\beta/2$ to the symmetry axis and the subtended angles of the linkage remain constant while the radius of the curve changes.

In the light of these findings, a ring assembly seemed plausible. When such an assembly was made as in Figure 5.4.5, it was seen that the linkage was indeed deployable. When the joints are placed on radial axes and the mechanism is simulated in Solidworks®️ the linkage expands and contracts radially. At the fully-expanded state, the linkage forms

a polygon, short and long links aligning on top of each other. At this state, the edge length of the polygon is the sum of half-length of the short and long links.
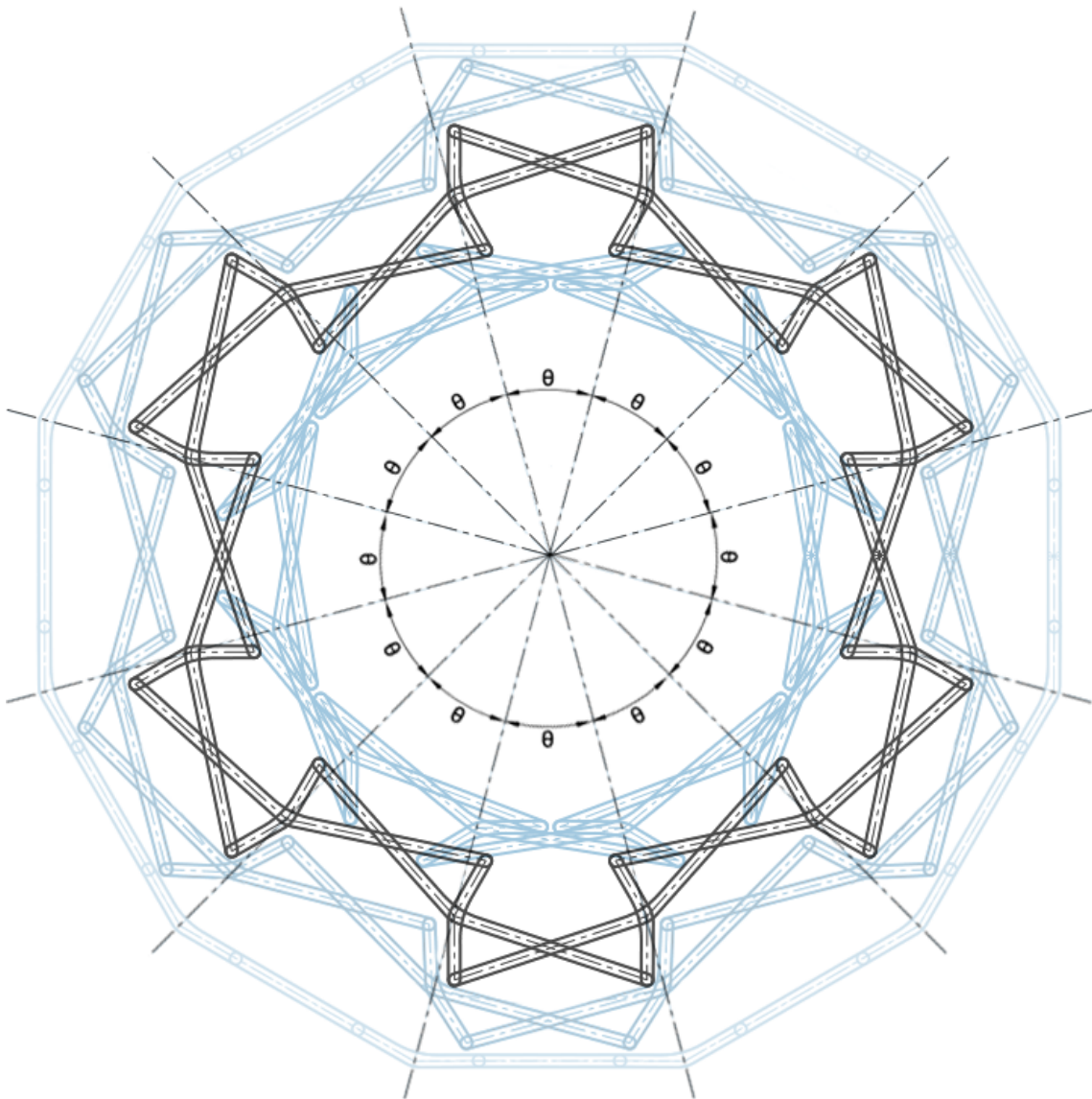
Figure 5.4.5 Ring assembly of cross-rectangle loops

The links formed in this linkage are one short and one long ternary angulated links with same kink angle and equal arms, connected by an intermediate hinge at the kink point. They are similar to the angulated scissors but as in Linkage 3, they connect differently than the other assemblies with angulated scissor unit in the literature. The links can be classified as Type II GAE defined by You & Pellegrino (Figure 2.1.13).

In his rhombus assemblies, Hoberman uses not only identical loops, but similar loops at different scales, such as in his patent (Figure 3.3.3) His work proves such assemblies can also deploy. Using the same principle, another assembly has been made

with different scale loops (Figure 5.4.6). Simulation of the linkage in Solidworks® shows that with cross-rectangle loops such a mechanism is also deployable.
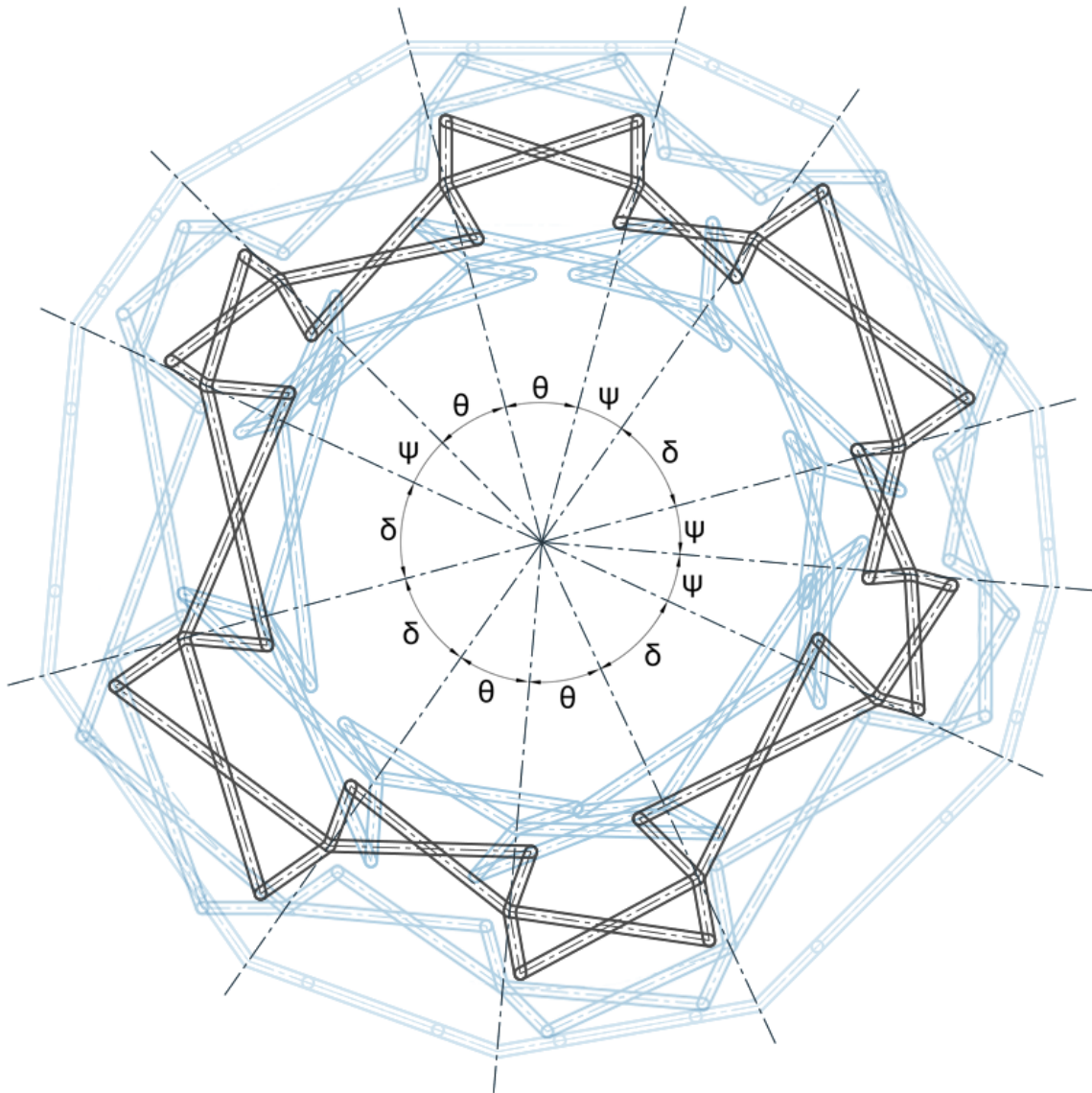
Figure 5.4.6 Ring assembly with different scale similar loops

The use of scaled loops lead to various angles between the joint axes, and the links formed are not the same either. In the figure below (Figure 5.4.7), each color represent one type of link. There are 6 pairs of links in this linkage; green-orange, cyan-purple, pink-light green, yellow-magenta, red-blue, and grey-maroon.
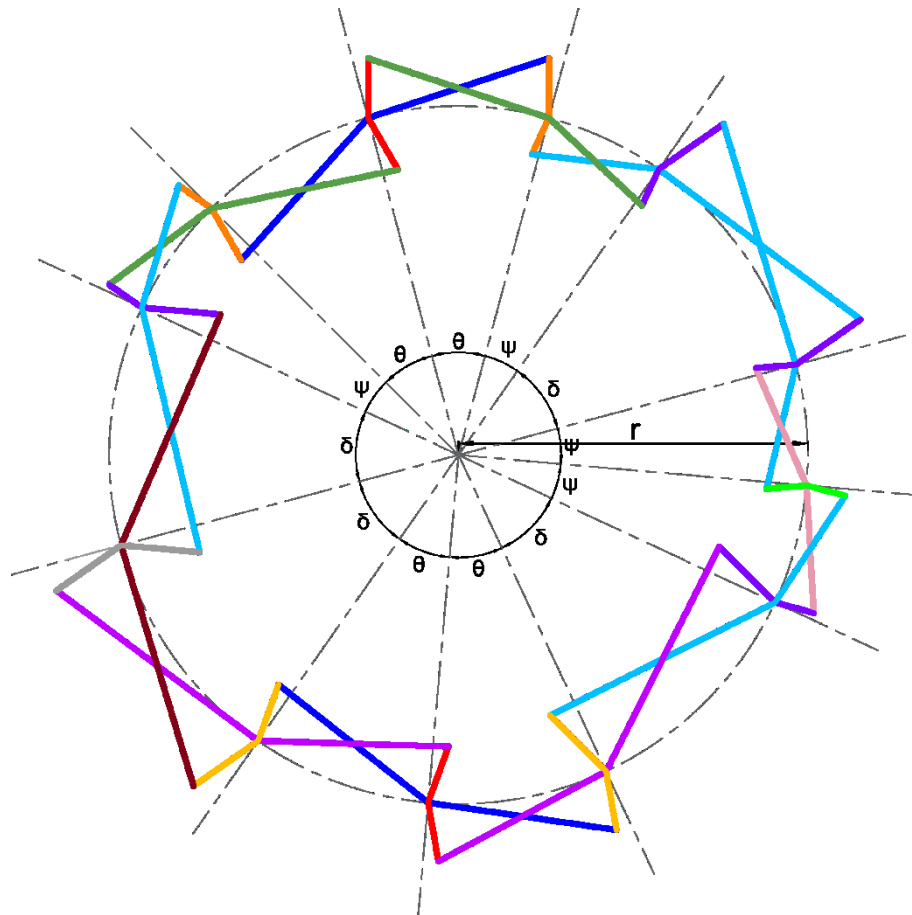
Figure 5.4.7 Link types of the assembly with similar loops

At start position, as seen in Figure 5.4.8 each loop have same inner angles since they are similar. When the axis passing from joint E is followed, it can be seen that it intersect with the symmetry axis of the first loop with a $\theta/2$ angle. Since $\overline{ED}$ edge is parallel to the symmetry axis, it intersects with $\theta/2$ angle with the edge, too.

For the next loop, an extension of the edge $\overline{EF}$ should be drawn. This extension is also parallel to the second loops symmetry axis, which bisects the angle ψ. So the angle between the axis passing through point E and the extension of $\overline{EF}$ is equal to $\psi/2$.

To find the kink angles, DEF link can be observed. On the extension of the edge $\overline{EF}$, two angles are known and kink angle of DEF is the complementary of those, that is $\pi - \psi/2 - \theta/2$. As it was proven for the start position, it can be proven that the kink angles of DEF and AEI are equal. Kink angles for all other link pairs can be found similarly. It is seen that the kink angle is equal to the sum of half of each loops rotation angles the links connect subtracted from π.
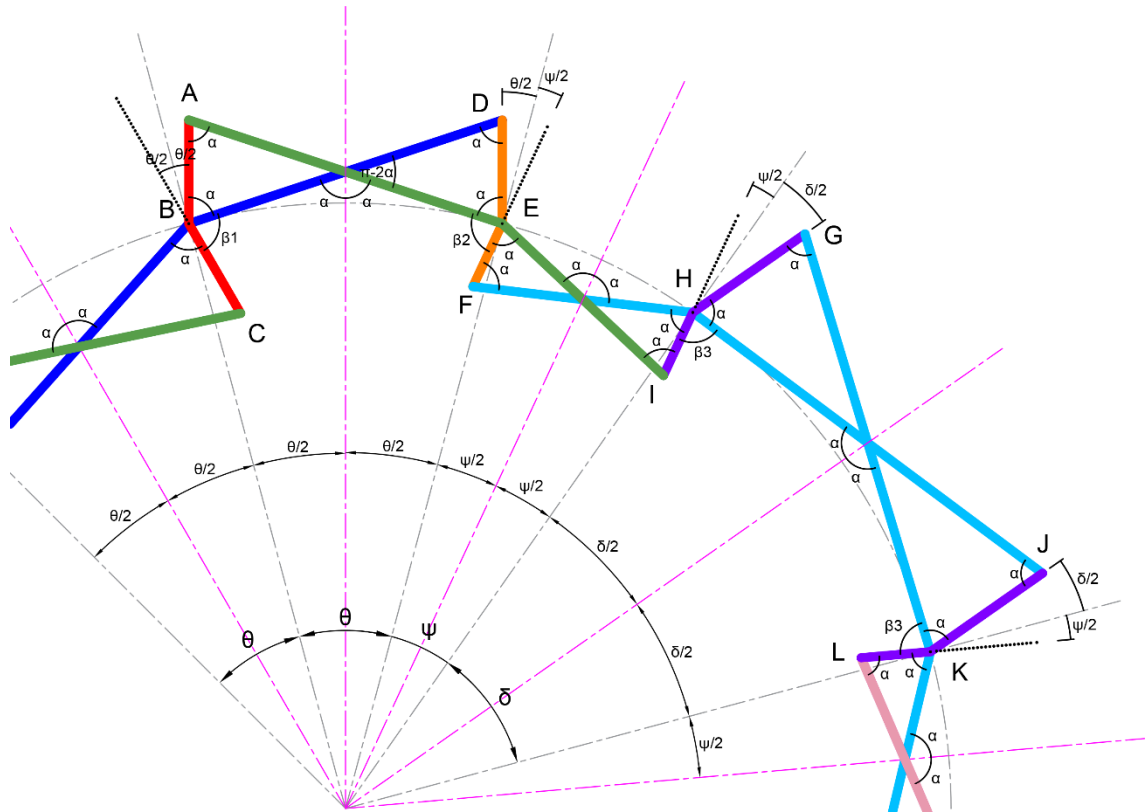
Figure 5.4.8 Geometric analysis of the assembly with similar loops

The assembly of similar cross-rectangles once again confirms that Hoberman's loop assembly method. The links formed in the linkage are again classified as Type II GAE defined by You & Pellegrino.

The findings on the deployability of linkages with similar loops as in the ring assembly case suggest that all the linkages examined in the previous cases could also be formed with similar loops. However they were not studied in the scope of this research.

5.5. Linkage 5

The last linkage is composed of antiparallelogram loops using the array *Spinning Sidle* as seen in Figure 5.5.1. This array is formed when a loop is vertically mirrored and then afterwards rotated by 180°. However, this formation is mistaken for repeating the loop twice in a row, due to the vertical symmetry axis of the loop itself.
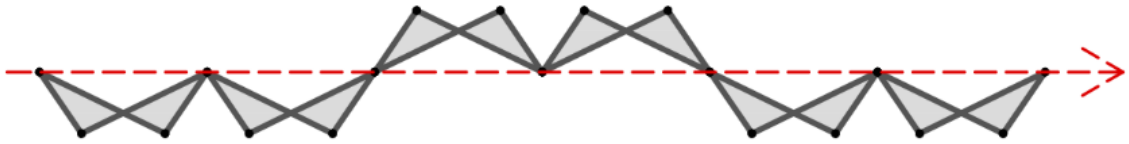
Figure 5.5.1 Array type of linkage-5

As in the cases before, there are two possible options to form the common links between the loops; either short edge connects with long one (Figure 5.5.2a), or short edges and long edges connect among themselves (Figure 5.5.2b).
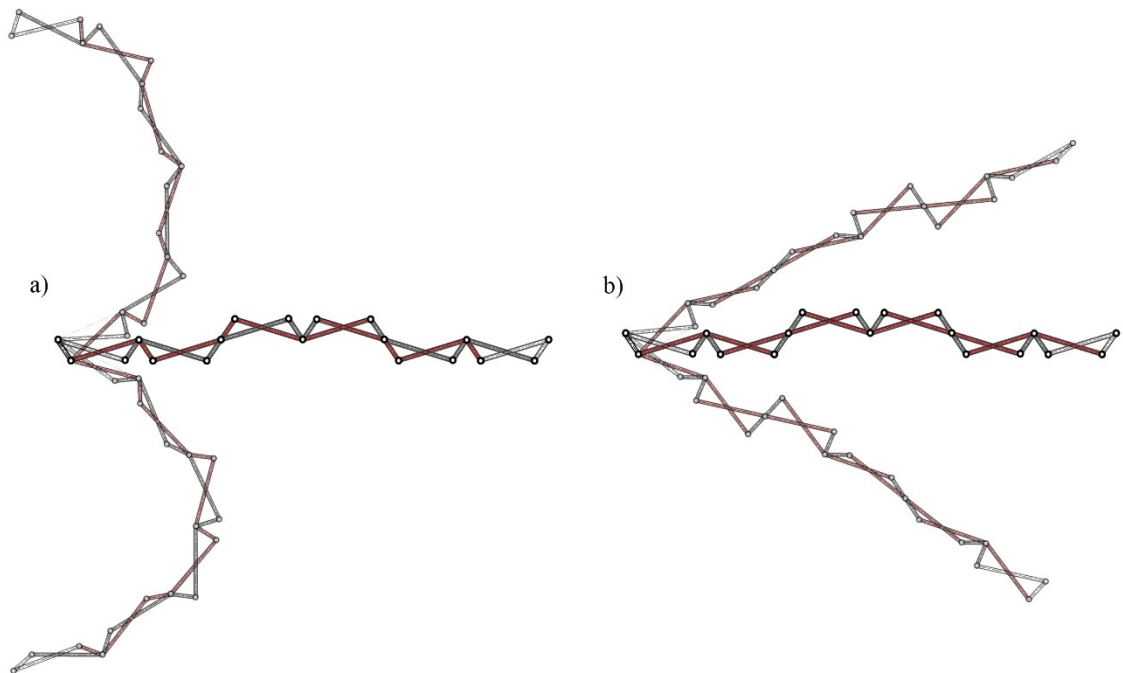
Figure 5.5.2 Linkage alternatives of the array and their motion

In Figure 5.5.2a, it is seen that the linkage is capable of transforming between concave and convex configurations like the linkages before. Up to this point, all of the arrays used to form the linkages led to either one or two types of common links. However, in this array only, there are four types of links formed. In Figure 5.5.3 these links are shown in dark red, grey, dark blue and lila colors. The geometrical relations are also shown on the figure for the start position.
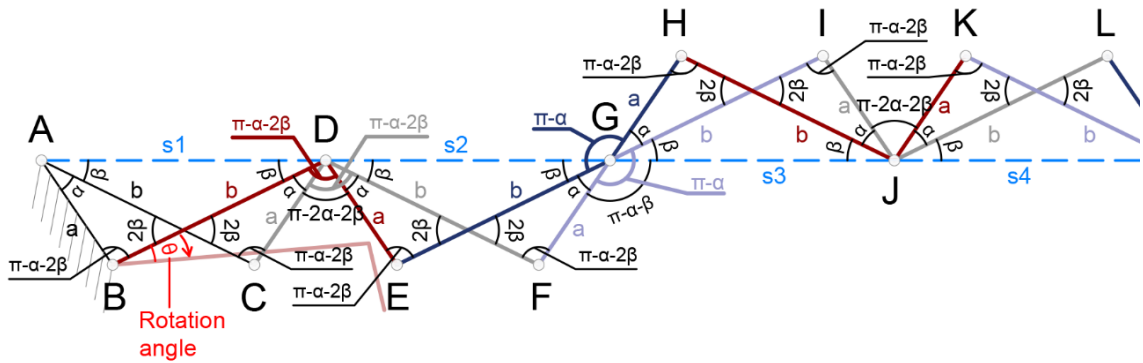
Figure 5.5.3 Geometry analysis at start position of the linkage-5

As done in previous linkages, one of the links is rotated by θ degrees to deploy the linkage. Using the same methods as in the previous linkages, all angles are possible to calculate. They are shown in Figure 5.5.4. The first and second loops deploy oppositely with the third and fourth loops. It is seen that the system forms a regular curve.
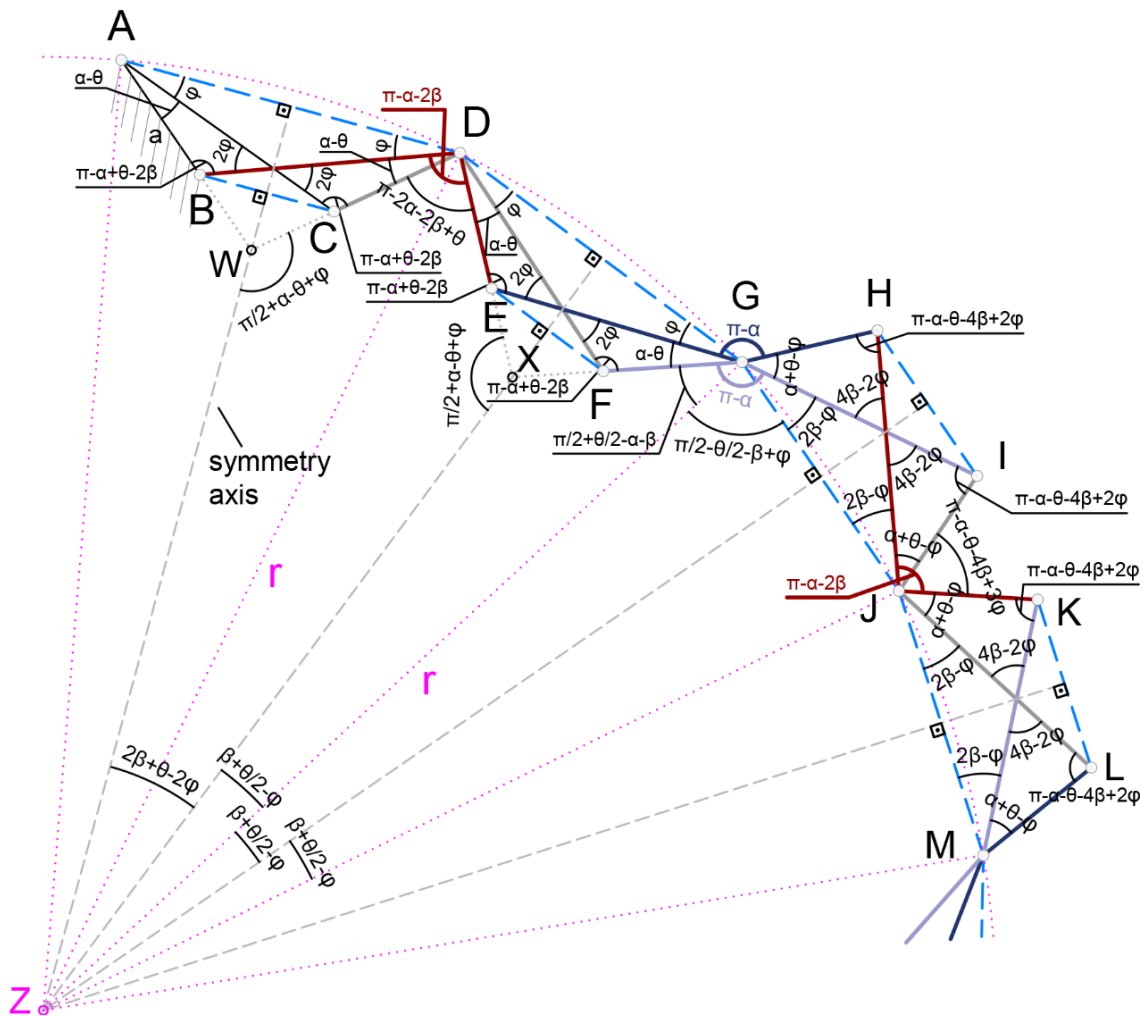
Figure 5.5.4 Analysis of relations and angles of the linkage-5

CHAPTER 6

CONCLUSIONS

Aim of this thesis research was to create novel deployable and transformable planar structural mechanisms using loop assembly method. Loop assembly method was formerly used with scissor mechanisms. Therefore, previous works on deployable and transformable scissor mechanisms were reviewed. The loops used in these mechanisms were examined and the antiparallelogram loop was not observed among them. Hence antiparallelogram loop was chosen for this research.

Producing various arrays is the primary step to form loop assemblies. To be able to produce arrays in a methodical way, geometrical approaches of unit multiplying methods, called symmetry operations, were examined. Among these methods Frieze Group operations found to be suitable for the aim of the research and were adopted to produce the arrays. After this step, single DoF linkages were formed. Within the many linkages produced, five of them were selected due to their novel aspects.

The analysis of the selected linkages shows that antiparallelogram linkages present novel motions with mostly known link types. For the first time in the literature, Frieze groups are used for the systematical classification of modular planar deployable structures composed of SLEs. As a result, 39 different loop assemblies comprising antiparallelogram loops were found (Figure 4.2.17). For each type, several different linkages can be obtained by fixing different portions of the loops to each other in order to form links. Kinematics of five of the hence obtained linkages are examined in detail.

Although Linkages 1, 2, 3 and 5 all perform a transformation from convex to straight and then to concave form, all have different types of links. Linkage 1 has angulated ternary links, but unlike the research of Yar et al. (2017), the loops are not connected in a linear fashion but rather in a one-over one-under order along a line. Also the links do not form scissor units. Linkage 2 has quaternary links, which is not common in the literature to do transformation motion. The quaternary links have two equal kink angles. Linkage 3 has straight bars very much like polar units. The links are connected with an intermediate hinge which is located eccentrically. However, each link pair is connected to the next in a reverse fashion than regular polar units. This connection makes the transformation motion possible, which was not observed with polar scissor units

before. Linkage 5 does not have special link forms, but the fact that there are four types of common links used in the linkage still resulting in the same motion makes it unique.

In linkage 4, there is a different motion compared to the rest. The linkage expands and contracts while maintaining the curvature. This specification is the key to form a ring-like mechanism. One short and one long ternary links both have equal arms with identical kink angles. As in Linkage 2, this pair of links is similar to angulated scissor units but the connection of the pairs to each other is different than the ones in the literature.

As the starting point of the research was loop assembly method utilized by Hoberman, another variation in his study was also examined. The ring assembly of Linkage 4 is composed again, this time with different scales of the same loop. It is seen that, such an assembly was also deployable. This time there were more than one type of link pair with same kink angles in each pair but differing from the rest.

The linkages observed with the ability to transform might be considered to be used in architectural applications such as building skin components, space covers, gates and more. As there are many other linkages composed of antiparallelogram loops that are not examined and analyzed as a case in the study, there are yet many characteristics and potentials to be explored.

Future studies may involve exploring more of the linkages defined in this study in detail. Seeking potential uses in architectural applications may also be considered as next step. In a kinematic point of view, exploration of possible linkages in three dimensional space could be another field to be studied.

REFERENCES

Ario, I., Nakazawa, M., Tanaka, Y., Tanikura, I. and Ono, S. (2013). Development of a prototype deployable bridge based on origami skill. *Automation in Construction*, 32, 104-111.

Belda, E. A. P. (2013). *The structures of Emilo Pérez Piñero: Evolution and types*. Seville, Starbooks.

Bouleau, E. and Guscetti, G. (2016). Scissor mechanisms for transformable structures with curved shape. *Advances in Architectural Geometry*, F. G. S. Adriaenssens, M. Kohler, A. Menges, M. Pauly, vdf: 222-239.

Cai, J. G., Zhou, Y. H., Zhu, Y. F., Feng, J., Xu, Y. X.and Zhang, J. (2016). Geometry and mechanical behaviour of radially retractable roof structures during the movement process. *International Journal of Steel Structures,* 16(3), 755-764.

Cook, P. (1967). *Architecture: action and plan*, Studio Vista; New York: Reinhold.

Coxeter, H. S. M. (1969). *Introduction to geometry*, Wiley New York.

De Temmerman, N. (2007). *Design and analysis of deployable bar structures for mobile architectural applications*, Ph. D. thesis, Vrije Universiteit Brussel, Brussels, Belgium.

Dictionary, O. E. (2007). *Oxford English dictionary online*, JSTOR. Retrieved from https://en.oxforddictionaries.com.

Escrig, F. (1984). Expandable space frame structures. *Proceedings of the 3rd International Conference on Space Structures*, ed: Nooshin, H., University of Surrey, Guildford, UK, Elsevier Applied Science Publishers, London.

Escrig, F. (1985). Expandable space structures. *International Journal of Space Structures,* 1(2), 79-91.

Escrig, F. (1996). *General survey of deployability in architecture*. Edited by F. Escrig and CA Brebbia. Proceedings of MARAS, 96, 3-22.

Escrig, F. and Valcarcel, J. (1986). Great size umbrellas with expendable bar structures. *Proceedings of the 1st International Conference on Lightweight Structures in Architecture*.

Escrig, F. and Valcarcel, J. (1986). Analysis of expendable space bar structures. *Proceeding of IASS symposium on shells, membranes, and space frames*.

Escrig, F. and Valcarcel, J. (1987). Curved expandable space grids. *Proceedings of the International Conference on the Design and Construction of Non-conventional Structures*, Civil-Comp Press London.

Escrig, F. and Valcarcel, J. (1993). Geometry of expandable space structures. *International Journal of Space Structures,* 8(1-2), 71-84.

Friedman, N. (2011). *Investigation of highly flexible, deployable structures: review, modelling, control, experiments and application*, École normale supérieure de Cachan-ENS Cachan.

Gantes, C. J., Connor, J. J., Logcher, R. D. and Rosenfeld, Y. (1989). Structural analysis and design of deployable structures. *Computers & Structures*, 32(3-4), 661-669.

Glassner, A. (1996). Frieze groups. *IEEE Computer Graphics and Applications*, 16(3), 78-83.

Guy, R. K. and Woodrow, R. E. (1994). *The Lighter Side of Mathematics: Proceedings of the Eugène Strens Memorial Conference on Recreational Mathematics and Its History*, Cambridge University Press.

Hanaor, A. and Levy, R. (2001). Evaluation of deployable structures for space enclosures. *International Journal of Space Structures*, 16(4), 211-229.

Merchan H., C. H. (1987). *Deployable structures*, Massachusetts Institute of Technology.

Hoberman, C. (1990). *Reversibly expandable doubly-curved truss structure*, US Patents, US4942700.

Hoberman, C. (1991). *Radial expansion/retraction truss structures*, US Patents, US5024031.

Hoberman, C., Demaine, E. and Rus, D. (2013). MIT Class 6.S080 (AUS) - Mechanical Invention through Computation, Mechanism Basics.

Jensen, F. V. (2004). *Concepts for retractable roof structures*, University of Cambridge.

Jiang, Y. B. and Wang, X. R. (2010). Movable roof design and analysis of retractable roof structures. C*ivil Engineering in China - Current Practice and Research Report,* 357-361.

Kassabian, P. E., You, Z. and Pellegrino, S. (1999). Retractable roof structures. *Proceedings of the Institution of Civil Engineers-Structures and Buildings,* 134(1), 45-56.

Kiper, G. and Söylemez, E. (2010). Irregular polygonal and polyhedral linkages comprising scissor and angulated elements. *Proceedings of the 1st IFToMM Asian Conference on Mechanism and Machine Science*, Taipei.

Kokawa, T. (2000). Structural idea of retractable loop-dome. *Journal of the International Association for Shell and Spatial Structures,* 41(2), 111-116.

Kovács, F. and Tarnai, T. (2004). *Symmetry-adapted mobility and stress analysis of spherical and polyhedral generalized bar-and-joint structures*, PhD dissertation submitted to the BME.

Langbecker, T. (1999). Kinematic Analysis of Deployable Scissor Structures. *International Journal of Space Structures*, 14(1), 1-15.

Langbecker, T. and Albermani, F. (2000). Foldable positive and negative curvature structures: geometric design and structural response. *Journal of the International Association for Shell and Spatial Structures,* 41(3), 147-161.

Langbecker, T. and Albermani, F. (2001). Kinematic and non-linear analysis of foldable barrel vaults. *Engineering Structures*, 23(2), 158-171.

Lederman, G., You, Z. and Glisic, B. (2014). A novel deployable tied arch bridge. *Engineering Structures*, 70, 1-10.

Leonard, I. E., Lewis, J. E., Liu, A. C.-F. and Tokarsky, G. (2014). *Classical Geometry: Euclidean, Transformational, Inversive, and Projective*, John Wiley & Sons.

Liao, Q. and Li, D. (2005). Mechanisms for scaling planar graphs. *Chinese Journal of Mechanical Engineering*, 8, 026.

Maden, F., Korkmaz, K., & Akgün, Y. (2011). A review of planar scissor structural mechanisms: geometric principles and design methods. *Architectural Science Review*, 54(3), 246-257.

Mao, D. and Luo, Y. (2008). Analysis and design of a type of retractable roof structure. *Advances in Structural Engineering,* 11(4), 343-354.

Perez, P. E. (1965). *Three dimensional reticular structure*, US Patents, US3185164.

Pesenti, M., Masera, G., Fiorito, F. and Sauchelli, M. (2015). Kinetic solar skin: a responsive folding technique. *International Conference on Solar Heating and Cooling for Buildings and Industry*, Shc 2014 70, 661-672.

Pinero, E. (1961). Project for a mobile theatre. *Architectural Design*, 12(1), 154-155.

Pinero, E. (1961). A reticular movable theatre. *The Architects'Journal*, 299.

Pinero, E. (1962). Expandable space framing. *Progressive Architecture,* 43(6), 154-155.

Pólya, G. (1924). XII. Über die Analogie der Kristallsymmetrie in der Ebene. *Zeitschrift für Kristallographie - Crystalline Materials*, 60(1-6), 278.

Qi, X. Z., Huang, H. L., Li, B. and Deng, Z. Q. (2016). A large ring deployable mechanism for space satellite antenna. *Aerospace Science and Technology*, 58, 498-510.

Rippmann, M. (2007). *Curtain Wall: Building Design Semesterarbeit*. Stuttgart: Universität Stuttgart-ILEK.

Singh, P. (2015). Frieze Groups and Frieze Patterns. *International Journal of Mathematical Sciences and Applications*, Volume 5(1), 59-66.

Söylemez, E. (2010). *Makina Teorisi-1 Mekanizma Tekniği*, Birsen, 3rd edition.

Usiskin, Z., J. Griffin, D. Witonsky and E. Willmore (2008). *The classification of quadrilaterals: A study of definition*, IAP.

Van Mele, T. (2008). *Scissor-hinged retractable membrane roofs*. Vrije Universiteit Brussel.

Wang, Y., Liang, T., Congi, Q., Liu, R. Q. and Yang, H. (2015). Satellite SAR Antenna Deployable Structure Design and Kinematic Analysis. *Proceedings of the First International Conference on Information Sciences*, Machinery, Materials and Energy (Icismme 2015) 126: 968-973.

Yar, M. (2016). Design of novel transformable planar structural linkages with angulated scissor units, Thesis, İzmir Institute of Technology.

Yar, M., Korkmaz, K., Kiper, G., Maden, F., Akgün, Y. and Aktaş, E., (2017). A novel planar scissor structure transforming between concave and convex configurations. *International Journal of Computational Methods and Experimental Measurements*, 5(4), 442-450.

You, Z. and Pellegrino, S. (1997). Foldable bar structures. *International Journal of Solids and Structures,* 34(15), 1825-1847.

Zheng, F. and Chen, M. (2015). New conceptual structure design for affordable space large deployable antenna. *Ieee Transactions on Antennas and Propagation,* 63(4), 1351-1358.